STUDY OF CONDUCTIVE POLYMERS FOR BIOELECTRONICS

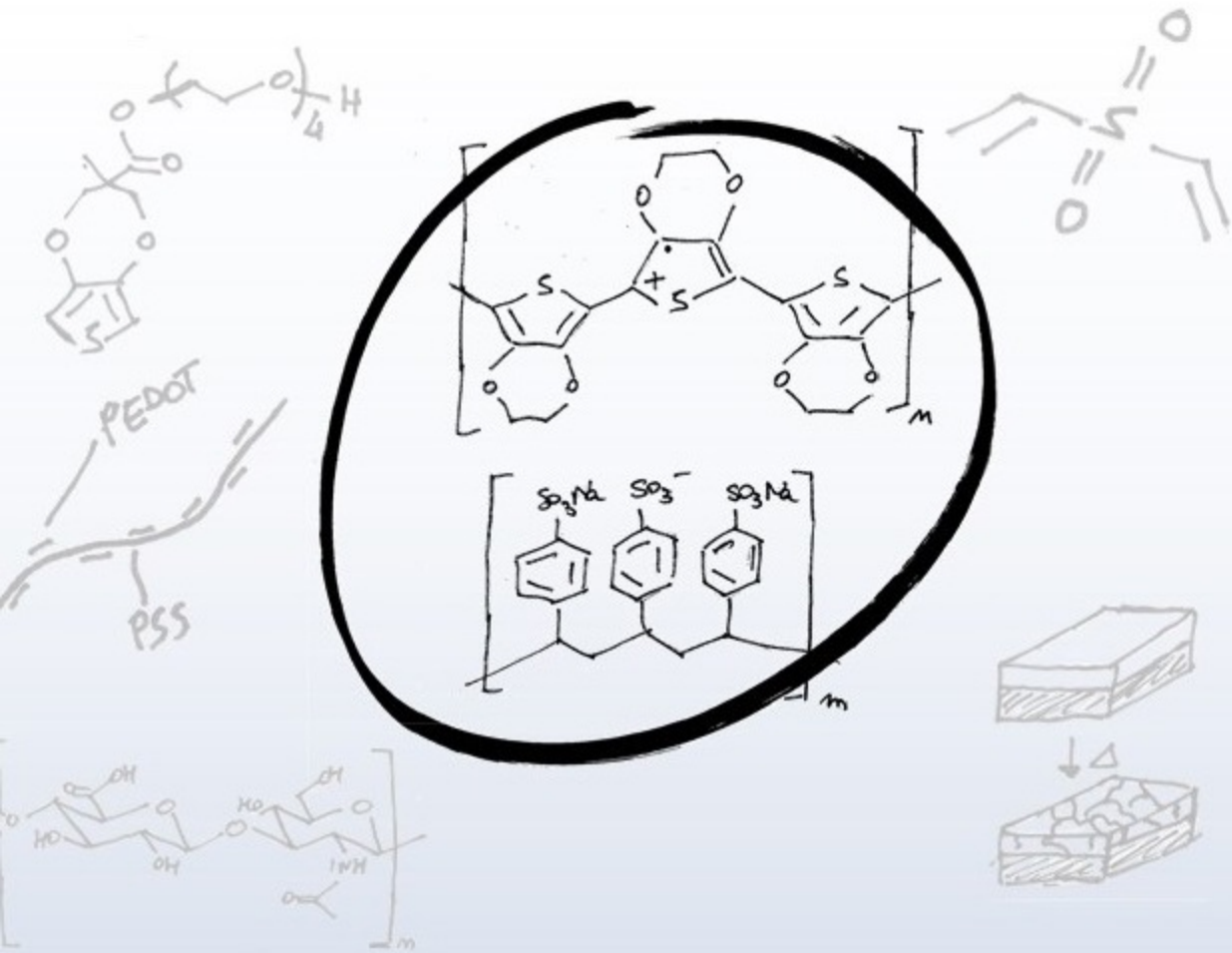

Daniele Mantione | PhD Thesis 2017

eman ta zabal zazu
Universidad del País Vasco
Euskal Herriko Unibertsitatea

POLYMAT
Basque Center for Macromolecular Design and Engineering

STUDY OF CONDUCTIVE POLYMERS FOR BIOELECTRONICS

Daniele Mantione

Thesis advisors:

Prof. David Mecerreyes

Dr. Haritz Sardon

University of the Basque Country UPV/EHU

Donostia-San Sebastian

2017

eman ta zabal zazu

Universidad del País Vasco

Euskal Herriko Unibertsitatea

POLYMAT

Basque Center for Macromolecular Design and Engineering

ES Más sabe el diablo por viejo que por diablo

EUS Azeriak, isatsa luze

EN The devil knows many things because he is old

IT L'eperienza paga

FR Vieux bœuf fait sillon droit

Table of contents

Introduction and objectives

I.1 Introduction

It is common knowledge that plastic acts as an insulator. In fact, from the early years of school, teachers explain us how polymeric materials are used in electronic to cover metal wires, or to create a protective layer, that insulate electricity, allowing us to manipulate them. That is only partially true. Chronologically, the first material based on a synthetic polymer, was electrically conductive. Weird? Let's explore these things in order.

The first broadly known synthetic polymer produced was named Bakelite. This polymer was synthesized by Leo Baekeland in Yonkers, New York in 1907 and is known to be an excellent insulator (**Scheme I.1a**).[1] However, in 1865, Alexander Parker synthesized what is considered as the first usable, plastic material. He started from a polymer, cellulose, functionalizing it with nitric acid, forming nitrocellulose or Parkesine. Even if this was considered as a milestone, the Parkesine never became as famous as the previously cited Bakelite.[2] Going deeply behind the scenes, browsing through the literature, almost at the same time, in 1862 H. Letheby, a professor in Chemistry at the London Hospital College, electropolymerized aniline sulfate to an apparently useless, bluish-black

solid layer on a platinum electrode and published his results in the Journal of the Chemical Society (**Scheme I.1b**), without highlighting the importance of his discovery.[3] This synthesis can be considered as the first event in the story of synthetic polymers and conductive polymers. Despite this, we had to wait almost one hundred years to find again in the literature an example about conductive polymeric materials; actually, around the 50s Herbert Naarmann discovered low resistivity materials based on polycyclic aromatic compounds[4] and, in 1963, B.A. Bolto and co- workers reported derivatives of polypyrrole with resistivity as low as 1 ohm·cm.[5]

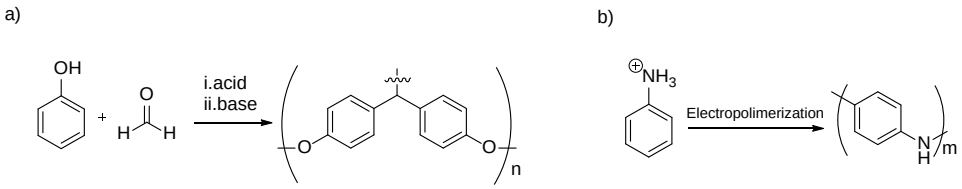

Scheme I.1 Reaction of polymerization and structure of Bakelite, b) reaction of electropolymerization and structure of polyaniline.

The first whole investigation about conductive polymers was published by McGinnes in 1972 in Science journal reporting a polymer based on melanin which owned a tunable electrical conductivity. This work is considered as the first complete example on a conductive polymer.[6] However, the first noteworthy investigations about polymeric conductive material were done in 1977 by the winners of the Nobel prize in chemistry in 2000: Alan J. Heeger, Alan MacDiarmid and Hideki Shirakawa.[7] They explained the synthesis and the characteristics of a polyacetylene doped conductive polymer. Even if polyacetylene showed great conductivity values, its instability against air did not permit the further application of this polymer.

At that time, it was envisioned that the insertion of heteroatoms inside the polymer chain, as we saw aniline and polypyrrole were easy to synthetize and handle. Here on, we are going to focused on thiophene backbone. Before entering in the scenes, thiophene had to wait until 1960 when Gronowitz et Al. discovered a new synthesis to merge thiophene rings.[8] From that time the research moved fast. In

1967 A. G. Davies and co-authors investigated the acid catalysed polymerization of furan, pyrrole, and thiophene heterocycles.[9] In 1973, researchers demonstrated that salts of tetrathiafulvalene showed almost metallic conductivity.[10] But we had to wait until 1982 when Tourillon and Garnier got a conductivity of 10–100 S/cm using a 3-alkyl-thiophene, opening officially a new era in thiophene based conductive polymers.[11] From that work, many other studies consisting in different protocols to prepare poly-3-alkyl-thiophenes regio-regularly or using different coupling reagents has been carried out.[12–14] All these work were fighting against the conductivity even if the main concern about these materials was the stability against air and moisture. Although polythiophenes are considerably more stable than the previously synthesized polyacetylenes, they de-doped easily and they are barely soluble in any solvent.

Across these studies, the importance to substitute the position 3 and 4 on the thiophene ring (**Scheme I.2**), to block side reaction during the polymerization[15] and to push up the conductivity was confirmed.[16] However, increasing too much the groups do not allow the correct polythiophene macrostructure decreasing the conductivity.[16,17] For that the interest was moving towards alkoxy thiophenes molecules: the same chemistry could be applied and they were more processable then the alkyl ones, they suffer less water and air exposition. This investigation lead to many different studies where the effect of the pendant group on the 3' position was studied and the different polymerization methods were investigated. The patents from Feldhues and Kampf demonstrated that the future was defined toward the small alkoxy substituents.[18–23] During these studies was clearly evidenced how blocking the position 3' was crucial, in fact the 3-alkyl-thiophene worked much better than the bare thiophene. Moreover, blocking also the position 4 in the thiophene ring lead to an amazing increase in the conductivity. This fact guided to a paper published by Daoust and Leclerc which stretched out the carpet for the best fusion of all these organic chemistry variables: a bicycle ring system.[24] Closing the upper ring in 3-4 position creating the 3,4-methylene dioxothiphene (MDOT) seemed to be the best method and researchers pay attention to that molecule (**Scheme I.2**). Moreover, closing the upper ring gives symmetric

molecules, avoiding the regioisomers formation and creating a more homogeneous polymer. Many people fight against the chemistry to synthetize this monomer in the 70-80s but they did never get the desired molecule.[25,26] It is good to know that only in 1997, so, years later, Ahonen et Al. synthetize and polymerize the MDOT (**Scheme I.2**) obtaining a fairly stable polymer with poor conductivity.[27]

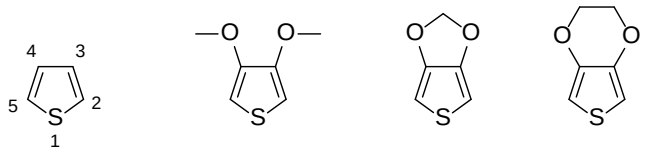

thiophene 3,4-dimethoxythiophene MDOT EDOT

Scheme I.2 Molecular structures of thiophene and derivates.

Coming back to the late 80s researchers from Bayer discovered the best scaffold so far: 3,4-ethylenedioxothophene EDOT and the relative polymer poly-3,4-ethylenedioxothophene PEDOT, simply by adding a carbon in the dioxygenated ring. This is one of the most important achievements of the last century (**Scheme I.2**). The patent application DE 38 13 589 A1 of the inventors Jonas, Heywang, and Werner Schmidtberg was filled in Germany on April 22, 1988 showing a 3,4-ethylenedioxothophene as base scaffold.[28] The bicyclic system of nine atoms immediately appeared to be outstanding. EDOT showed great stability, water stability and easy handling. In fact only one week later, on April 30, the same inventors filled another patent (DE 38 14 730 A1) applying the material to capacitors in collaboration with Agfa.[29] The synthesis was afterwards published in Advanced Material.[30] It is worth to precise that in all these works, PEDOT was coupled with other small molecules that acted as counter-anions. The challenge at that time was to discover a counter chain that allowed processing doped PEDOT from an aqueous solution/dispersion. The solution came when the researches from Agfa and Bayer jointly mixed PEDOT to the well-known Sodium Polystyrene sulfonate (NaPSS). NaPSS was known as water soluble antistatic

agent due to its ionic conductivity. The combination of the two polymers resulted in a stable aqueous dispersion which could be processed by several casting methods as a coating and pushed the limits of Polymer Electronics, named PEDOT:PSS (**Scheme I.3**).[31]

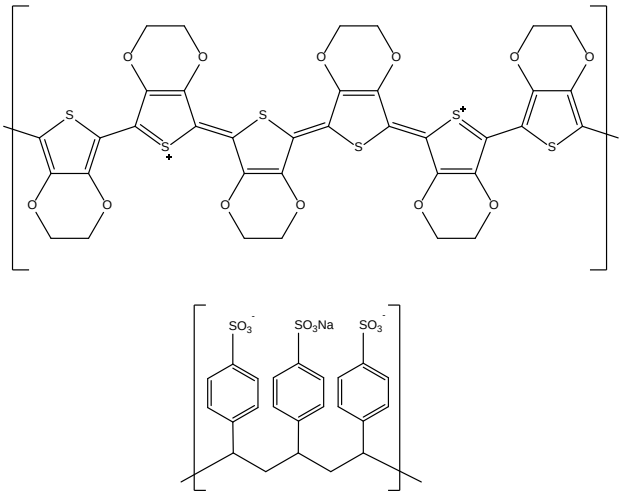

Scheme I.3 Structure of poly-3,4-ethylenedioxothophene (on the top) and polystyrene sulfonate (down).

Poly-3,4-ethylenedioxothophene: polystyrene sulfonate (PEDOT:PSS) is nowadays the most successful industrial conductive polymer due to its wide range of applications. **Figure I.1** illustrates some of the most important areas where PEDOT:PSS is in use such as organic electronics, organic optoelectronics and medical devices and sensors.

Bare electronics was how PEDOT:PSS entered in the scenes of the industrial world. The excellent electronic properties such as low surface resistivity, 10^{-6} Ω/□, the absence of heavy metals, transparency and the easy processability made it

an excellent anti-static agent for different application including coatings as well as bulk materials. Agfa, one of the main retailers of this suspension, made a great business around it in the 80-90's coating millions of square meters of photographic film.[32,33] Antistatic coating in cathode ray tubes (the old televisions), was another huge market where the conductive polymer was used extensively.[34] More recently, PEDOT:PSS is being used in touchscreen applications in a range of electronic devices such as mobile phones or tablets.[35] Due to its electronic properties, PEDOT/PSS is also finding applications in electrochemical energy storage technologies in supercapacitors[36] or electrodes for Lithium-air batteries.[37]

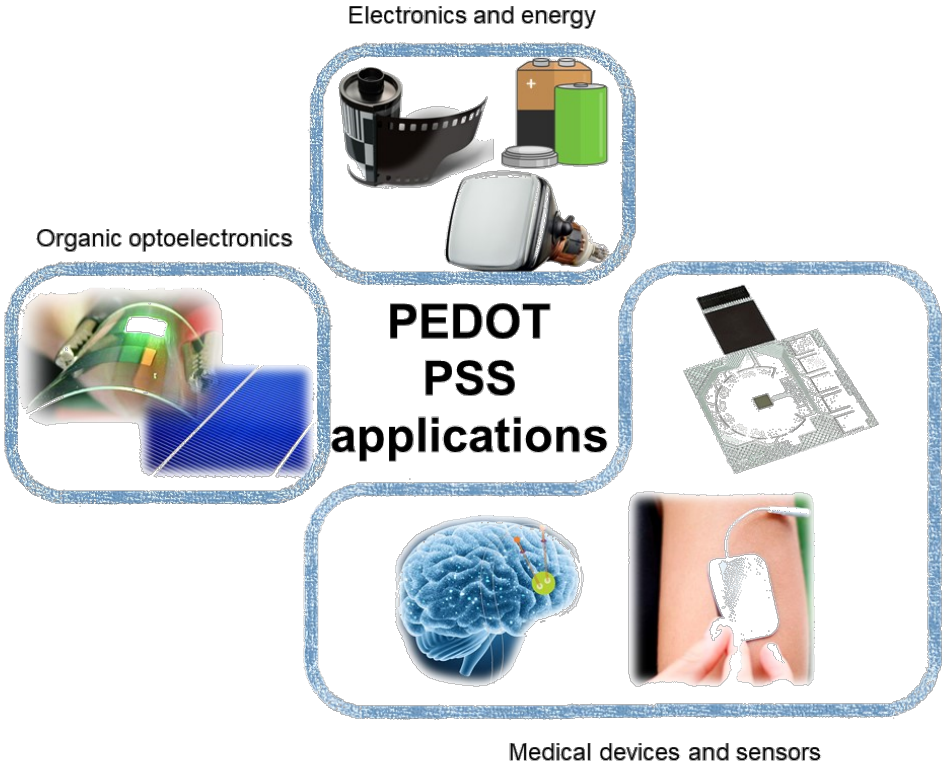

Figure I.1 Four different main areas where PEDOT:PSS is applied: organic electronics, organic optoelectronics, sensors and medical devices

However, the most explored field where PEDOT:PSS has been, and is used in research, is organic optoelectronics. Cavendish Laboratory pioneered its use in

an organic photodiode in 1999,[38] followed by other attempts to use PEDOT:PSS as electrode Organic Light Emitting Diodes (OLEDs) and for organic solar cells.[38]

In this area Indium tin oxide (ITO) is the most used transparent conducting oxice layer in electrodes. Despite its good combination of transparency and conductivity, ITO is too expensive and rigid to fulfil a flexible and chap goal. PEDOT:PSS finds applications to substitute ITO as transparent electrode with flexibility and low prize.[39–41] Further, PEDOT:PSS has been also used in other optoelectronic devices such as electrochromic smart windows and more recently in thermo-electric energy devices, etc.[42].

The last application area where PEDOT:PSS is actively being applied is in sensors and medical devices. It is worth to combine these two topics together, as usually, the majority of the literature threating this area consist of devices to sense biologically relevant molecules or want to measure biological phenomena. The general principle of these devices is being able to transform a variation of concentration of molecule, or ions, into an electronic signal. In the case of the sensors we have a large variety, sensing humidity,[43] pressure,[44] gases[45,46] and using different geometry. But, among these, organic thin-film transistors (OTFTs) offer several advantages for use as transducers due to their high signal amplification, respect of the current applied, that allows high efficient and small dimensions.[47] For these reasons, OTFTs have been used in sensor applications for gaseous analytes (e.g., H_2O_2 and O_2,[48] NO_2,[49] and O_3[50]), humidity sensing,[51] acidity,[52] ion concentrations,[53] and a variety of biologically important analytes like enzymes,[54] antibodies[55] and deoxyribonucleic acid (DNA).[56] An interesting class of OTFTs is organic electrochemical transistors (OECTs). These devices have been used widely in recent years due to their low operating voltages and their simply structure. Furthermore, OECTs have the ability to operate in aqueous environments that are essential for biological applications, worth to cite are deep brain implants and cutaneous electrodes.[57]

During the years, PEDOT:PSS has been optimized for the different application needs. For instance, one common challenge has been and still is to push the

electronic conductivity as high as possible. To do that, several organic molecules have been added to the PEDO:PSS formulation followed by a post-treatment step. Additives considered as secondary dopants to increase the conductivity include ethylene glycol[58,59], meso-erythritol,[58,59] DMSO,[60–62] surfactants and ionic liquids. Severak post-treatment have been carried out to optimize the best conductivity value: like bake the final film at high temperature,[63] or soaking the film in different organic molecules or acidic treatments.[63–65] Noteworthily, with these method the highest conductivity reached for PEDOT/PSS is about 3300 S/cm.[65] It is worth to remark that the record conductivity right now is 8797 S/cm which may be the theoretical limit, obtained by single crystal growing of PEDOT without PSS.[66]

Even though PEDOT:PSS is a stable material in contact with a living tissue, in a long-term point of view, cross-linking is needed to prevent delamination and eventual re-dispersion of the conducting film, especially on glass substrate.[67,68] In order to achieve this, numerous methods were used such as UV light or polyethylene oxide treatment.[69–71] Among them, one of the most studied is the use of silanes,[72,73] and in particular glycidoxy propyltrimethoxysilane (GOPS).[74–79] The drawbacks of these molecules are multiple, in fact, normally are insulators, low biocompatibility and the excess is difficult to remove. This makes that one of the challenges of the application of PEDOT:PSS in medical devices or bioelectronics is to develop robust and high-performance cross-linking method.

Another limitation of PEDOT:PSS is its biocompatibility. Although PEDOT:PSS is considered nowadays a biocompatible polymer, in a long-term point of view, the conductive polymer chains, and mostly the counter chain like PSS, can suffer side reactions, or with the residual acidity of the sulfonate groups, result in a poor bio-tolerability. Various strategies have been used to overcome these side effects, enhancing the biocompatibility and reduce the cytotoxicity. First of all substituting PSS for biomolecules.[80–82] A variety of negatively charged biomolecules have been studied, such as alginate, dextran sulfate, chondroitin

sulfate,[83–85] heparin and hyaluronic acid.[86–88] In most of these reports the conducting polymer/biomolecule complexes were prepared electrochemically limiting their scalability due to the low area of the electrode where the polymer is usually deposited.[89]

Observing the structure of EDOT or PEDOT another logical strategy to enhance the bio-compatibility or biofunctionality could be to modify and act directly on the conductive polymeric backbone. To do that, we must insert a pendant group in the dioxolane ring. At this respect, in the literature there is a clear disequilibrium about the few works done in order to modify the proper monomer EDOT and the many works concerning the modification of all the matrix: anionic chain, solvents, dopants, crosslinkers etc.[90,91] This is due principally to the fact that the material (PEDOT:PSS) is commercially available, stable and already many research groups use it which creates a huge amount of useful literature behind. The second, but not less important factor, is that to modify the scaffold, many synthetic chemical steps are needed. And, even if afterwards the result could be a better polymer with better properties, the efforts have to be worth.

I.2 Objectives

The aim of this thesis is to develop new PEDOT:PSS-base and -like materials, for bioelectronic applications. As the figure suggests we have tried to improve three of the limitations of PEDOT:PSS. First its limited biocompatibility was tackled by substituting PSS by natural biopolymers. Second, a new additive was introduced into the formulation in order to cross-link in an efficient manner the PEDOT:PSS while maintaining its electronic conductivity. Third, a synthetic strategy was developed to obtain (bio)functional monomers and new conductive polymers. Following this, the thesis is going to be divided in three chapters, each one concerning one modification as display in **Figure I.2**.

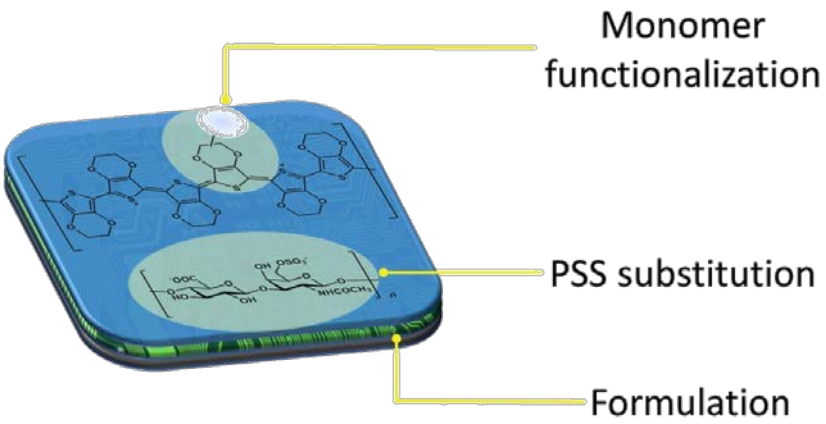

Figure I.2 Key points in the modification of PEDOT:PSS.

The first chapter of this thesis is centered in changing the whole PSS chain, with a more bioactive anionic chain. Screening the possible anionic biocompatible polymers, GAGs (glycosaminoglycanes) are a class of anionic polymer naturally present in the body that, bearing anionic groups, can couple with PEDOT and substitute PSS. Due to the residual acidity of the protonated sulfonate groups, PSS, could result less bio-tolerated than GAGs. More precisely in this chapter we are going to investigate, among all the GAGs, of three polymers: Hyaluronic acid, Chondroitin sulfate and Heparine. The goal here is to obtain PEDOT:GAGS dispersion which are more bioactive than PSS without depleting the conductivity and the mechanical properties.

In the second chapter, our target is to modify the formulation of PEDOT:PSS and to search for new cross-linking additives. As cited in the introduction, GOPS is one of the most used crosslinkers of PEDOT:PSS. However, the easy to use and effective epoxy-silane, GOPS presents some drawbacks. First of all it creates an insulating network, requires high temperatures to crosslink (more than 100 °C) and, the excess, is difficult to remove. In this chapter, we focused our attention to DVS: acronym for divinylsulfone. This is a commonly used crosslinker for biomolecules and many study of biocompatibility has been done using this

scaffold. The goal here is to investigate the use of DVS as cross-linker for PEDOT:PSS and to investigate the biocompatibility and application of the PEDOT:PSS crosslinked layers in bioelectronics.

The third chapter is focused on the monomer modification. The goal of this chapter is to develop a simple synthetic methodology for a versatile monomer molecule. For this reason, we shifted to ProDOT (3,4-propilenedioxothiophene), a close scaffold that own similar properties than EDOT. The goal of this chapter was to synthesize an acid functionalized ProDOT monomer in a limited number of steps. The acid functionalization will allow easy and various (bio)functionalizations. As examples, the synthesis of monomers/polymers of ProDOT-acid with dopamine, TEMPO (2,2,6,6-Tetramethyl-1-piperidinyloxy) derivate and tetraethyleneglycol will be investigated.

In the last chapter, the conclusions of each part of this thesis are commented.

I.3 References

(1) https://www.acs.org/content/acs/en/education/whatischemistry/landmarks/bakelite.html (accessed March 2, 2017). .
(2) Parkes, A. Improvement in the manufacture of Parkesine. UK 1313, 1865.
(3) Letheby, H. *J. Chem. Soc.* **1862**, *15* (0), 161.
(4) Naarmann, H. In *Ullmann's Encyclopedia of Industrial Chemistry*; Wiley-VCH Verlag GmbH & Co. KGaA: Weinheim, Germany, 2000.
(5) Bolto, B.; Weiss, D. *Aust. J. Chem.* **1963**, *16* (6), 1076.
(6) McGinness, J.; Corry, P.; Proctor, P. *Science (80-.).* **1974**, *183* (4127), 853.
(7) Shirakawa, H.; Louis, E. J.; MacDiarmid, A. G.; Chiang, C. K.; Heeger, A. J. *J. Chem. Soc. Chem. Commun.* **1977**, No. 16, 578.
(8) Gronowitz, S.; Karlsson, H.-O. *Ark. Kemi* **1960**, No. 17, 89.
(9) Armour, M.; Davies, A. G.; Upadhyay, J.; Wassermann, A. *J. Polym. Sci. Part A-1 Polym. Chem.* **1967**, *5* (7), 1527.
(10) Ferraris, J.; Cowan, D. O.; Walatka, V.; Perlstein, J. H. *J. Am. Chem. Soc.* **1973**, *95* (3), 948.
(11) Tourillon, G.; Garnier, F. *J. Electroanal. Chem. Interfacial Electrochem.* **1982**, *135* (1), 173.
(12) McCullough, R. D.; Lowe, R. D.; Gu, H. B.; Yoshino, K.; Wudl, F.; Spinelli, D. *J. Chem. Soc. Chem. Commun.* **1992**, *24* (1), 70.
(13) Chen, T. A.; Rieke, R. D. *J. Am. Chem. Soc.* **1992**, *114* (25), 10087.
(14) Guillerez, S.; Bidan, G. *Synth. Met.* **1998**, *93* (2), 123.
(15) Roncali, J. *Chem. Rev.* **1992**, *92* (4), 711.
(16) Feldhues, M.; Kämpf, G.; Litterer, H.; Mecklenburg, T.; Wegener, P. *Synth. Met.* **1989**, *28* (1–2), 487.
(17) Tourillon, G.; Garnier, F. *J. Electroanal. Chem. Interfacial Electrochem.* **1984**, *161* (1), 51.
(18) Wegener, P.; Feldhues, M.; Litterer, H. No Title. EP328984, 1988.
(19) Feldhues, M.; Kämpf, G.; Mecklenburg, T. No Title. EP328983, 1988.
(20) Kämpf, G.; Feldhues, M. No Title. EP328981, EP328982, 1988.
(21) Feldhues, M.; Kämpf, G.; Mecklenburg, T. No Title. EP313998, 1987.
(22) Kämpf, G.; Feldhues, M. No Title. EP292905, 1987.
(23) Feldhues, M.; Mecklenburg, T.; Wegener, P.; Kämpf, G. No Title. EP257573, 1987.
(24) Daoust, G.; Leclerc, M. *Macromolecules* **1991**, *24* (2), 455.
(25) Dallacker, F.; Mues, V. *Chem. Ber.* **1975**, *108* (2), 576.
(26) Dallacker, F.; Mues, V. *Chem. Ber.* **1975**, *108* (2), 569.
(27) Ahonen, H. J.; Kankare, J.; Lukkari, J.; Pasanen, P. *Synth. Met.* **1997**, *84* (1–3), 215.
(28) Jonas, F.; Heywang, G.; Schmidtberg, W. Neue polythiophene, verfahren zu ihrer herstellung und ihre verwendung. DE3813589, 1988.
(29) Jonas, F.; Heywang, G.; Schmidtberg, W. Feststoff-elektrolyte und diese enthaltende elektrolyt-kondensatoren. DE3814730, 1988.
(30) Heywang, G.; Jonas, F. *Adv. Mater.* **1992**, *4* (2), 116.

(31) Jonas, F.; Werner, K. Polythiophene dispersions, their production and their use. EP0440957, 1990.
(32) Jonas, F.; Krafft, W.; Muys, B. *Macromol. Symp.* **1995**, *100* (1), 169.
(33) Jonas, F.; Morrison, J. T. *Synth. Met.* **1997**, *85* (1–3), 1397.
(34) Hotta O.,Soga S., N. S. N. No Title. JP 02129284, 1988.
(35) Bishop, C. A. *Transparent conducting coatings on polymer substrates for touchscreens and displays*; 2016.
(36) Liu, Y.; Weng, B.; Razal, J. M.; Xu, Q.; Zhao, C.; Hou, Y.; Seyedin, S.; Jalili, R.; Wallace, G. G.; Chen, J. *Sci. Rep.* **2015**, *5* (1), 17045.
(37) Yoon, D. H.; Yoon, S. H.; Ryu, K.-S.; Park, Y. J. *Sci. Rep.* **2016**, *6* (1), 19962.
(38) Arias, A. C.; Granström, M.; Petritsch, K.; Friend, R. H. *Synth. Met.* **1999**, *102* (1–3), 953.
(39) Sun, K.; Zhang, H.; Ouyang, J. *J. Mater. Chem.* **2011**, *21* (45), 18339.
(40) Sun, K.; Xiao, Z.; Lu, S.; Zajaczkowski, W.; Pisula, W.; Hanssen, E.; White, J. M.; Williamson, R. M.; Subbiah, J.; Ouyang, J.; Holmes, A. B.; Wong, W. W. H.; Jones, D. J. *Nat. Commun.* **2015**, *6*, 6013.
(41) Dam, H. H.; Sun, K.; Hanssen, E.; White, J. M.; Marszalek, T.; Pisula, W.; Czolk, J.; Ludwig, J.; Colsmann, A.; Pfaff, M.; Gerthsen, D.; Wong, W. W. H.; Jones, D. J. *ACS Appl. Mater. Interfaces* **2014**, *6* (11), 8824.
(42) Kirchmeyer, S.; Reuter, K. *J. Mater. Chem.* **2005**, *15* (21), 2077.
(43) Jaruwongrungsee, K.; Sriprachuabwong, C.; Sappat, A.; Wisitsoraat, A.; Phasukkit, P.; Sangworasil, M.; Tuantranont, A. In *The 8th Electrical Engineering/ Electronics, Computer, Telecommunications and Information Technology (ECTI) Association of Thailand - Conference 2011*; IEEE, 2011; pp 66–69.
(44) Muckley, E. S.; Lynch, J.; Kumar, R.; Sumpter, B.; Ivanov, I. N. *Sensors Actuators B Chem.* **2016**, *236*, 91.
(45) Hui-Hisn Lu; Chia-Yu Lin; Yueh-Yuan Fang; Tzu-Chien Hsiao; Kuo-Chuan Ho; Dongfang Yang; Chii-Wann Lin. In *2008 30th Annual International Conference of the IEEE Engineering in Medicine and Biology Society*; IEEE, 2008; pp 3208–3211.
(46) Seekaew, Y.; Lokavee, S.; Phokharatkul, D.; Wisitsoraat, A.; Kerdcharoen, T.; Wongchoosuk, C. *Org. Electron.* **2014**, *15* (11), 2971.
(47) Nilsson, D.; Robinson, N.; Berggren, M.; Forchheimer, R. *Adv. Mater.* **2005**, *17* (3), 353.
(48) Torsi, L.; Dodabalapur, A.; Sabbatini, L.; Zambonin, P. . *Sensors Actuators B Chem.* **2000**, *67* (3), 312.
(49) Hu, W.; Liu, Y.; Xu, Y.; Liu, S.; Zhou, S.; Zhu, D.; Xu, B.; Bai, C.; Wang, C. *Thin Solid Films* **2000**, *360* (1–2), 256.
(50) Bouvet, M.; Leroy, A.; Simon, J.; Tournilhac, F.; Guillaud, G.; Lessnick, P.; Maillard, A.; Spirkovitch, S.; Debliquy, M.; de Haan, A.; Decroly, A. *Sensors Actuators B Chem.* **2001**, *72* (1), 86.
(51) Nilsson, D. *Sensors Actuators B Chem.* **2002**, *86* (2–3), 193.
(52) Bartic, C.; Palan, B.; Campitelli, A.; Borghs, G. *Sensors Actuators B Chem.* **2002**, *83* (1–3), 115.
(53) Dabke, R. B.; Singh, G. D.; Dhanabalan, A.; Lal, R.; Contractor, A. Q. *Anal. Chem.* **1997**, *69* (4), 724.

(54) Bartlett, P. N.; Wang, J. H.; Wallace, E. N. K. *Chem. Commun.* **1996**, No. 3, 359.
(55) Kanungo, M.; Srivastava, D. N.; Kumar, A.; Contractor, A. Q. *Chem. Commun.* **2002**, No. 7, 680.
(56) Krishnamoorthy, K.; Gokhale, R. S.; Contractor, A. Q.; Kumar, A. *Chem. Commun.* **2004**, No. 7, 820.
(57) Nikolou, M.; Malliaras, G. G. *Chem. Rec.* **2008**, *8* (1), 13.
(58) Ouyang, J.; Chu, C.; Chen, F.; Xu, Q.; Yang, Y. *J. Macromol. Sci. Part A* **2004**, *41* (12), 1497.
(59) Ouyang, J.; Chu, C.-W.; Chen, F.-C.; Xu, Q.; Yang, Y. *Adv. Funct. Mater.* **2005**, *15* (2), 203.
(60) Na, S.-I.; Kim, S.-S.; Jo, J.; Kim, D.-Y. *Adv. Mater.* **2008**, *20* (21), 4061.
(61) Na, S.-I.; Wang, G.; Kim, S.-S.; Kim, T.-W.; Oh, S.-H.; Yu, B.-K.; Lee, T.; Kim, D.-Y. *J. Mater. Chem.* **2009**, *19* (47), 9045.
(62) Do, H.; Reinhard, M.; Vogeler, H.; Puetz, A.; Klein, M. F. G.; Schabel, W.; Colsmann, A.; Lemmer, U. *Thin Solid Films* **2009**, *517* (20), 5900.
(63) Zhou, J.; Anjum, D. H.; Chen, L.; Xu, X.; Ventura, I. A.; Jiang, L.; Lubineau, G. *J. Mater. Chem. C* **2014**, *2* (46), 9903.
(64) Xia, Y.; Ouyang, J. *Org. Electron.* **2012**, *13* (10), 1785.
(65) Ouyang, J. *ACS Appl. Mater. Interfaces* **2013**, *5* (24), 13082.
(66) Cho, B.; Park, K. S.; Baek, J.; Oh, H. S.; Koo Lee, Y.-E.; Sung, M. M. *Nano Lett.* **2014**, *14* (6), 3321.
(67) Elschner, A.; Kirchmeyer, S.; Lövenich, W.; Merker, U.; Reuter, K.; Lovenich, W.; Merker, U.; Reuter, K. *PEDOT*, 1st ed.; CRC Press: Boca Raton FL USA, 2011.
(68) Zhang, S.; Hubis, E.; Girard, C.; Kumar, P.; DeFranco, J.; Cicoira, F. *J. Mater. Chem. C* **2016**, *4* (7), 1.
(69) Huang, T.-M.; Batra, S.; Hu, J.; Miyoshi, T.; Cakmak, M. *Polymer (Guildf).* **2013**, *54* (23), 6455.
(70) Xing, Y.; Qian, M.; Wang, G.; Zhang, G.; Guo, D.; Wu, J. *Sci. China Technol. Sci.* **2014**, *57* (1), 44.
(71) Ghosh, S.; Inganäs, O. *Synth. Met.* **1999**, *101* (1–3), 413.
(72) Kim, S.; Cho, A.; Kim, S.; Cho, W.; Chung, M. H.; Kim, F. S.; Kim, J. H. *RSC Adv.* **2016**, *6* (23), 19280.
(73) Cho, W.; Im, S.; Kim, S.; Kim, S.; Kim, J. *Polymers (Basel).* **2016**, *8* (5), 189.
(74) Mu Yang; Yushi Zhang; Hongze Zhang; Zhihong Li. In *10th IEEE International Conference on Nano/Micro Engineered and Molecular Systems*; IEEE, 2015; pp 149–151.
(75) Sessolo, M.; Khodagholy, D.; Rivnay, J.; Maddalena, F.; Gleyzes, M.; Steidl, E.; Buisson, B.; Malliaras, G. G. *Adv. Mater.* **2013**, *25* (15), 2135.
(76) Khodagholy, D.; Doublet, T.; Quilichini, P.; Gurfinkel, M.; Leleux, P.; Ghestem, A.; Ismailova, E.; Hervé, T.; Sanaur, S.; Bernard, C.; Malliaras, G. G. *Nat. Commun.* **2013**, *4*, 1575.
(77) Leleux, P.; Johnson, C.; Strakosas, X.; Rivnay, J.; Hervé, T.; Owens, R. M.; Malliaras, G. G. *Adv. Healthc. Mater.* **2014**, *3* (9), 1377.
(78) Berezhetska, O.; Liberelle, B.; De Crescenzo, G.; Cicoira, F. *J. Mater. Chem. B* **2015**, *3* (25), 5087.

(79) Williamson, A.; Rivnay, J.; Kergoat, L.; Jonsson, A.; Inal, S.; Uguz, I.; Ferro, M.; Ivanov, A.; Sjöström, T. A.; Simon, D. T.; Berggren, M.; Malliaras, G. G.; Bernard, C. *Adv. Mater.* **2015**, *27* (20), 3138.
(80) Serra Moreno, J.; Panero, S.; Materazzi, S.; Martinelli, A.; Sabbieti, M. G.; Agas, D.; Materazzi, G. *J. Biomed. Mater. Res. Part A* **2009**, *88A* (3), 832.
(81) Collier, J. H.; Camp, J. P.; Hudson, T. W.; Schmidt, C. E. *J. Biomed. Mater. Res.* **2000**, *50* (4), 574.
(82) Pérez-Madrigal, M. M.; del Valle, L. J.; Armelin, E.; Michaux, C.; Roussel, G.; Perpète, E. A.; Alemán, C. *ACS Appl. Mater. Interfaces* **2015**, *7* (3), 1632.
(83) Molino, P. J.; Tibbens, A.; Kapsa, R. M. I.; Wallace, G. G. *MRS Proc.* **2013**, *1569*, mrss13.
(84) Molino, P. J.; Yue, Z.; Zhang, B.; Tibbens, A.; Liu, X.; Kapsa, R. M. I.; Higgins, M. J.; Wallace, G. G. *Adv. Mater. Interfaces* **2014**, *1* (3), n/a.
(85) Pérez-Madrigal, M. M.; Estrany, F.; Armelin, E.; Díaz, D. D.; Alemán, C. *J. Mater. Chem. A* **2016**, *4* (5), 1792.
(86) Thaning, E. M.; Asplund, M. L. M.; Nyberg, T. A.; Inganäs, O. W.; von Holst, H. *J. Biomed. Mater. Res. Part B Appl. Biomater.* **2010**, *93B* (2), 407.
(87) Moulton, S. E.; Higgins, M. J.; Kapsa, R. M. I.; Wallace, G. G. *Adv. Funct. Mater.* **2012**, *22* (10), 2003.
(88) Asplund, M.; Thaning, E.; Lundberg, J.; Sandberg-Nordqvist, A. C.; Kostyszyn, B.; Inganäs, O.; von Holst, H. *Biomed. Mater.* **2009**, *4* (4), 45009.
(89) Ocampo, C.; Oliver, R.; Armelin, E.; Alemán, C.; Estrany, F. *J. Polym. Res.* **2005**, *13* (3), 193.
(90) Wen, Y.; Xu, J. *J. Polym. Sci. Part A Polym. Chem.* **2017**, *55* (7), 1121.
(91) Mantione, D.; Agua, I. del; Sanchez-Sanchez, A.; Mecerreyes, D. *Polym. 2017, Vol. 9, Page 354* **2017**, *9* (8), 354.

Chapter 1. PEDOT:GAG aqueous Dispersions: Towards Electrically Conductive Bioactive Materials

1.1 Introduction

Electrically conductive polymers are showing great promise in the field of bioelectronics as materials able to act at the interface between electronics and biology. Among conducting polymers, poly(3,4-ethylenedioxythiophene) (PEDOT) coupled with polystyrene sulfonate (PSS) is catching more interest day by day due to its high conductivity, easy processing and commercial availability.[1,2] This organic polymer dispersion commonly used in organic electronics is being widely applied in bioelectronic devices in applications as transparent electrodes, a variety of biosensors, organic electrochemical transistors and more.[3–10] One of the key factors to its wide utilization in this area is the low toxicity presented with several cell types such as endothelial, epithelial, fibroblast, macrophage and most importantly human neuronal cell lines *in vitro*.[11,12] Furthermore, the applicability and biocompatibility of devices such as an organic electrochemical

transistor (OECT) based on PEDOT:PSS has been shown *in vivo* in an experimental rat model of epileptiform.[13]

Regardless of how promising this material has proven to be, long-term effects of degradation and possible release of acidic PSS degradation products in the brain remain unexplored. It is known that upon implantation of neural devices a considerable amount of damage to the surrounding tissue can occur. Indeed, in neuronal recording devices, it has been reported that the glial scar increases the distance between target neuronal populations, insulates the electrode and increases impedance, preventing a stable device-CNS interface.[14] A widely used strategy to improve the side effects of organic electrochemical transistors and to enhance the biocompatibility and reduce the cytotoxicity of conducting polymers such as polypirrole, polyaniline or PEDOT is the use of biomolecules as dopants.[15–17] A variety of negatively charged biomolecules have been studied as dopants, such as alginate, dextran sulfate, chondroitin sulfate,[18–20] heparin and hyaluronic acid.[11,21,22] In most of these reports the conducting polymer/biomolecule complexes were prepared electrochemically limiting their scalability due to the low area of the electrode where the polymer is usually deposited.[23] Only recently, Wallace and coworkers[24] have reported the synthesis of PEDOT:dextran sulfate aqueous dispersions which allow the production of high amounts of conductive materials and the coatings of large areas by casting using dextran sulfate dopant. They found that after drop casting, PEDOT:dextran sulphate films showed around 25% superior cell growth after 4 days. This fact inspired us to investigate other negatively charged polymers naturally present in the body, more specifically in the neural tissue, to create PEDOT materials with improved biocompatibility and bioactivity.

Glycosaminoglycans (GAGs) are natural heteropolysaccharides that are present in every mammalian tissue. They are composed by repeating disaccharide units and are negatively charged even with carboxylic and sulfated groups. In addition, GAGs play important roles in physiological and pathological conditions and they are considered key macromolecules that affect cell properties and functions. Therefore, GAGs not only could act as dopant for PEDOT but as well induce

protection for cells or increase proliferation of neural cells. For instance, Hyaluronic acid (HA) has been shown to facilitate nerve regeneration and limit perineural scar formation.[25] Heparin (HEP) is one of the highest negatively charged molecules present in the body and it can bind to several growth factors such as Heparin Binding Growth Factors, (HBGFs) and nerve growth factor (NGF), which stimulates neuronal survival and neurite outgrowth.[26,27] Likewise, Chondroitin Sulfate (CS) is a major constituent of perineuronal nets and it is involved in the maintenance of neuronal plasticity, where it serves mainly as an inhibitory signal and protected cells against hydrogen peroxide induced cell death.[28] These advantages are of major importance when materials are used for devices to be implanted into the Central Nervous System (CNS) environment. In this chapter, biocompatibility was first assessed according to the international organization for standardization (ISO) guidelines ISO10993-5:2009 using the L929 mouse fibroblast cell line and the extraction method. To evaluate the PEDOT:GAGs presented here in a CNS related context, biocompatibility and functional tests were performed with human neuroblastoma cell line SH-SY5Y and human astrocytoma cell line CCF-STTG1. SH-SY5Y is an established cell line commonly used in neurodegeneration studies and neurotoxicity screens. [29,30] CCF-STTG1 cell line was used as a human astrocytic cells model, these cells show comparable characteristics and can be used as a model for the human astrocytic response in toxicological screenings.[31,32] In this chapter we show the synthesis and biocompatibility properties of new poly(3,4-ethylenedioxythiophene):GlycosAminoGlycan (PEDOT:GAG) aqueous dispersions and its resulting films.[33]

1.2 Results and Discussion

1.2.1 Synthesis and characterization of PEDOT:GAGs aqueous dispersions

In this chapter, three different GAGs were successfully used as dopants to prepare PEDOT dispersions by oxidative chemical polymerization of EDOT: HA (Hyaluronic acid), HEP (Heparine) and CS (Chondroitin Sulfate), and compared to commercially used PSS (**Scheme 1.1a**; in the scheme has been use CS, the other difference structures of GAG molecules are HA **Scheme 1.1b** and HEP **Scheme 1.1c**). Briefly, the stabilizer, (PSS, HA, CS or HEP) was first dissolved in water and stirred for 30 min at 25 ºC. When the dopant was completely dissolved, EDOT monomer was added and after 15 min, the oxidant $(NH_4)_2S_2O_8$ and a catalytic amount of catalysts $Fe_2(SO_4)_3$ were added. After completing the reaction, the reaction became a deep blue aqueous dispersion, indicative of the presence of PEDOT.

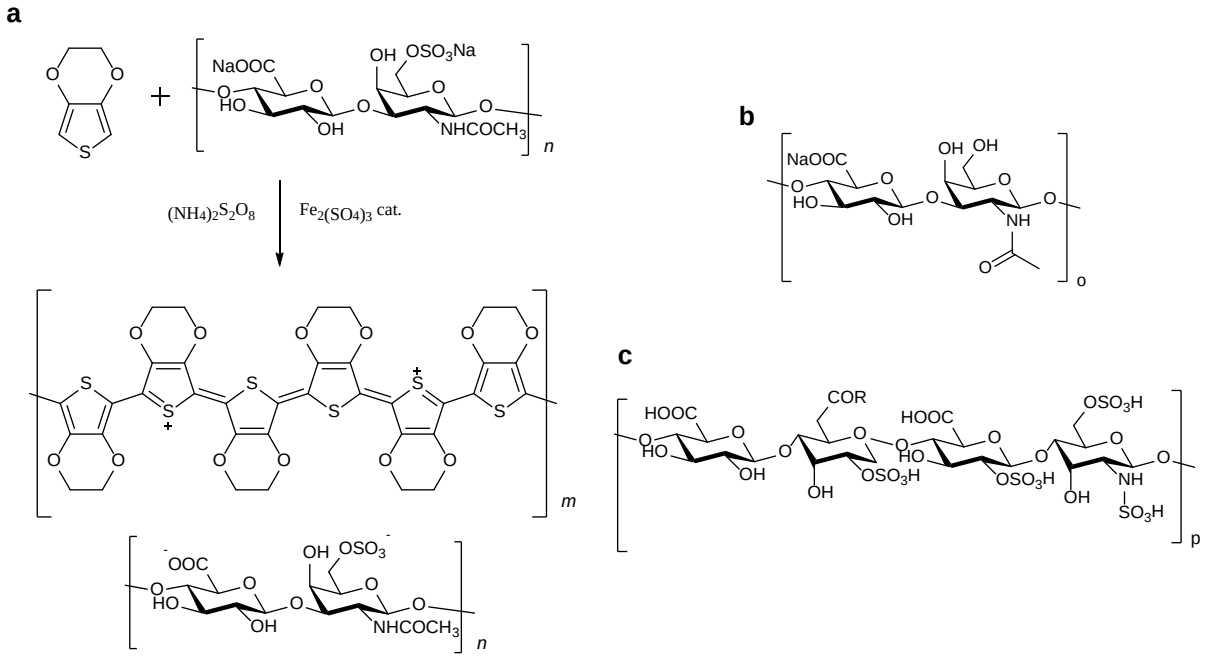

Scheme 1.1 a) Oxidative chemical polymerization of EDOT with GAG (e.g. CS), b) Chemical structure of Hyaluronic Acid, c) Chemical structure of Heparin.

To further verify the efficient polymerization of EDOT in the presence of GAGs as dopants, a kinetic study was carried out by HPLC measuring monomer consumption *vs* time with the 3 different GAGs and compared to commonly used PSS dopant (**Figure 1.1**). The measurement has been carried with an internal standard, precipitating an aliquot of the suspension in ACN (Acetonitrile) to ride of the already polymerized PEDOT.

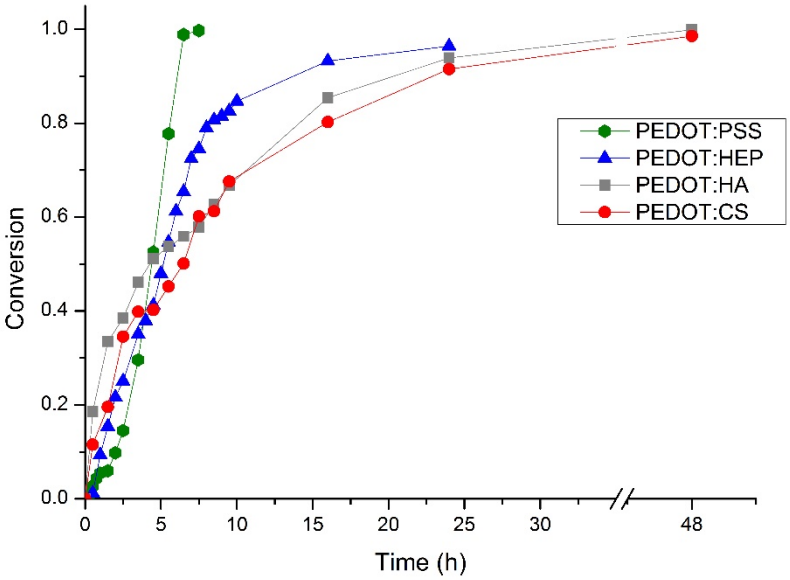

Figure 1.1 Kinetic reaction profiles of chemically oxidative polymerization.

As observed in all cases, we were able to reach full conversation in all the cases. However, in the case of using HA (48h), CS (48h) and HEP (24h) as dopants and stabilizers the reaction was considerably slower than in the case of PSS (8h). In our opinion this fact can be attributed to a much higher viscosity of initial GAGs solutions compared to PSS solutions. This increase on the viscosity could reduce the diffusion of radicals necessary to promote the oxidative polymerization, reducing the polymerization rate.[34,35] Hence, in the case of HEP (with intermediate viscosity), the reaction was much faster, 24 h, than in the case of HA and CS, 48 h.

In order to confirm the initial high viscosity of GAGs dispersions respect to PSS dopant, absolute viscosity was calculated for entry 1 and entry 2 of **Table 1.1**: containing PSS and HA dopants respectively.

#	% EDOT [wt]	Dopant	% Dopant [wt]	Conductivity [S/cm]
1	*50*	*PSS*	*50*	*0.070*
2	*50*	*HA*	*50*	*0.012*
3	*50*	*CS*	*50*	*0.015*
4	*50*	*HEP*	*50*	*0.004*
5	*33*	*HA*	*67*	*0.003*
6	*67*	*HA*	*33*	*0.060*
7	*85*	*HA*	*15*	*0.071*
8	*33*	*CS*	*67*	*0.002*
9	*67*	*CS*	*33*	*0.055*
10	*85*	*CS*	*15*	*0.075*
11	*33*	*HEP*	*67*	*0.001*
12	*67*	*HEP*	*33*	*0.013*
13	*85*	*HEP*	*15*	*0.050*

Table 1.1 Conductivity values measured by FPP of drop-casted films of PEDOT:GAGs at different ratios.

As observed in **Figure 1.2**, when GAGs are used as dopant, the initial viscosity is around 1Pa·s, higher than the PEDOT:PSS that is around 1mPa·s. As the reaction proceeded we observed a sharp decrease of the viscosity as the EDOT started polymerizing.

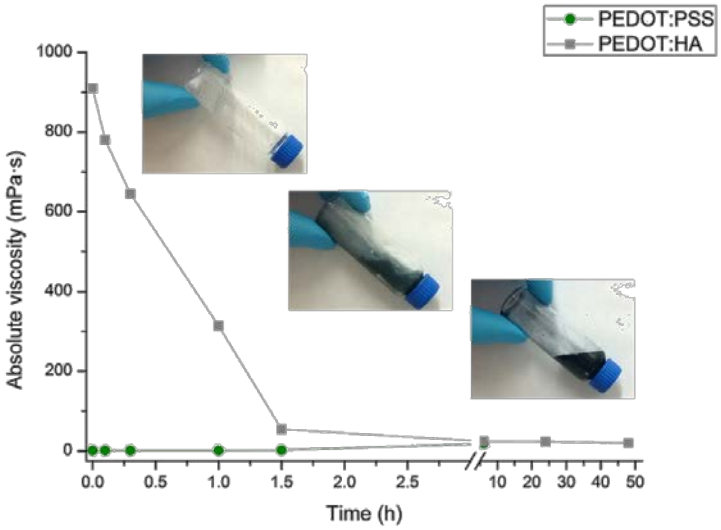

Figure 1.2 Color and viscosity changes during the reaction.

In our opinion, this fact occurred because at the beginning the negatively charged species of the GAGs were able to form strong intermolecular hydrogen bonding. As soon as the polymerization of EDOT started, some charged PEDOT species were formed which were stabilized by the negatively charged GAGs, reducing considerably their ability to form intermolecular hydrogen bonding with water. As a consequence, the viscosity of the dispersions is reduced and the reactions are able to proceed to full conversion. It is worth to note that a similar decrease of viscosity is also observed in other dispersion polymerization processes such as the preparation of poly(vinyl acetate) latexes using poly(vinyl alcohol) as stabilizer.[36]

After confirming the successful polymerization of EDOT in the presence of GAGs, we prepared different PEDOT/GAGs dispersions varying both the nature of the GAG (HA, CS and HEP) and the weight ratio between PEDOT/GAG (50:50, 67:33, 33:67, 85:15) as shown in **Table 1.1**. The synthesized dispersions were characterized by Transmission Electron Microscopy (TEM) and Dynamic Light Scattering (DLS). By DLS, **Figure 1.3**, we observed that increasing the amount of HA and CS, the particle size did not change significantly, staying around 200 nm and 500 nm for HA and CS

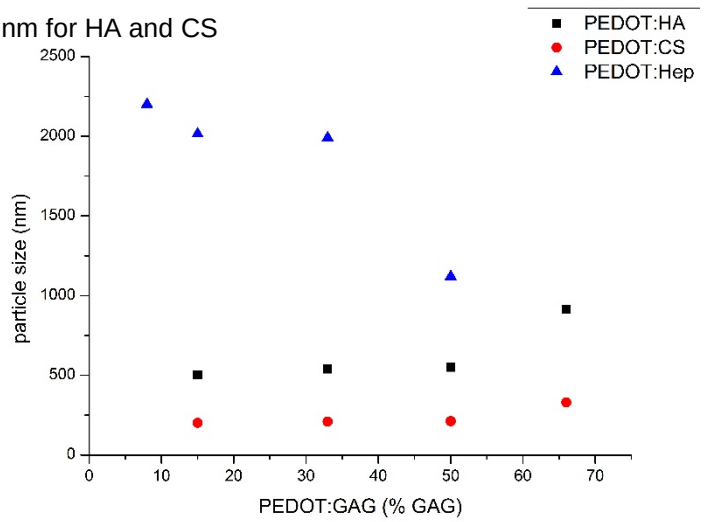

Figure 1.3 Particle sizes plot measured by DLS of PEDOT:GAG dispersions at different ratios.

respectively. In the case of HEP the final particle size measured by DLS, in all the cases, is more than a micron: out of the range of the instrument. The TEM images, **Figure 1.4** (PEDOT: a,b)HA c)HEP and d)CS) of all the GAGs shown not perfectly spherical particles, even if HA and CS look rounder than HEP. Looking closer is possible to distinguish an inner spherical core surrounded by irregular layer. As the inner cores appear darker than the rest, we can hypothesize are PEDOT domains and the outer lighter material are the biomolecules that stabilize them.[37,38] It is also possible to notice how in the case of HEP, even though the solution was diluted, more aggregates are presented and the shape is non-uniform.

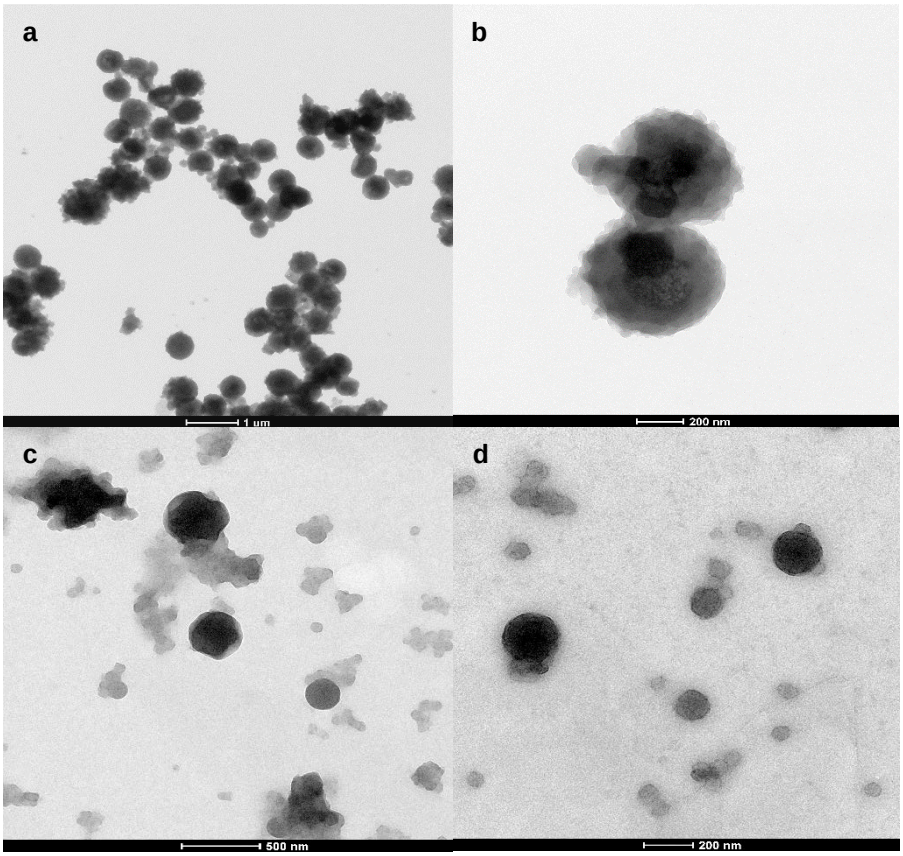

Figure 1.4 a,b)TEM images of PEDOT:HA c) PEDOT:HEP and d) PEDOT:CS.

The PEDOT:GAGs dispersions were further characterized by Ultraviolet - Near Infra-Red Spectroscopy and compared to commercially available PEDOT:PSS **(Figure 1.5).**

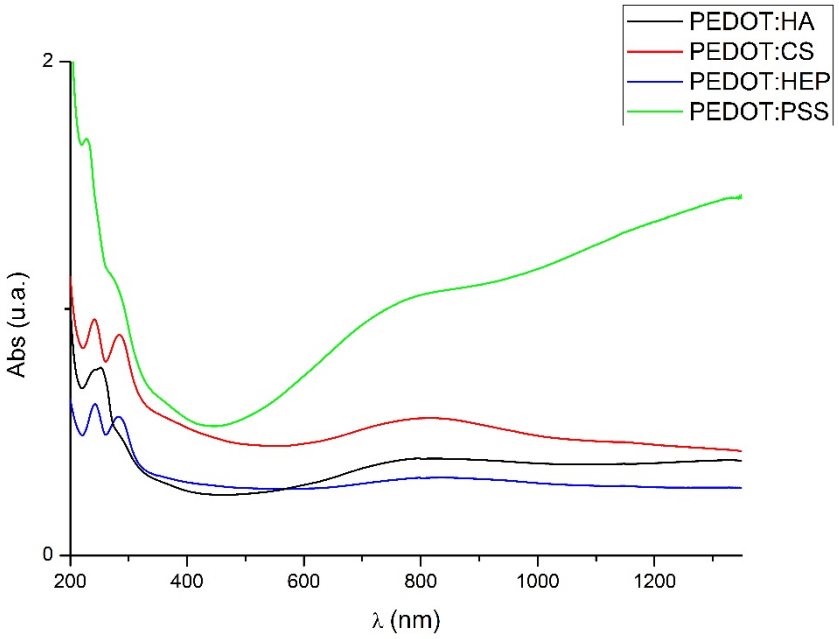

Figure 1.5 UV-Vis-NIR spectra of PEDOT:GAGs 1:1 2%wt and PEDOT:PSS 1:1 2%wt.

We observed two bands that in the case of PEDOT:PSS: the characteristic absorption band of PEDOT π - π^* centered at 800 nm and a broad polaron band that extends in the NIR region, centered at 1150 nm were presented. With respect to PEDOT:GAGs the band centered at 700 nm was similar to the PEDOT:PSS, the band centered at 1150 nm is less intense tough. This broad band in the NIR is generally attributed to the doped material and it is related to the conductivity of the material. [39] It is worth noting that we did not observe any significant difference in the UV using different PEDOT:GAG ratios.

Next the electronic conductivity of PEDOT:GAGs was measured by four point probe and compared with PEDOT:PSS films (**Table 1.1**). As expected,

decreasing the ratio between insulating GAGs molecules and conductive PEDOT, the conductivity increased. The values increased from 10^{-2} S/cm at high GAGs ratios (67 wt. %) to values close to 10^{-1} S/cm at low GAGs ratio (15 wt. %). It is worthy to note that 10^{-1} S/cm value is similar to the one obtained for PEDOT:PSS without any additional post-treatment.[40,41] When different GAGs were compared, the films obtained using CS showed slightly higher conductivity than the ones stabilized by HA and HEP. In the case of HA the lack of sulfonate anionic groups reduced considerably its ability to show high conductivity values and in the case of HEP the low stability and the presence of large aggregates could be the main explanation for this lower conductivity.

1.2.2 Biocompatibility of PEDOT:GAGs films

For the following bio-tests, films obtained by casting PEDOT:GAGs 1:1 (50% GAGs content) at 2%wt and PEDOT:PSS® by Heraeus as landmark, since is broadly used in literature, have been chosen as representative materials. Adding a known cross-linker to the suspensions leaded to conductive water-insoluble films that were sterilized and used into a fairly high throughput process In order to build a potential library with different types of functional organic conductive PEDOT materials with biomolecules, a pre-screen for cytotoxic properties of PEDOT materials on murine L929 fibroblasts was performed according to ISO 10993-5 guidelines. Biomolecules selected for this initial library were hyaluronic acid (HA), chondroitin sulfate (CS) and heparine (HEP),–culture medium was conditioned for 24h with these PEDOT materials and thereafter medium of L929 cells was refreshed with this conditioned medium. L929 cells cultured in all PEDOT extracts showed comparable cell viability with the inert control (high density polyethylene; **Figure 1.6**). Based on these findings, all PEDOT substrates were suitable to continue further experimentation.

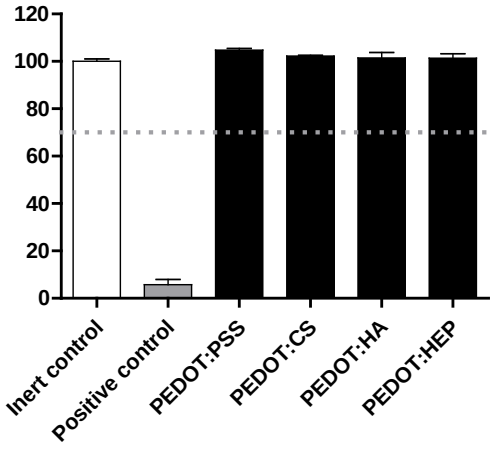

Figura 1.6 Cell viability of L929 cells, cultured in medium extracts of materials, measured by means of an MTT assay according to ISO 10993-5-2009 standards (n=3). Inert control: High density polyethylene, Positive control: Polyvinyl chloride (PVC). Viability shown as % of inert control (unpaired Student's t-test: *** p<0.001)

1.2.3 Cellular attachment and proliferation of CCF-STTG1 and SH-SY5Y cells

In the research presented here, neuroblastoma cell line SH-SY5Y and astrocytoma cell line CCF-STTG1 were used as CNS model cell lines for neuronal and astrocytic cells, respectively. Neurons in the CNS are responsible for neurotransmission connecting and coordinating brain areas by the generation and maintenance of neurites that send and receive neuronal signals. The composition of the tissue matrix influences the adequate growth and development of neurites. Injury or disease can lead to inflammatory conditions negatively influencing the extracellular environment such that is ends up in severe neuronal connectivity impairments. One strategy to overcome these impairments ideally would be to produce biomaterials that provide a favorable matrix for neuroregeneration. [42,43] Being the most abundant cell type in the CNS, astrocytes are indispensable for the brain. They are involved in synaptic formation and pruning, functioning of synapses and establishment of neuronal circuitries.

Additionally, they are intricately involved in regulation of cerebral blood flow and in maintaining integrity and regulation of the blood brain barrier.[44–46] Moreover, astrocytes also play a paramount role in the CNS immune response and inflammatory processes induced by disease or injury, including invasive surgeries for the implantation of neural devices.[47] For neuronal recording devices, it has been reported that the glial scar increases the distance between target neuronal populations, insulates the electrode and increases impedance, preventing a stable device-CNS interface.[14] With this in mind, it is of importance in future devices to fabricate materials that support normal functioning of neurons and astrocytes and provide an interface that does not evoke extra activation of the immune system on top of that already done by the mechanical stress due to implantation. In addition, materials are preferred that do not induce or stimulate extra proliferation of astrocytes and provide an environment stimulating neuronal regeneration.

For assessment of the suitability of our novel PEDOT dispersions for use in devices to be implanted in the CNS, cellular attachment and proliferation of CCF-STTG1 and SH-SY5Y cells were determined with use of a MTT assay[48] Cells were allowed to attach for 24 h, where after cell viability was measured and defined as time point 0 h. Hence, this time point could be taken as a measure for cellular attachment. For CCF-STTG1 cells, all three PEDOT:GAGs showed a higher cell viability at time point 0h (**Figure 1.7**). This indicates that these PEDOT:GAGs, provide a more compatible and thus less hostile substrate for attachment. However, this significant difference was not observed anymore at 24h and 48h, suggesting a higher proliferation of CCF-STTG1 cells cultured the PEDOT:PSS substrate. To compare rates of proliferation, non-linear regression was performed and the slopes from curve fits were compared. Cells cultured on PEDOT:PSS and PEDOT:CS did not show significantly different proliferation rates ($p=0.132$). However, cells cultured on PEDOT:HA ($p=0.028$) and PEDOT:HEP ($p=0.017$) showed lower proliferation rates. As well for SH-SY5Y cells, all the PEDOT:GAGs were shown to be a more preferred substrate indicated by higher cell attachment at time point 0h.

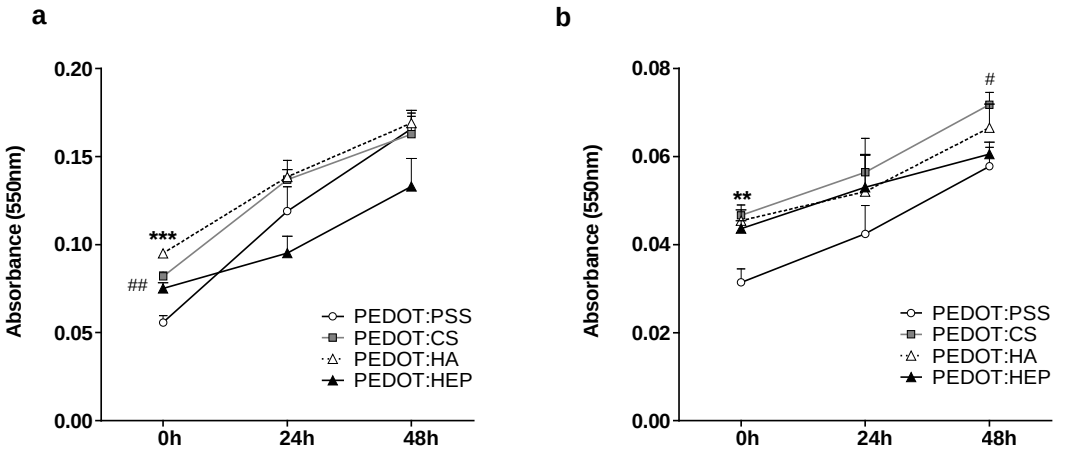

Figure 1.7 a) CCF-STTG1 cell proliferation was measured by means of MTT over 48h (unpaired Student's t-test: ## p<0.01 (PEDOT:CS vs PEDOT:PSS and PEDOT:HEP vs PEDOT:PSS); *** p<0.001 – n=4 per timepoint). b) SH-SY5Y cell proliferation was measured by means of MTT over 48h (unpaired Student's t-test: # p<0.05; ** p<0.01– n=4 per timepoint).

At time point 48h, still a significant higher cell viability was measured of cells cultured on PEDOT:CS compared to PEDOT:PSS. However, this was most probably caused by higher initial attachment of cells to PEDOT:CS since the slopes of curve fits by nonlinear regression did not differ significantly between PEDOT:PSS and PEDOT:CS (p=0.902). Nevertheless, as in the previous case PEDOT:HA (p=0.627) and PEDOT:HEP (p=0.349) showed lower proliferation rates. Together these results suggested that PEDOT:GAGs provided more compatible and preferred substrates for CNS cells types, specially PEDOT:CS substrate.

1.2.4 Calcium response of CCF-TTG1 cells induced by ATP

Calcium cation is one of the most dominant signalling elements in biology. As we know, calcium fluxes are involved in the birth of cells, proliferation and cell death

and has functions in nearly every cell type, from muscle contractions to complex roles in neuronal circuitry where neurite growth, plasticity, neurotransmitter dynamics, depolarization and synaptic activity are all dependent on this signalling element.[49–52] Although the functions of different types of intra- and intercellular calcium signals are still under extensive investigation, it is clear that astrocytes use calcium signalling to communicate which each other, neurons and other glia cells.[50] Astrocytes release ATP in response to rises in intracellular Ca^{2+}. In turn, ATP functions as an extracellular messenger acting on purinergic receptors of neighbouring astrocytes initiating rises in intracellular Ca^{2+} and subsequent release of ATP, thus propagating the calcium wave.[53] Here, we utilized this property of ATP to induce intracellular calcium responses in the astrocyte model cell line CCF-STTG1 in a high throughput model where changes in intracellular Ca^{2+} were visualized with the use of organic calcium dye Fluo-4 and fluorescent microscopy.

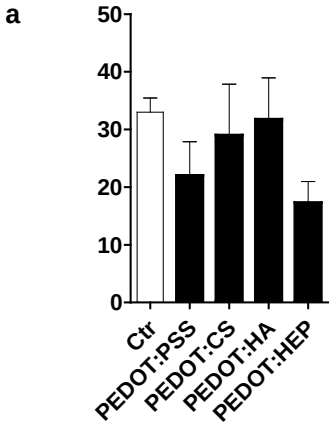

Figure 1.8 CCF-STTG1 cells were stimulated with ATP (50 mM) and the % of responsive cells was calculated (unpaired Student's t-test: ** $p<0.01$)

After preliminary investigations, it was determined that 50mM ATP induced a substantial intracellular calcium response in CCF-STTG1 cells cultured on tissue culture plastic, but would allow to detect differences in responses of cells cultured

on PEDOT materials with possible higher or lower amplitudes. It was observed that not all cells showed responsivity to ATP and that roughly 30% of the cells showed a rise in intracellular Ca^{2+} when stimulated with ATP (**Figure 1.8**).

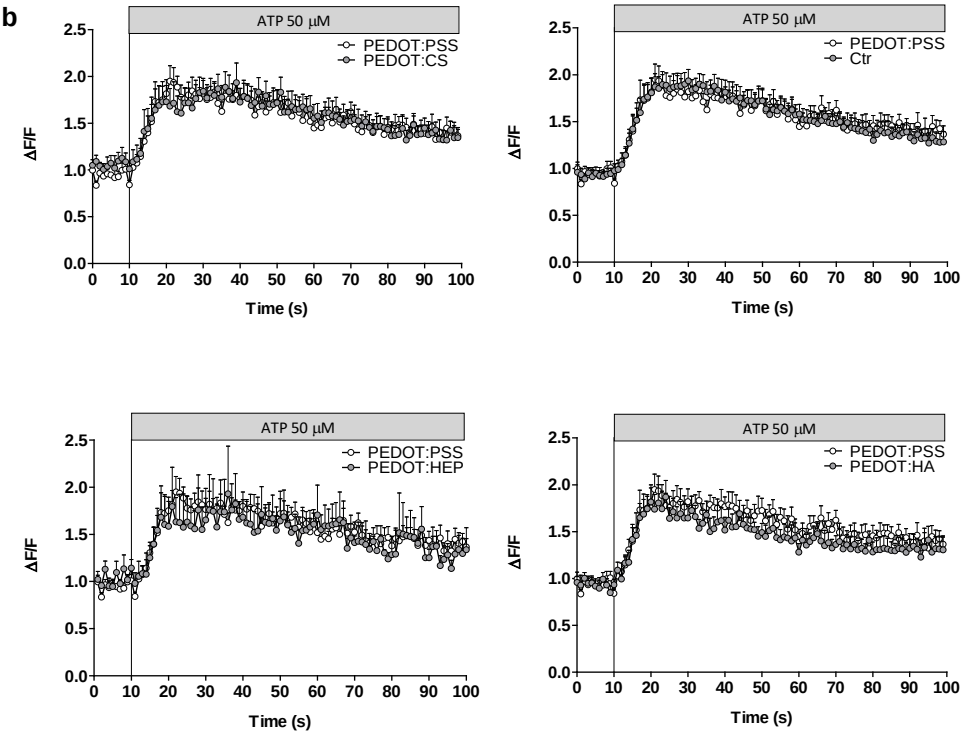

Figure 1.9 Response of CCF-STTG1 cells cultured on PEDOT substrates when stimulated with ATP (50 mM) were measured. Graphs depict average of responsive cell population of multiple samples and per sample 50-200 cells were analyzed (Ctr n=10, PEDOT:PSS n=8, PEDOT:CS n=6, PEDOT:HA n=7, PEDOT:HEP n=4). Chondroitin Sulfate

This percentage of responsive cells significantly differed from CCF-STTG1 cells cultured on PEDOT:HEP ($p<0.01$) but did not significantly differ from CCF-STTG1 cells cultured on PEDOT:PSS, PEDOT:CS and PEDOT:HA substrates, although PEDOT:PSS showed a lower tendency. Nonetheless, when novel PEDOT:GAGs were compared to PEDOT:PSS, no significant differences were observed

between the percentages of ATP responsive cells (**Figure 1.9**). To analyse actual intracellular calcium responses of cells cultured on PEDOT substrates, only signals of responsive cells were plotted and compared. Fluorescent signals were corrected for background and normalized to their own baseline measurement and plotted as ΔF/F. Although the percentage of responses appeared to have minor differences between cells cultured on different PEDOT substrates, intracellular calcium responses upon ATP stimulation of responsive cells did not show any significant differences. Cells cultured on normal tissue culture plastic or cultured on the PEDOT materials, all showed similar response dynamics, peaking around 10 seconds after stimulation with ATP followed by a slow decrease of the signal. It should be noted that the results shown here are a summation of responsive cells, and no individual cell profiles were compared. In summary, these experiments showed that all PEDOT materials tested here, PEDOT:PSS, PEDOT:CS, PEDOT:HA and PEDOT:HEP showed functional compatibility with astrocytic like cells, in terms of collective intracellular calcium response upon ATP stimulation.

1.2.5 Calcium response of SH-SY5Y cells upon KCl-induced depolarization

As previously discussed, calcium plays a large role in neuronal signal transduction. In neurons, after depolarization, influx of calcium is observed mainly by the action of voltage gated calcium channels and measuring of intracellular calcium is widely used to assess action potential activity *in vitro* as well as *in vivo.*[51] Here we used KCl-induced membrane depolarization of SH-SY5Y neuroblastoma cells to assess possible differences in rise of intracellular calcium after this event. KCl-induced depolarization has been previously established as an in vitro model of neuronal activity.[54] Before starting, a KCl concentration-response curve (45 mM-70mM) was generated to identify the most suitable concentration of use, which was identified to be KCl 55mM (data not shown). KCl was shown to be highly effective in inducing rises in intracellular calcium in SH-SY5Y cells, since nearly 90% of cells in all conditions was responsive to the

stimulus, with the exception of cells cultured on PEDOT:PSS, which showed a slightly lower percentage of responsive cells, albeit not significant (**Figure 1.10a**).

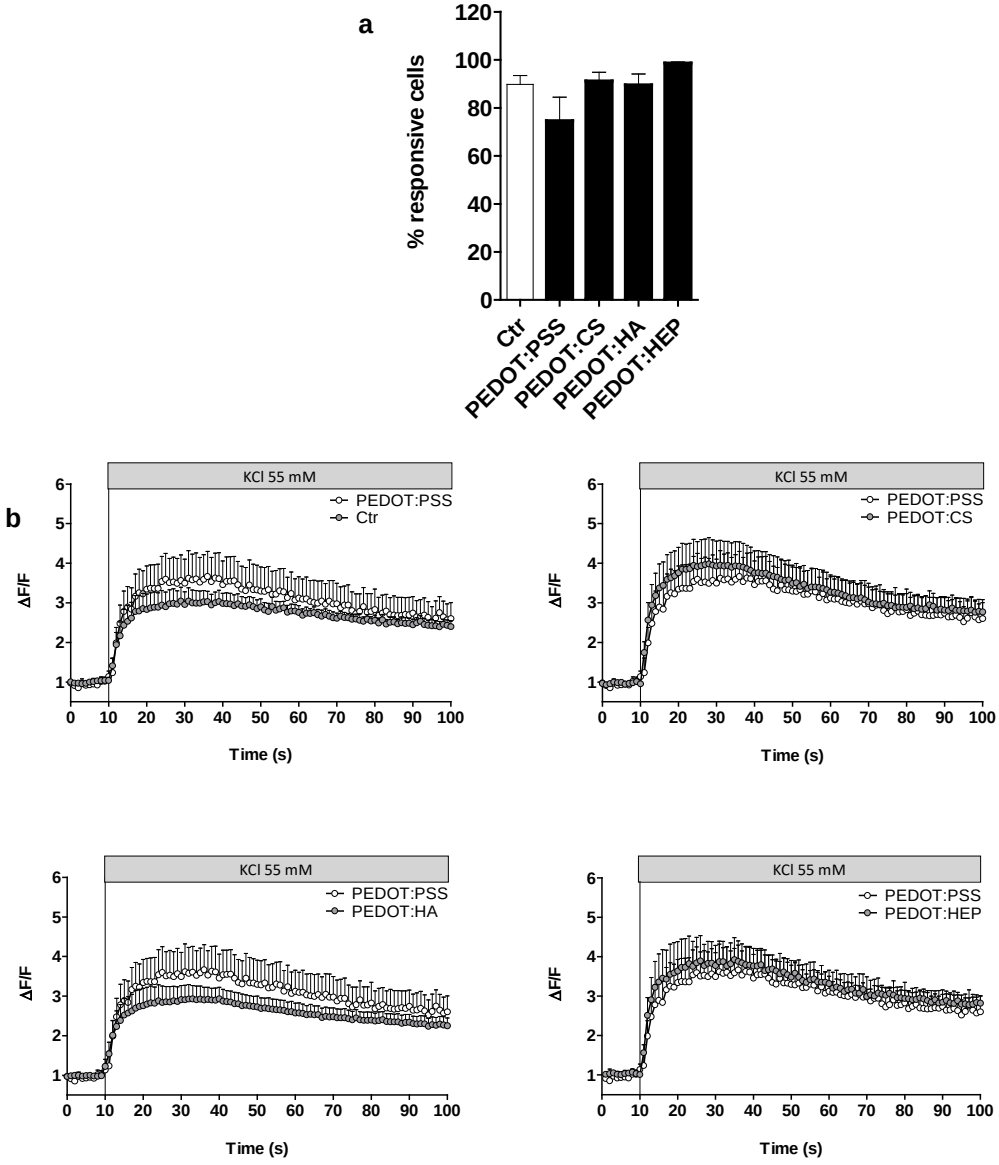

Figure 1.10 a) SH-SY5Y cells were stimulated with KCl (55 mM) and the % of responsive cells was calculated. b) Response of SH-SY5Y cells cultured on PEDOT substrates when stimulated with KCl (50 mM). Graphs depict average of responsive cell population of multiple samples and per sample 100-300 cells were analysed (Ctr n=8, PEDOT:PSS n=7, PEDOT:CS n=9, PEDOT:HA n=8, PEDOT:HEP n=5).

Intracellular calcium responses, expressed as ΔF/F, after KCl induced depolarization did not differ significantly between any of the conditions and showed similar patterns showing instant increase of intracellular Ca^{2+} after the stimulus, peaking between 20-30s, followed by a gradual decrease thereafter. However, PEDOT:CS and PEDOT:HA non-significantly deviated from this description where PEDOT:CS showed a higher value and PEDOT:HA a lower value (**Figure 1.10b**). In summary, these results suggest that all PEDOT materials tested here, support and did not negatively influence neuronal activity and thereby were shown to be functionally compatible with this cell type.

1.2.6 Neurite formation of differentiated SH-SY5Y cells cultured on PEDOT substrates

As described previously, upon implantation of neural devices a considerable amount of damage to the surrounding tissue can occur. Hence, neurons directly in the surrounding of the device can be damaged and dye. Furthermore, formation of the glial scar is a more than often observed problem, not only insulating the device, but as well preventing neuronal regeneration at the site of injury. With this in mind, the search for biomaterials that support and enhance neuronal regeneration is one of the main necessities. Measurement of neurite length of differentiated neuronal cell lines such as SH-SY5Y and PC12 cells, is generally used to identify neuronal biocompatibility and to assess if materials support neuroregeneration.[55] Here, we differentiated SH-SY5Y cells, cultured on PEDOT:PSS, PEDOT:CS, PEDOT:HA and PEDOT:HEP, by treating the cells for 3 days with synthetic retinoid EC23 in serum free medium, followed by a 3 day treatment with Brain-derived neurotrophic factor (BDNF) in serum free medium. Cells were immunostained for neurofilament (NF-200) and neurite length was measured using imageJ plugin simple neurite tracer. As a positive control, SH-SY5Y cells were differentiated on laminin, which has previously been shown to be the optimal substrate for stimulating differentiation of SH-SY5Y cells.[56]

As expected, undifferentiated cells stained 24h after seeding, did not show NF-200 positive neurite outgrowth (**Figure 1.11b**).

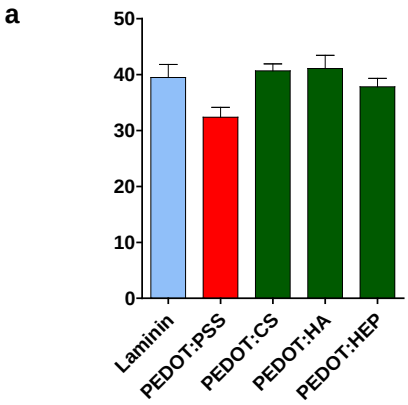

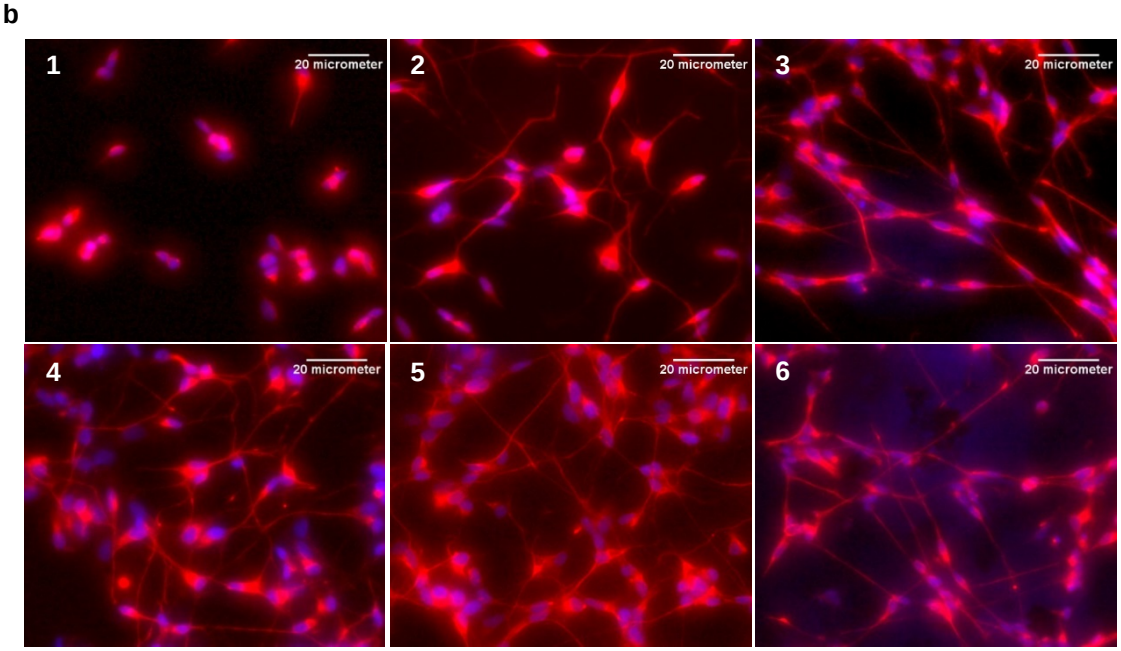

Figure 1.11 a) Immunohistochemistry (red: NF-200, blue: hoechst) of SH-SY5Y cells undifferentiated (A.1) or differentiated after culturing on control substrate laminin (A.2), PEDOT:PSS (A.3), PEDOT:CS (A.4), PEDOT:HA (A.5), PEDOT:HEP (A.6). b) Neurite length analysis of NF-200 expressing neurites (n=3, per sample a minimum of 10 cells were measured; all were compared to PEDOT:PSS using unpaired Student's t-test: * $p<0.05$; ** $p<0.01$).

Cells differentiated on laminin however, showed clear and long neurite outgrowth (**Figure 1.11a**). All substrates, PEDOT:PSS, PEDOT:CS, PEDOT:HA and PEDOT:HEP showed differentiated cells with NF-200 positive neurites (**Figure 1.11b** 3-6). Nonetheless, SH-SY5Y cells differentiated on PEDOT:PSS showed significantly shorter neurite length when compared to all other conditions (Figure 8B). The activity of individual GAGs regarding neuritogenesis has been previously shown to be concentration-dependent [57] and this critical aspect has been considered in the design of the stoichiometry for the PEDOT:GAGs materials. As discussed before, both HEP [26,27] and HA[25] have been described to support neurite survival and formation. Interestingly, here we show that CS, a well-known neurite growth inhibitor,[58] when combined with PEDOT promotes neuronal differentiation. All GAGs combined here with PEDOT, CS, HA and HEP, reach the scaffolding supportive capacity that laminin, a nervous system extracellular matrix molecule does. These results show that all PEDOT substrates support neuroregeneration, and that the novel PEDOT:GAGs show a stimulating environment.

1.2.7 Protection from hydrogen peroxide induced cell death

Implantation of neural devices induces a primary inflammatory response, mainly mediated by microglia and astrocytes. During this process of acute local inflammation, reactive oxygen species (ROS) such as hydrogen peroxide (H_2O_2) are produced, which has neurotoxic effects.[14] This makes the need to protect cells from this damage an important factor in selecting biomaterials to use in such implants. In order to test for possible neuroprotective properties of novel PEDOT:GAGs, the cytotoxicity protocol normally used for biocompatibility testing according to ISO 10993-5:2009 guidelines in that L929 cells was replaced with neuronal model cell line SH-SY5Y and additionally medium extracts were supplemented with H_2O_2. First a H_2O_2 kill curve experiment was performed (data not shown) where a significant amount of cell death was observed at a H_2O_2 concentration of 0.25mM.

Thereafter, MTT analyses was performed on SH-SY5Y cells which were cultured for 24h in normal cell culture medium or medium extracts 24h conditioned with PEDOT:PSS, PEDOT:CS, PEDOT:HA and PEDOT:HEP with or without H_2O_2 (0.25mM) present in the medium. All material extracts were shown to be non-cytotoxic to SH-SY5Y cells showing cell viabilities of 95-100% for all conditions. In control cells, H_2O_2 induced cell death of more than 60% and comparable cell viabilities were observed for cells cultured in H_2O_2 supplemented medium extracts of PEDOT:PSS, PEDOT:HA and PEDOT:HEP. However, cells cultured in PEDOT:CS extracts showed significantly higher cell viability compared to all other conditions, with a protection of over 20% (**Figure 1.12**). These results suggested that CS not only acted as a structural dopant but also possessed a neuroprotective effect against H_2O_2 induced cell death on SH-SY5Y cells, in agreement with the oxidative stress preventive role described previously in literature for CS alone in SH-SY5Y cells.[28]

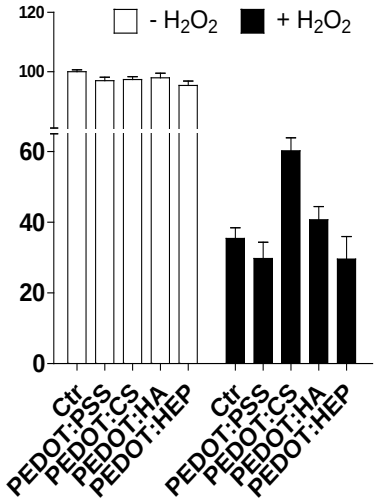

Figure 1.12 SH-SY5Y cell were cultured in 24h conditioned medium extracts from PEDOT substrates without or within the presence of H2O2 (0.25mM; n=5; unpaired Student's t-test: *** p<0.001).

1.3 Conclusion

In this chapter, we present a simple synthetic strategy to create PEDOT dispersion doped with glycosaminoglycans biopolymers. The resulting multi-purpose conductive suspensions were broadly characterized by following the kinetics of the reaction, DLS and UV-Vis-NIR. PEDOT/GAGS materials assessed not only biocompatibility in terms of cell viability, but also gave an indication on functional biocompatibility. Thus, we showed that all PEDOT materials tested here do not interfere with physiological functions by showing that ATP induced increases in intracellular calcium in astrocytic cell line CCF-STTG1 and that SH-SY5Y cells showed normal KCl depolarization induced increases in intracellular calcium. A remarkable observation was that the novel PEDOT:GAGs were shown to be more supportive for neuroregenerative processes, compared to commercial PEDOT:PPS, as shown by longer neurite length of differentiated SH-SY5Y cells. In addition, a neuroprotective effect of PEDOT:CS was shown where SH-SY5Y cells were partially protected from H_2O_2 induced cell death. In summary, these PEDOT:GAGs materials are ideal candidates for organic electrochemical transistors because of their functional support in neuroregenerative processes and their protection against the oxidative environment likely to occur when recording/stimulating devices would be implanted in vivo. To conclude, a useful and more bio-active substitutes of PSS were chosen and fruitfully tested, opening up to further modification and studies toward other biopolymers.

1.4 Experimental section

1.4.1 Reagents and instruments

EDOT was purchased from Acros Organic, Sodium Hyaluronate (HA) (250-800kDa) medium molecular weight, Chondroitin Sulfate sodium salt USP Bovine, Heparin sodium salt is purchased from Bioiberica s.a. and used without further purifications. Poly Styrene Sulfonate sodium salt MW70000 30%wt used to prepare PEDOT:PSS for kinetic measure was supplied by Sigma. Clevios P® (PEDOT:PSS) was supplied by Heraeus. All other chemicals were supplied from Sigma-Aldrich. Round-shaped coverslips were supplied by OPPAC S.A. in two different sizes 1.3cm and 2.5cm of diameter. To produce thin films, a KLM SCC spin coater was used for 10s at 200rpm and for 40s at 3000rpm. The measurements of conductivity were performed on a Four Point Probe Veeco/Miller FPP5000 using layer resistivity function, sampling more than three different zones of the film more than three times and doing the reciprocal. The kinetic studies were performed in a Hewlett-Packard HPLC series 1100 apparatus using a Lichrosphere 100 CN (5µm) column in static conditions, water:ACN 1:1 1mL/min at room temperature (r.t.). The solubility tests were performed using a solution of Phosphate Buffer Solution (PBS) 0.01M (1x). The UV-Vis-NIR measures were obtained using a Perkin Elmer Lambda 950 between 200nm and 1350nm. Particle size was measured with dynamic light scattering (DLS) Malvern Zetasizer Nano ZS90 at 20ºC. The thickness of the films was measured with a micrometer screw gauge. The TEM images were performed on a TECNAI G2 20 TWIN at 75kV. For all the biological assays suspensions PEDOT:GAGs 50:50 2%wt has been used and as, PEDOT:PSS, Clevios P®.

1.4.2 Synthesis of PEDOT:GAGs and PEDOT:PSS dispersions, general procedure

In a 250mL reactor filled with 100mL of deionized (DI) water, 1g of GAG, or PSS solution, is placed and stirred at 600rpm for 30min at r.t. until a clear viscous

solution is formed. 1g EDOT is added and after 15min at r.t., then 1.5 eq. of $(NH_4)_2S_2O_8$ and a catalytic amount of $Fe_2(SO_4)_3$ were added. This lead to dispersions of 2% solid content. Each GAG dispersion was stirred until complete conversion, usually for 48h. Similarly, the dispersions of 10%wt were prepared starting from 5g of EDOT and 5g of GAG. Finally, dispersions containing different PEDOT:GAG ratios were obtained varying the initial amount of grams.

1.4.3 PEDOT:GAGs films creations

Glass coverslips used for the measurements were previously treated for 2h with piranha solution which was freshly prepared mixing one part of H_2O_2 and another part of H_2SO_4.

Normal drop-casting has been performed by filling the surface of the coverslips and drying them firstly at r.t. for one night and secondly in a vacuum oven at 55°C for 1h.

To form insoluble spin coated films suitable for biological analysis we used the following protocol: to a 5 mL of aqueous dispersion, 250µL of ethylene glycol, 1 drop of dodecylbenzenesulfonicacid (DBSA), and 100µL of 3-glycidoxypropyltrimethoxysilane (GOPS, as a cross-linker) were added.[10] Homogeneous films are formed and cured at 55ºC under vacuum for 1h.

Spin-coated films were made by pipetting in the center of the coverslip the material and spin coating them for 10s at 100rpm and 40s at 2000rpm. The films have been dried for 1h at 50°C in a vacuum oven. To check the solubility, the resulting coverslips after the drying step were put in a beaker with 20mL of PBS 0.01M changing this solution 3 times every 8h.

1.4.4 Kinetic study of PEDOT:GAGs dispersions

The kinetic studies were performed sampling the reactor at different times using a HPLC. Samples of 10µL of mixture were extracted from the reactor and put in

5mL of acetonitrile (ACN) containing 1 µL of benzyl alcohol as internal standard. 20 µL of supernatant were taken and injected directly into the HPLC. The retention times of benzyl alcohol and EDOT are 2.8min and 4.6min respectively. The areas were plotted in a calibration line to calculate concentrations.

1.4.5 DLS and UV-Vis-NIR measurements

A quartz made couvette was filled according with the instrument indications with a solution 1% v-v in water of the dispersion of each PEDOT:GAG and analyzed directly. For the UV-Vis-NIR all the spectra were normalized.

1.4.6 Cell culture

murine fibroblast cells L929 were maintained in high glucose Dulbecco's Modified Eagles Medium (DMEM; Sigma, Ref. D5796) supplemented with 10% Fetal Bovine Serum (FBS; Biochrom, Ref. A1020S0115) and 1% Penicillin-Streptomycin (Pen/Strep; Lonza, Ref. A3717-745E). Human neuroblastoma cells SH-SY5Y were maintained in Advanced D-MEM/F12 (Gibco, Ref:12634-010) supplemented with 10% FBS and 1% Pen/Strep. Human astrocytoma cells CCF-STTG1 were maintained in RPMI medium 1640 (Life technologies, Ref.A10491-01) supplemented with 10% FBS and 1% Pen/Strep. All cells were cultured in a humidified incubator at 37°C, 5% CO_2. In normal maintenance culture, passaging of cells was done when cells reached a confluency of 80-85%. In short, cells were rinsed with PBS 1x and treated for 5 min with trypsin-EDTA (0.05%; Invitrogen, Ref. 25300-054) at 37°C followed by centrifuging for 5min, 500g. Cell pellet was re-suspended in 1ml of culture medium and seeded in desired cell numbers.

1.4.7 Cytotoxicity assay

Cytotoxicity of PEDOT material was evaluated using an MTT assay (Roche, Cell proliferation kit I) according to ISO 10993-5 guidelines for tests on extracts and

use of L929 cells. MTT was performed according to manufacturer instructions and all cultures and incubation steps were performed in a humidified incubator at 37°C, 5% CO_2. In short, L929 cells were seeded 104 cells/well in a 96-well plate and after 24h MTT was added to cells representing t=0h. In test conditions, cell culture medium was refreshed with medium extracts. Medium extracts were produced by immersing appropriate surfaces (thickness < 0,5mm = 6cm2 , If thickness > 0,5mm = 3 cm2, If thickness > 1 mm = 1.25cm2) of PEDOT materials, negative control (high-density polyethylene, USP, Ref. 1546707) and positive control (positive bioreaction, USP, Ref. 1071439) in cell culture medium for 24h. Cells were cultured in medium extracts for 24h where after MTT was added. In experiments using SH-SY5Y cells, where H_2O_2 induced cells death was used, media were supplemented with 0.25mM H_2O_2 (Sigma-Aldrich, Ref. 31642). After 4h of incubation with MTT, cell proliferation kit I solubilization solution was added for 24h, to dissolve the purple formazan salt crystals. Thereafter, absorbance was measured at wavelength 550nm using a Multiskan Ascent (Thermo Scientific) plater reader. Results were compared by means of unpaired Student's t-test where $p<0.05$ was considered as significant.

1.4.8 Proliferation assay

Proliferation studies were performed using thin PEDOT films spin coated onto coverslips. SH-SY5Y or CCF-STTG1 cells were seeded directly on to the material substrates, which were put in a 24-well plate, with a density of 2x104 cells. As a control condition, cells were seeded on normal tissue culture plastic (24-well plate). After 24h medium was refreshed with normal cell culture medium or, for the t=0h time point, with medium containing MTT. After all time points, MTT assay was performed as described above. For plate reading, after solubilizing, solutions were transferred to a 96 well plate and read out was done at a wavelength of 550 nm. Results of individual time points were compared by means of unpaired Student's t-test where $p<0.05$ was considered as significant. For assessment of

proliferation rate, non-linear regression was performed and the slopes from curve fits were compared with $p<0.05$ considered as significant.

1.4.9 Intracellular calcium measurements

For measurement of intracellular Ca^{2+} levels cells were seeded on thin PEDOT films spin coated into coverslips with a density of 6x104 cells in 24-well plate. Culture medium was removed and adherent cells were briefly washed with external standard solution (ESS; 140mM NaCl, 2mM KCl, 2.5mM $CaCl_2$, 1mM MgCl2, 40mM Glucose, 5.5mM HEPES, pH7.3). Thereafter, cells were incubated with calcium dye Fluo-4-AM cell permeant (1µM; Invitrogen, Ref. F14201) diluted in ESS for 45min at 37°C and 5% CO_2. Cells were rinsed twice with ESS after Fluo-4 incubation. Intracellular calcium changes, directly after stimulation with high potassium solution (55mM KCl) for SH-SY5Y cells or ATP (50 µM) for CCF-STTG1 cells, were monitored using fluorescence microscopy. Every second an image was taken and for every condition, an intrinsic baseline was measured 10s prior to the stimulus. Results were analyzed by importing image sequences into ImageJ where cells could be analyzed individually by measuring pixel densities in regions of interest (ROIs). Fluorescence values were corrected for blank and normalized to own baseline measurements using the following formula: $\frac{\Delta F}{F} = \frac{Fmeasurement - Fblank}{Fo - Fblank}$. Percentage of response cells were compared by means of unpaired Student's t-test where $p<0.05$ was considered as significant. To assess for differences in response between cells cultured on different materials over time, 2-way ANOVA was performed.

1.4.10 SH-SY5Y differentiation and Immunocytochemistry

SH-SY5Y cells were seeded with a density of 6x104 cells on thin PEDOT films spin coated onto coverslips or laminin coated (10µg/ml; Sigma-Aldrich, Ref. L2020) coverslips which served as controls. To induce neuronal differentiation of SH-SY5Y cells, cell culture medium was refreshed with serum free Advanced D-MEM/F12 medium supplemented with 1µM synthetic retinoid ec23 (Amsbio, Ref.

SPR002), 24h after seeding and maintained in this medium for 3 days. Following ec23 treatment, medium was refreshed with serum free Advanced D-MEM/F12 medium supplemented with human brain derived neurotrophic factor (BDNF; Sigma-Aldrich, Ref. B3795). For immunocytochemistry, cells were rinsed with PBS 1x and fixed in 4% formaldehyde in PBS 1x (0.1% Triton X-100) for 1min at 4°C. Thereafter, cells were rinsed twice with PBS 1x for 10min at r.t. followed by 1h blocking in 1% BSA in PBS 1x. Cells were incubated with Anti-neurofilament 200 primary antibody (1:500) produced in rabbit (Sigma-Aldrich, Ref. N4142) for 1.5h at r.t. followed by rinsing 2 times with PBS 1x and incubation (1:500) with Alexa 568 Goat anti-Rb IgG (H+L; Invitrogen, Ref. A11011) for 1.5h at r.t. Incubation with secondary antibody was followed by washing with PBS 1x supplemented with Hoechst (1:1000) for nuclear staining and 2 times normal rinsing with PBS 1x for 5min. Coverslips were briefly rinsed in distilled water and mounted onto glass slides with Permafluor (Thermo scientific, Ref. TA-006-FM) for fluorescence imaging. Neurite length analysis was performed using ImageJ software with simple neurite tracer plugin. Results were compared by means of unpaired Student's t-test where $p<0.05$ was considered as significant.

1.5 References

(1) Povlich, L. K.; Feldman, K. E.; Shim, B. S.; Martin, D. C. In *Comprehensive Biomaterials*; Ducheyne, P., Ed.; Elsevier: Oxford, 2011; pp 547–561.

(2) Rivnay, J.; Owens, R. M.; Malliaras, G. G. *Chem. Mater.* **2014**, *26* (1), 679.

(3) Elschner, A.; Kirchmeyer, S.; Lövenich, W.; Merker, U.; Reuter, K.; Lovenich, W.; Merker, U.; Reuter, K. *PEDOT*, 1st ed.; CRC Press: Boca Raton FL USA, 2011.

(4) Jimison, Leslie H.Khodagholy, D.; Doublet, T.; Bernard, C.; Malliaras, G. G.; Owens, R. M. *Applications of Conducting Polymer Devices in Life Sciences*; 2013; Vol. 8.

(5) Abidian, M. R.; Martin, D. C. *Adv. Funct. Mater.* **2009**, *19* (4), 573.

(6) Abidian, M. R.; Ludwig, K. A.; Marzullo, T. C.; Martin, D. C.; Kipke, D. R. *Adv. Mater.* **2009**, *21* (37), 3764.

(7) Kim, D.-H.; Richardson-Burns, S. M.; Hendricks, J. L.; Sequera, C.; Martin, D. C. *Adv. Funct. Mater.* **2007**, *17* (1), 79.

(8) Sasaki, M.; Karikkineth, B. C.; Nagamine, K.; Kaji, H.; Torimitsu, K.; Nishizawa, M. *Adv. Healthc. Mater.* **2014**, *3* (11), 1919.

(9) Seyedin, M. Z.; Razal, J. M.; Innis, P. C.; Wallace, G. G. *Adv. Funct. Mater.* **2014**, *24* (20), 2957.

(10) Khodagholy, D.; Doublet, T.; Gurfinkel, M.; Quilichini, P.; Ismailova, E.; Leleux, P.; Herve, T.; Sanaur, S.; Bernard, C.; Malliaras, G. G. *Adv. Mater.* **2011**, *23* (36), H268.

(11) Asplund, M.; Thaning, E.; Lundberg, J.; Sandberg-Nordqvist, A. C.; Kostyszyn, B.; Inganäs, O.; von Holst, H. *Biomed. Mater.* **2009**, *4* (4), 45009.

(12) Isaksson, J.; Kjäll, P.; Nilsson, D.; Robinson, N. D.; Berggren, M.; Richter-Dahlfors, A. *Nat. Mater.* **2007**, *6* (9), 673.

(13) Khodagholy, D.; Doublet, T.; Quilichini, P.; Gurfinkel, M.; Leleux, P.; Ghestem, A.; Ismailova, E.; Hervé, T.; Sanaur, S.; Bernard, C.; Malliaras, G. G. *Nat. Commun.* **2013**, *4*, 1575.

(14) Fattahi, P.; Yang, G.; Kim, G.; Abidian, M. R. *Adv. Mater.* **2014**, *26* (12), 1846.

(15) Serra Moreno, J.; Panero, S.; Materazzi, S.; Martinelli, A.; Sabbieti, M. G.; Agas, D.; Materazzi, G. *J. Biomed. Mater. Res. Part A* **2009**, *88A* (3), 832.

(16) Collier, J. H.; Camp, J. P.; Hudson, T. W.; Schmidt, C. E. *J. Biomed. Mater. Res.* **2000**, *50* (4), 574.

(17) Pérez-Madrigal, M. M.; del Valle, L. J.; Armelin, E.; Michaux, C.; Roussel, G.; Perpète, E. A.; Alemán, C. *ACS Appl. Mater. Interfaces* **2015**, *7* (3), 1632.

(18) Molino, P. J.; Tibbens, A.; Kapsa, R. M. I.; Wallace, G. G. *MRS Proc.* **2013**, *1569*, mrss13.

(19) Molino, P. J.; Yue, Z.; Zhang, B.; Tibbens, A.; Liu, X.; Kapsa, R. M. I.; Higgins, M. J.; Wallace, G. G. *Adv. Mater. Interfaces* **2014**, *1* (3), n/a.

(20) Pérez-Madrigal, M. M.; Estrany, F.; Armelin, E.; Díaz, D. D.; Alemán, C. *J. Mater. Chem. A* **2016**, *4* (5), 1792.
(21) Thaning, E. M.; Asplund, M. L. M.; Nyberg, T. A.; Inganäs, O. W.; von Holst, H. *J. Biomed. Mater. Res. Part B Appl. Biomater.* **2010**, *93B* (2), 407.
(22) Moulton, S. E.; Higgins, M. J.; Kapsa, R. M. I.; Wallace, G. G. *Adv. Funct. Mater.* **2012**, *22* (10), 2003.
(23) Ocampo, C.; Oliver, R.; Armelin, E.; Alemán, C.; Estrany, F. *J. Polym. Res.* **2005**, *13* (3), 193.
(24) Harman, D. G.; Gorkin, R.; Stevens, L.; Thompson, B.; Wagner, K.; Weng, B.; Chung, J. H. Y.; in het Panhuis, M.; Wallace, G. G. *Acta Biomater.* **2015**, *14*, 33.
(25) Özgenel, G. Y. *Microsurgery* **2003**, *23* (6), 575.
(26) Joung, Y. K.; Bae, J. W.; Park, K. D. *Expert Opin. Drug Deliv.* **2008**, *5* (11), 1173.
(27) Wood, M. D.; Hunter, D.; Mackinnon, S. E.; Sakiyama-Elbert, S. E. *J. Biomater. Sci. Polym. Ed.* **2010**, *21* (6), 771.
(28) Canas, N.; Valero, T.; Villarroya, M.; Montell, E.; Verges, J.; Garcia, A. G.; Lopez, M. G. *J. Pharmacol. Exp. Ther.* **2007**, *323* (3), 946.
(29) Cheung, Y. T.; Lau, W. K. W.; Yu, M. S.; Lai, C. S. W.; Yeung, S. C.; So, K. F.; Chang, R. C. C. *Neurotoxicology* **2009**, *30* (1), 127.
(30) Kovalevich, J.; Langford, D. In *Neuronal Cell Culture: Methods and Protocols*; Amini, S., White, M. K., Eds.; Methods in Molecular Biology; Humana Press, 2013; Vol. 1078, pp 9–21.
(31) Holden, L. J.; Coleman, M. D. *Toxicology* **2007**, *241* (1–2), 75.
(32) Holden, L. J.; Coleman, M. D. *Environ. Toxicol. Pharmacol.* **2008**, *26* (3), 290.
(33) Mantione, D.; del Agua, I.; Schaafsma, W.; Diez-Garcia, J.; Castro, B.; Sardon, H.; Mecerreyes, D. *Macromol. Biosci.* **2016**, *16* (8), 1227.
(34) Lakowicz, J. R. *Principles of Fluorescence Spectroscopy Principles of Fluorescence Spectroscopy*; 2006.
(35) *Polymer Reaction Engineering*; Wiley-Blackwell, Ed.
(36) Hayashi, S. *Polym. Plast. Technol. Eng.* **1988**, *27* (1), 61.
(37) Takano, T.; Masunaga, H.; Fujiwara, A.; Okuzaki, H.; Sasaki, T. *Macromolecules* **2012**, *45* (9), 3859.
(38) Lang, U.; Müller, E.; Naujoks, N.; Dual, J. *Adv. Funct. Mater.* **2009**, *19* (8), 1215.
(39) Xia, Y.; Ouyang, J. *ACS Appl. Mater. Interfaces* **2012**, *4* (8), 4131.
(40) Cruz-Cruz, I.; Reyes-Reyes, M.; Aguilar-Frutis, M. a.; Rodriguez, a. G.; López-Sandoval, R. *Synth. Met.* **2010**, *160*, 1501.
(41) Cruz-Cruz, I.; Reyes-Reyes, M.; López-Sandoval, R. *Thin Solid Films* **2013**, *531*, 385.
(42) Huang, Y.; Li, Y.; Chen, J.; Zhou, H.; Tan, S. *Front. Hum. Neurosci.* **2015**, *9*, 586.
(43) Tsintou, M.; Dalamagkas, K.; Seifalian, A. M. *Neural Regen. Res.* **2015**, *10* (5), 726.
(44) Clarke, L. E.; Barres, B. a. *Nat. Rev. Neurosci.* **2013**, *14* (5), 311.
(45) Kimelberg, H. K.; Nedergaard, M. *Neurotherapeutics* **2010**, *7* (4), 338.

(46) Pekny, M.; Pekna, M. *Physiol. Rev.* **2014**, *94* (4), 1077.
(47) Sofroniew, M. V. *Nat Rev Neurosci* **2015**, *16* (5), 249.
(48) Mosmann, T. *J. Immunol. Methods* **1983**, *65* (1–2), 55.
(49) Clapham, D. E. *Cell* **2007**, *131* (6), 1047.
(50) Khakh, B. S.; McCarthy, K. D. *Cold Spring Harb. Perspect. Biol.* **2015**, *7* (4), a020404.
(51) Grienberger, C.; Konnerth, A. *Neuron*. 2012, pp 862–885.
(52) Cornell-Bell, A.; Finkbeiner, S.; Cooper, M.; Smith, S. *Science (80-.).* **1990**, *247* (4941), 470.
(53) Guthrie, P. B.; Knappenberger, J.; Segal, M.; Bennett, M. V; Charles, a C.; Kater, S. B. *J. Neurosci.* **1999**, *19* (2), 520.
(54) Kim, Y.; Seo, M.; Lee, Y. Il; Kim, S. Y.; Cho, E. A.; Kim, S. H.; Ahn, Y. M.; Kang, U. G.; Kim, Y. S.; Juhnn, Y. S. *Psychiatry Investig.* **2008**, *5* (2), 94.
(55) Thompson, B. C.; Murray, E.; Wallace, G. G. *Adv. Mater.* **2015**, *27* (46), 7563.
(56) Dwane, S.; Durack, E.; Kiely, P. A. *BMC Res. Notes* **2013**, *6*, 366.
(57) Lesma, E.; Di Giulio, A. M.; Ferro, L.; Prino, G.; Gorio, A. *J. Neurosci. Res.* **1996**, *46* (5), 565.
(58) Ohtake, Y.; Li, S. *Brain Res.* **2015**, *1619*, 22.

Chapter 2. Low temperature cross-linking of PEDOT:PSS films using divinylsulfone

2.1 Introduction

Bioelectronics nowadays is a fast growing field driven by many new discoveries by an everyday more dedicated scientific community.[1,2] Prominent topics are the creation and design of implantable electronic medical devices (IEMDs) that require long-term stability, such as cochlear implants, retinal prostheses, microfabricated cortical electrodes, cutaneous electrodes and more. In literature, polythiophenes and in particular PEDOT, acronym for poly(3,4-ethylenedioxythiophene), is considered to be the main protagonist in these applications. PEDOT is mainly doped with an anionic polymer poly(styrene sulfonate) (PSS) and it is commercially available on the market as a blue dispersion in liter scale, bearing the name Clevios®. The conductivity of the pristine film that could result from spin-coating of Clevios, ranges between 0.1 to 1 S cm-1. In order to be processable and create films for application in most organic electronic devices, it is necessary to elevate this value. Many studies have been carried out within this race, leading to conductivity values up to 3,000 S cm-1.[3]

Biocompatibility is another key point in designing new bioelectronics devices.[4] Many studies are presented in literature demonstrating that films of PEDOT:PSS are stable and compatible *in vivo* and *in vitro*.[5–8] Even though many of these strategies present a stable material in contact with a living tissue, in a long term point of view, cross-linking is needed to prevent delamination and eventual re-dispersion of the conducting film, especially on glass substrate.[9,10] In order to achieve this, numerous methods were used such as UV light or polyethylene oxide treatment.[11–13] Among them, one of the most studied is the use of silanes,[14,15] and in particular glycidoxy propyltrimethoxysilane (GOPS).[7,16–20] In spite of the excellent ability to cross-link PEDOT:PSS film, GOPS presented some important drawbacks such as its high curing temperature (140 ºC for 1 h) and a negative effect onto the conductivity values. Due to the natural insulating properties of the siloxane network, this cross-linker is normally used together with doping agents such as ethylene glycol or DMSO, to reduce the loss of conductivity generated by GOPS.[21] Its main inconvenience is the high temperature curing needed (>100 ºC) which avoids to apply the process in the presence of any biological content. In our search for a better candidate to cross-link PEDOT:PSS, we explored the possibility to use divinylsulfone (DVS), which is a broadly studied cross-linker for biomolecules. DVS is a reactive molecule against nucleophiles, with two active sites, in correspondence of the outer carbons in the double bond.[22] It has been fruitfully applied many times to cross-link biomolecules such as glycosaminoglycanes (GAGs), hyaluronic acid for example, and has already been implemented in many products for in vivo applications.[23] The advantages of DVS are the high reactivity, the possibility to work in an aqueous environment and the low boiling point that facilitate the elimination of excess.

Conducting polymer based devices are commonly used in the field of bioelectronics for electrophysiology and *in vivo* and *in vitro* biosensing applications. One promising candidate emerging from this field is the organic electrochemical transistor (OECT) as a transducer of biological events with local amplification such as the movement of biomolecules, electroencephalography

activity, probe cell adhesion and more.[24–26] In OECTs, the conducting polymer film, deposited between source and drain contacts is placed in direct contact with an electrolyte. Upon application of a bias at an external gate, that is immersed in the electrolyte, ions are injected in the bulk of the polymer. This, subsequently, alters the hole density of the film, thus the current flowing between source and drain electrodes. Therefore, OECTs are effective ion-electron transducers which is governed by the channel materials ability to conduct holes as well as ions. This phenomenon can be analysed using transconductance as a figure of merit, which determines the conversion between gate voltage (VG) and drain current (ID). A small increase in transconductance means a much higher recording capacity of small biological signals. How reliable and stable an OECT is, is determined by the stability of this parameter, which becomes especially relevant in the case of long-term *in vivo* recordings.[17]

In this chapter, we applied DVS as an alternative cross-linker of PEDOT:PSS to enhance the stability for long term applications and allow the resultant thin films of the suspension to be cured at ambient temperature.[27] The suspension of cross-linked material was characterized chemically: through NIR-UV-Vis, Raman and FT-IR. For physical assessment of cross-linked films, measuring conductivity showed that DVS cross-linked PEDOT:PSS showed an enhanced conductivity by two-fold compared to GOPS cross-linked PEDOT:PSS. Although biocompatibility of PEDOT:PSS has been widely described in literature,[28] we confirmed biocompatibility of DVS cross-linked PEDOT:PSS by cytotoxicity testing according to ISO 10993-5 guidelines and additional biocompatibility tests were performed using the neuroblastoma cell line SH-SY5Y. We further tested the PEDOT:PSS:DVS formulation in Organic Electrochemical Transistor (OECT configuration) by employing thin films of PEDOT:PSS:DVS as the channel material. We investigated the transconductance as a function of time for subsequent comparison of performance and stability of it to traditional PEDOT:PSS channels.

2.2 Results and Discussion

2.2.1 Cross-linking mechanisms of PEDOT:PSS:DVS

The chemical structure of DVS is shown in **Figure 2.1** (in red on the left side). Different amounts (1-40 by %v/v) were added to a commercial PEDOT:PSS solution (Clevios PH1000) and films were prepared by casting or spin-coating. After curing at room temperature for 14 h, the films were cross-linked. Raising the temperature to 50 °C speeds up the cross-linking process to only 1 h. In order to proof the cross-linking, the films were immersed in water or PBS. As it can be seen in the pictures of **Figure 2.2**, a not cross-linked film is going to delaminate in less than a minute while the films crosslinked using DVS are stable and do not disperse or delaminate.[10] In order to investigate in detail the chemical nature of the relevant cross-linking mechanism, we first looked at the dispersions. The easy preparation of dispersions for characterization consisted only in mixing the desired amount of DVS with the commercial aqueous suspension of PEDOT:PSS. The solution was sonicated to homogenize the suspension and left overnight in a closed vial, to avoid the evaporation of DVS. UV-Vis-NIR spectra (**Figure 2.3b**) show only one strong band between 800 nm and 1100 nm arising from the polarons present in the PEDOT chains.[29]

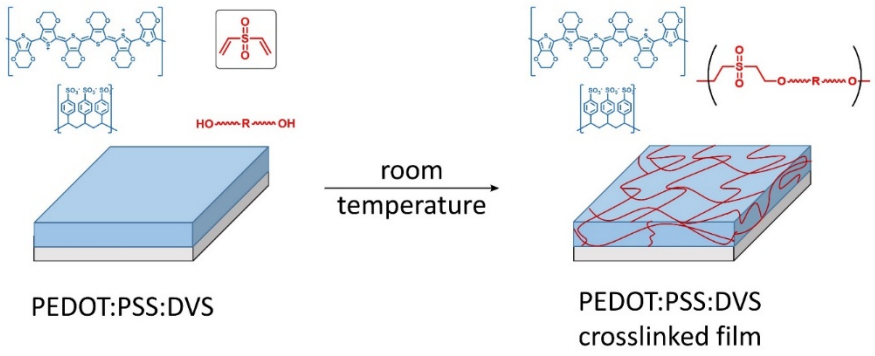

Figure 2.1 Schematic representation of cross-linking reaction of PEDOT:PSS film by DVS.

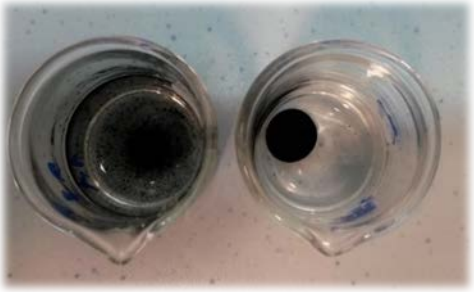

Figure 2.2 Not cross-linked (left) and cross-linked (right) PEDOT:PSS:DVS films.

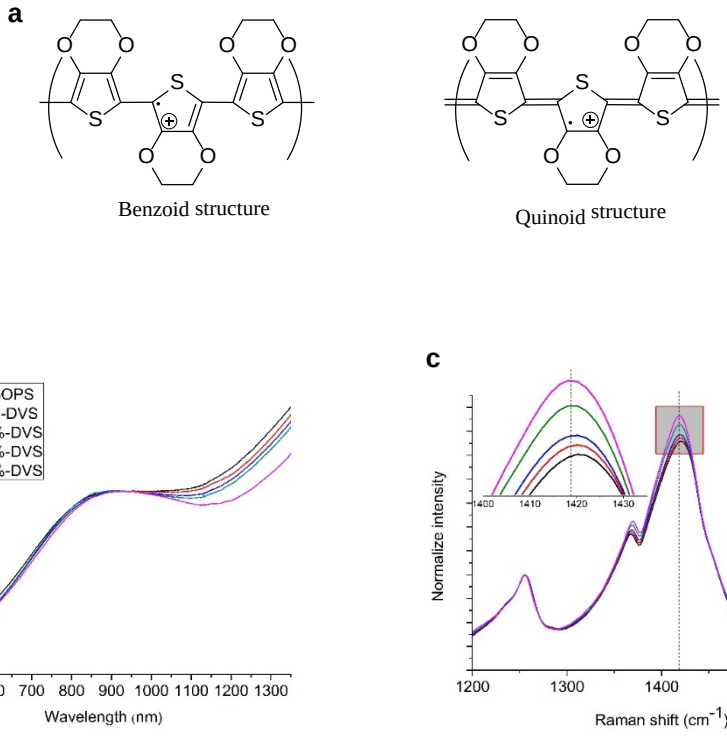

Figure 2.3 a) Resonance structure of PEDOT chain in “benzoid” and “quinoid” form, b) UV-Vis-NIR, c) Raman spectrum of PEDOT:PSS:DVS at different concentration of DVS.

With increasing amount of DVS, a decrease in the intensity at higher wavelengths can be seen. As reported by Massonet and coworkers in 2014, this reduce can be interpret as a decrease in the quantity of bipolarons and increasing of the radical species of the conjugated thiophene backbone.[30]

This confirms that the material is highly doped and the addition of DVS does not deplete it. Also in the Raman spectroscopy, as is shown in **Figure 2.3c**, the addition of DVS does not change drastically the aspect of the spectra as we can see from the comparison between the black line and the others. Analyzing the spectra, we can notice how the bands at 1433 cm^{-1} and 1260 cm^{-1} corresponding to symmetrical Cα-Cα' inter-ring stretching vibrations, remain unchanged.[31–33] The highest band located at 1420 cm^{-1} and the one at 1522 cm^{-1} remain, also, barely unchanged by size but, analyzing closely, are red-shifted. These two bands correspond to symmetrical and unsymmetrical stretching vibrations of the Cα=Cβ. The red shift is indicating that the structure of the carbon backbone is turning more into the quinoid form as is shown in **Figure 2.3a**.[34,35] Another confirmation of this phenomena is the blue shift of the band at 1360 cm^{-1}. This band corresponds to the stretching deformations of aromatic Cβ=Cβ: in this case our structure, tending to the quinoid structure, is losing aromaticity and bond order is decreasing.[36] The small increase in both bands is possibly due to the formation of hydroxide anions, as pointed out in the work of Cruz-Cruz et al.[37] In fact, adding DBU (1,5-diazabiciclo(5.4.0)undec-5-ene) they noticed the formation of hydroxide anions that quench the polarons, increasing the intensity of the Raman shifts. This is due to strong resonant effects of the neutral form of thiophene.

The same results can be observed from the FT-IR (**Figure 2.4**) spectra, conducted on dry films. As affirmed in literature a growth of the bands between 1600 and 100 cm^{-1} is corresponding of a more doped material, affordable with solvent treatment as shown by Nguyen et al.[38,39] To confirm the presence of the sulfone moiety, bands at 1360 and 1152 cm^{-1} are strong evidence, but unluckily only in the last spectrum, when the concentration of DVS is 20%, those bands overtake the rest and become visible.

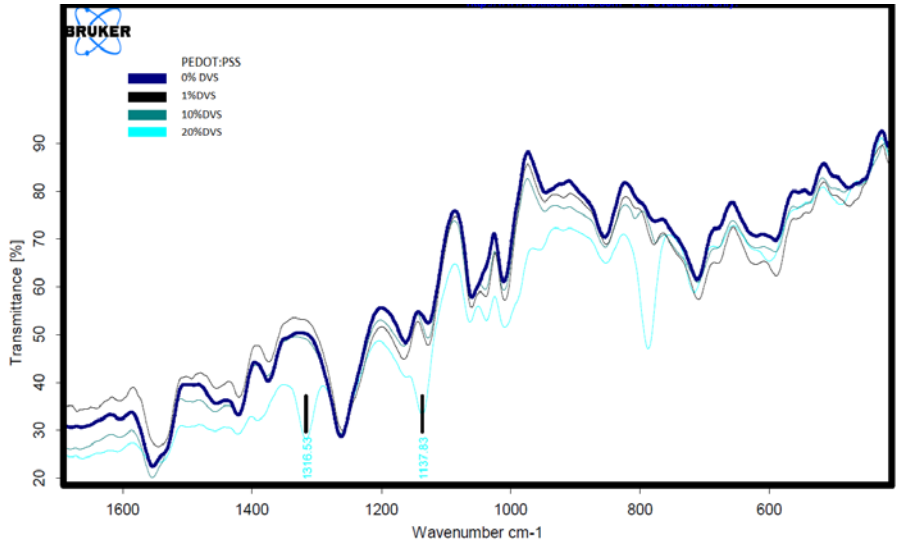

Figure 2.4 FT-IR spectra of PEDOT:PSS with different percentage of Divinylsulfone.

2.2.2 Film formation electrical properties and conductivity measurements of PEDOT:PSS:DVS films

Next we investigated the formation of PEDOT:PSS:DVS films obtained by curing the dispersions at 50 ºC for 1h. Unfortunately, comparison of the FT-IR and NMR spectra between the DVS-treated and non-treated films did not show any clear difference. In order to explain the cross-linking nature we synthesized a model suspension of PEDOT:PSS, respecting the same ratio and solid content declared by the producer, using different oxidant agents in order to demonstrate the uninfluential of it. At this purpose, we used 3 equivalents of $Na_2S_2O_8$, $(NH_4)_2S_2O_8$, $FeCl_3$ and $Fe(Tos)_3$, with a catalytic amount of Iron (III) (except in the case of Iron-based oxidants). With this model suspensions, we were not able to obtain an insoluble film after curing with DVS, but when we add ethylene glycol (20%), the result is a cross-linked film, this is because DVS reacts very fast with nucleophiles such as alcohols, thiols and amines.[22] It is known that Clevios PH1000 is a product of a spread range of suspensions, which the complete and detailed composition is unknown but includes stabilizers, viscosity additives, dopant improvers and conductivity enhancers such as ethylene glycol.[40,41] The model

reaction between DVS and ethylene glycol has been tested and followed by ^{1}H-NMR, leaving DVS and ethylene glycol in water at the same pH of the suspension of PEDOT:PSS (pH~2) (**Figure 2.5**).

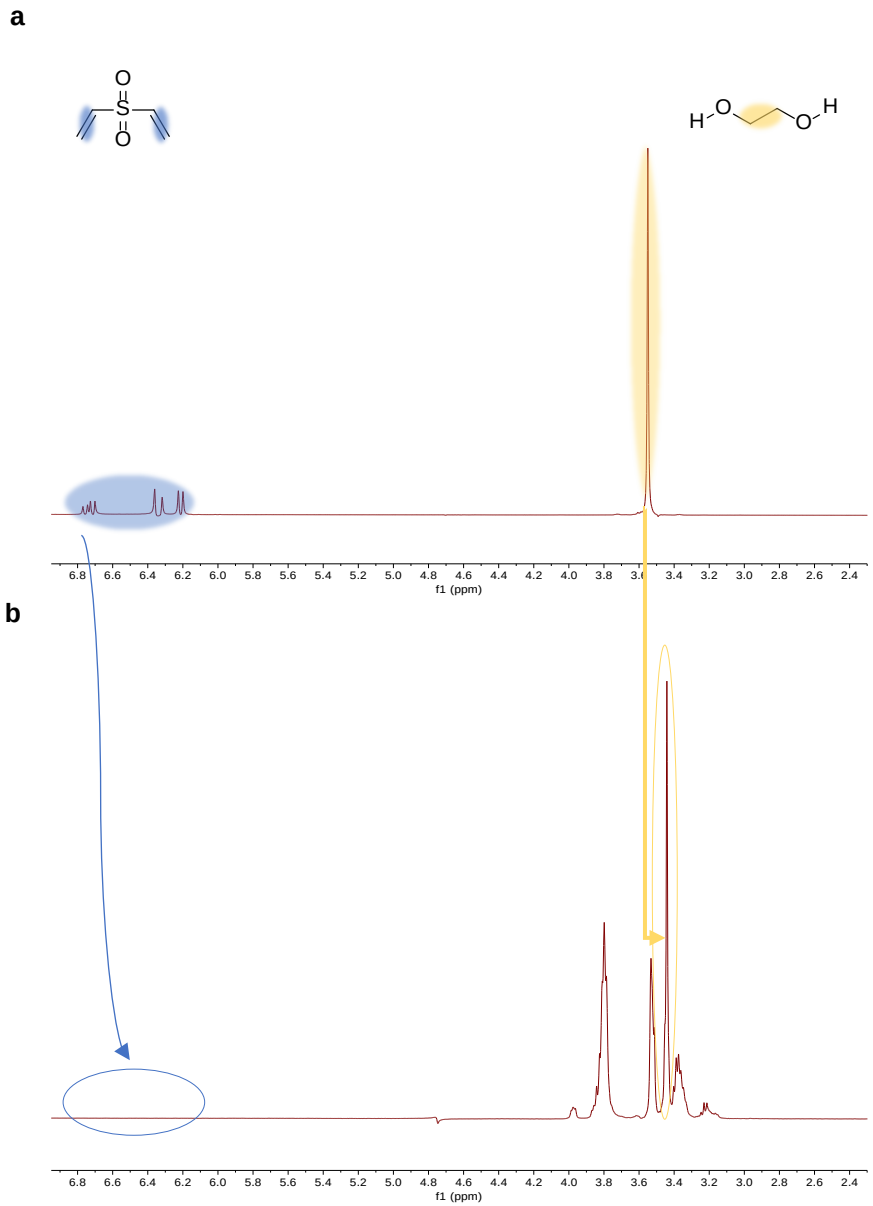

Figure 2.5 1H-NMR WATERGATE spectra of: a) Divinylsulfone and b) Ehtylene glycol-Divinylsulfone mixture

The analysis confirms the reaction between DVS and the diol, shielding the singlet of the methylenes of the diol and quitting the signals at high frequency of the vinyl moiety. All-in-all we can conclude that the chemical nature of the cross-linking its by reacting with some existing nucleophiles (alcohols and amines) in the PEDOT:PSS formulation. In the **Scheme 2.1** we can observe in detail the reaction occurring in this case.

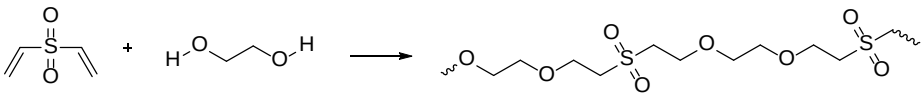

Scheme 2.1 Chemical structure of the sample reaction between ethylene glycol and divinylsulfone

Next we investigated the effect of the DVS cross-linking into the conductivity of the PEDOT:PSS films. To measure film conductivity, the Four Point Probe (4PP) method was used.[42,43] For this study, the conductivity of several PEDOT:PSS:DVS formulations were measured and compared with reported values for the widely applied PEDOT:PSS:GOPS cross-linked films (**Figure 2.6b**). PEDOT films cross-linked with DVS present conductivity in between 550-750 S cm^{-1} which are 200-300 S cm^{-1} higher than GOPS, at any given cross-linker concentration. Measurement fluctuations are explained due to the soft nature of PEDOT films (**Figure 2.6a**), which difficult the precision of the measurements obtained by the 4PP technique, phenomena already observed in a previous study.[42] Interestingly, the conductivity values stay constant with the DVS content whereas in the case of GOPS a fast decrease in conductivity is observed when the DVS concentration increases above 1%. With these results, we can conclude that DVS is a more appropriate PEDOT cross-linker than GOPS, as it does not reduce PEDOT film conductivity. In fact, the low boiling point of DVS, 25 °C/2mmHg, and the high reactivity of the divinyl scaffold make it react totally and the excess being eliminated during the baking treatment at 50 °C under vacuum; is good to point out that as DVS is high volatile, the use of vacuum could be

avoided if the baking process is done at higher temperature as normally used in OECT preparations (above 140 ºC). On the other hand, this is not occurring when GOPS is used as cross-linker because it has a higher boiling point (120 °C/2mmHg) and siloxanes are lower reactive groups. Moreover, it has been reported that adding solvents such as DMSO or additives such as ethylene glycol or ionic liquids inside the formulation improves the electrical conductivity. In our case, DVS acts as a conductivity enhancer additive and the cross-linked films show very high conductivity values.[21,44,45]

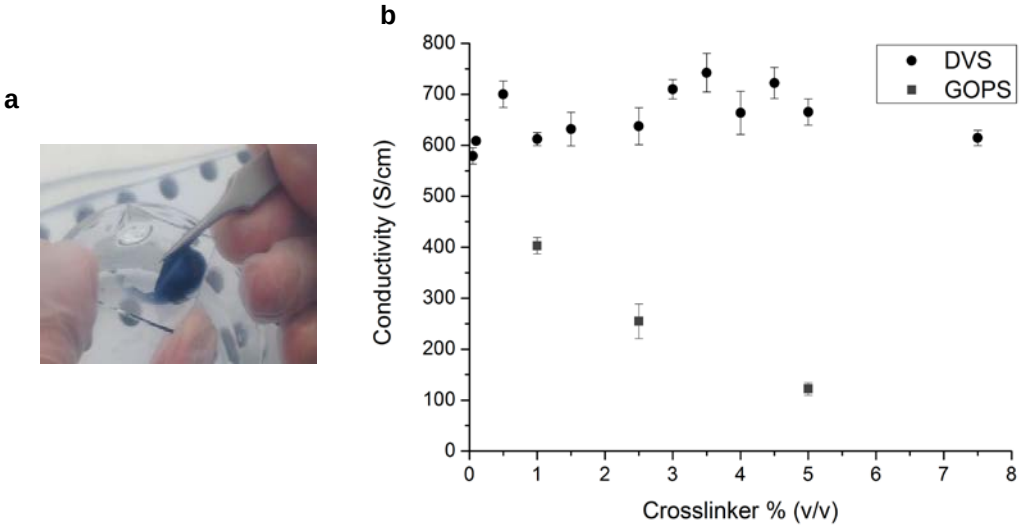

Figure 2.6 a) Lifting and manipulation of PEDOT:PSS:DVS from a glass substrate. b) Conductivity measurements of films prepared with solution containing different amount of DVS or GOPS cross-linker.

2.2.3 OECT transduction measurements

We further tested ion and hole transport capabilities of the PEDOT:PSS:DVS in an OECT configuration (**Figure 2.7a**).[24] Among all measurable parameters in these devices, transconductance is the most important parameter as it indicates its amplification capacity,[26] in other words, it quantifies its efficiency of signal transduction. Transconductance is defined as $g_m=\Delta I_D/\Delta V_G$, where I_D is the drain current and V_G is the gate voltage. In most of OECTs present in literature, the channel is formed by the conducting polymer PEDOT:PSS,[46–48] which is

previously treated with cross-linkers to avoid its dissolution.[49,50] In this study we measure transconductance of an OECT which channel is formed by a thin film of PEDOT:PSS:DVS, the design of the device is visible in **Figure 2.7b**. PEDOT formulation with 3% v/v DVS was chosen for the device fabrication because it ensures stable films with high conductivity. To the latter one, 0.2% of GOPS was included in the formulation to provide attachment to the substrate as DVS only provides fixation but not attachment. Conductivity suffered almost no decrease with GOPS addition at this concentration (623±19 S cm^{-1}, n=4). In graph (**Figure 2.7d**), transconductance along time is measured for a channel geometry of 10*100 µm and 100 nm thickness (**Figure 2.7c**). Measurements were taken after OECT conditioning to avoid data fluctuations due to an initial PEDOT layer degradation. The OECT was kept in sterile phosphate buffered saline solution in between measurements and after rinsing with MilliQ water, drops of NaCl 0.1M solution were deposited on the channel for measurements. As it is visible in the graph, at day 10, transconductance has a value of 13.2±0.65 mS (n=4) which is an outstanding value when compared to studies employing PEDOT:PSS:GOPS channels. For channel sizes of 10*100 µm and 400 nm thickness, values of 2-3 mS were obtained.[26] Moreover PEDOT:PSS:DVS channels seem to stable in the long term, showing 6% and 20% decay in transconductance after 20 and 64 days, respectively.

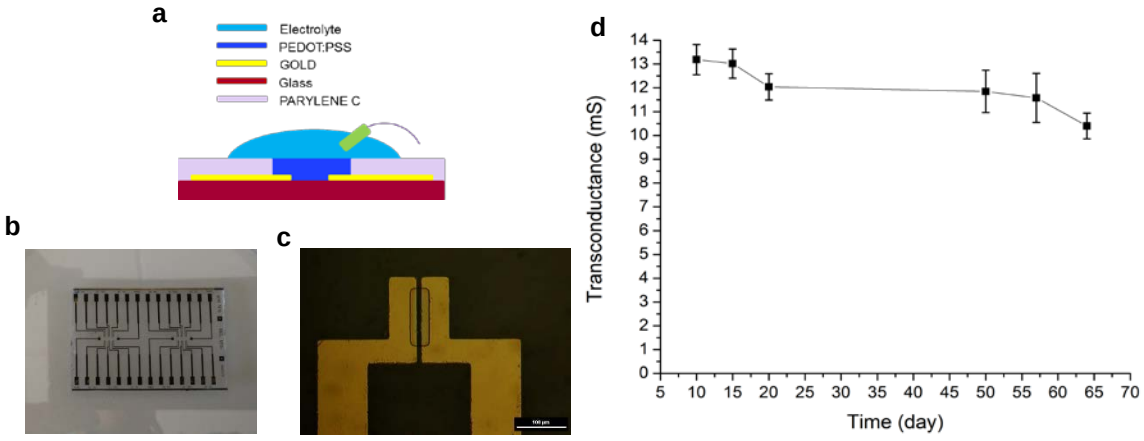

Figure 2.7 a) OECTs design b) OECT device c) OECT PEDOT:PSS:DVS channel 100µm*10 µm d) Transconductance evolution with time for channel formulation PEDOT:PSS:DVS with channel size 100µm*10 µm.

PEDOT:PSS:DVS channel shows outstanding transconductance values and good stability in a wide range of frequency and over time (**Figure 2.8**). This means, in respect with GOPS that also shown good stability over time, a big amplification capacity of the OECT when PEDOT:PSS is cross-linked by DVS than by other cross-linkers, as is visible either in the high value on the y axis in **Figure 2.8a** or in the constant oscillations of **Figure 2.8b**.[10,25,51] This difference in transconductance is determined by ion transport through the channel which depends on its structure and swelling degree.[52] Implying that PEDOT:PSS:DVS film absorbs more water, and induces greater phase segregation and structural modification in between PEDOT and PSS chains.

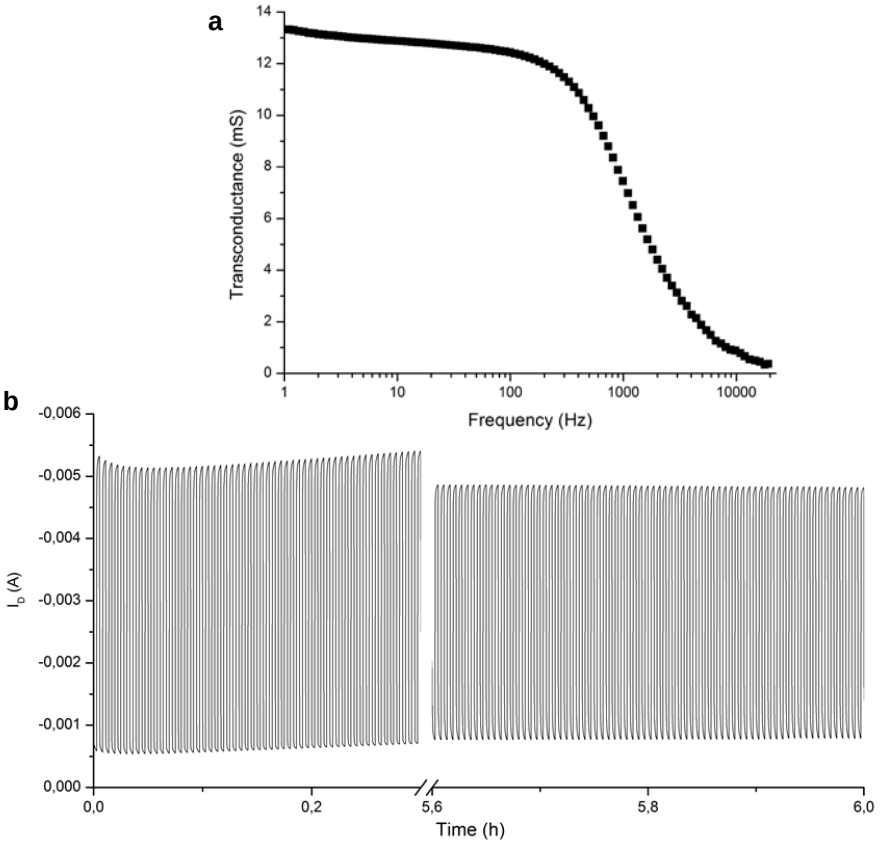

Figure 2.8 a) Frequency-dependent transconductance of PEDOT:PSS:DVS OECT after conditioning (Gate voltage offset VG=0.3V, channel dimensions L=10 µm, W=100 µm). b) 6 h operation cycle test. A gate voltage pulse (V_G=0.5 V) was applied for 10 s with an interval time of 10 s between the successive pulses (Drain Voltage, V_D=-0.5 V).

2.2.4 Biocompatibility of PEDOT:PSS:DVS films

In order to assess the biocompatibility of PEDOT:PSS:DVS, cytotoxicity of PEDOT:PSS:GOPS was compared to PEDOT:PSS cross-linked with DVS and all samples were compared to an inert (high density polyethylene) and positive control (Polyvinyl chloride). Cytotoxicity testing was performed by MTT assay according to ISO 10993-5 guidelines using the murine L929 fibroblast cell line.

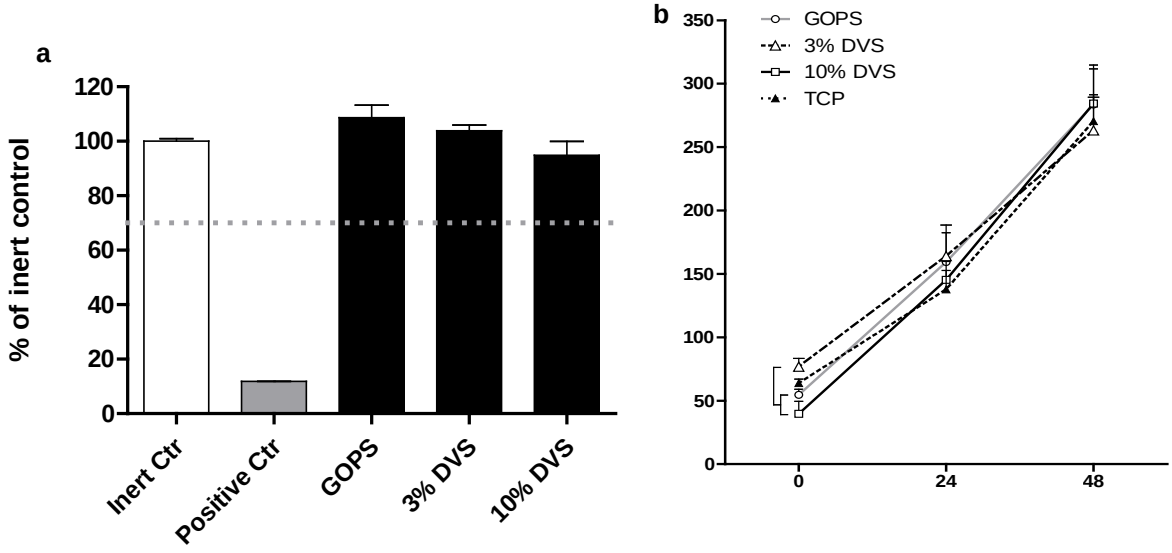

Figure 2.9 a) MTT cytotoxicity assay was performed according to ISO 10993-5 guidelines for extracts, using L929 cells and medium extracts of PEDOT cross-linked with 3% GOPS, 5% DVS or 10% DVS v/v. b) Proliferation assay of SH-SY5Y cells cultured on tissue culture plastic (TCP) or PEDOT cross-linked with GOPS, 5% DVS or 10% DVS during 48 h (t=0h represents 24 h after seeding). After live/dead assay, analysis was performed by counting live cells. Statistical analysis performed with unpaired student's t-

L929 cell culture medium was conditioned with PEDOT:PSS:GOPS and DVS cross-linked films, as well as with the inert and positive controls. L929 cells were cultured thereafter for 24 h in this conditioned medium and cytotoxicity was determined. As expected the positive control showed high cytotoxicity (~10% cell viability), all other samples showed comparable cell viability to the inert control around 100%, as shown in **Figure 2.9a**. These results show that the films do not release toxic degradation products during the 24h incubation period.

2.2.5 Proliferation of SH-SY5Y neuroblastoma cells on PEDOT:PSS:DVS films

Since a large part of IEMD's using PEDOT are destined to be used in the CNS environment, SH-SY5Y cells were chosen to serve as an *in vitro* neuronal model cell line to assess biocompatibility in such an environment. In addition to biocompatibility in the sense of cell survival, to be able to perform long-term recordings or stimulations of neural tissue, extensive research has been dedicated to create materials or coatings of electrodes that present conditions for optimal cellular attachment and thus minimalize the gap of tissue-electrode interface for optimal performance.[53,54] To assess the effect of PEDOT:PSS:DVS on these factors live/dead staining was performed on SH-SY5Y cells cultured on films prepared as described in previous sections in 24-well plates. After seeding, 24 h later live and dead cells were stained with Calcein-AM and EthD-1, respectively, and cells were manually counted using the ImageJ cell counter plugin. This procedure was repeated at timepoints 24 h and 48 h. At timepoint 0 h, PEDOT:PSS:DVS (3%) showed a significantly higher amount of live cells compared to PEDOT:PSS:GOPS and PEDOT:PSS:DVS (10%). This indicates, that of the samples analyzed here cross-linking with 3% DVS provides the best conditions for initial cellular attachment. Regarding proliferation, no significant differences between samples and tissue culture plastic control were found over the 48 h time course of the proliferation experiments (**Figure 2.9b**). These results show that PEDOT:PSS cross-linked with 3% and 10% DVS, support cellular attachment and proliferation, where 3% v/v would be preferred due to the initial difference in cellular attachment at 0 h.

2.2.6 Neurite length of differentiated SH-SY5Y cells on PEDOT:PSS substrates

When IEMD's are implanted in a CNS environment it is of importance that these biomaterials support and possibly stimulate neuronal regeneration. A general method used to assess whether or not a biomaterial supports neurobiocompatibility and neuroregeneration is the measurement of neurite

lengths of newly formed neurites in differentiated neuronal cell lines such as SH-SY5Y.[55] In experiments performed here, SH-SY5Y cells were differentiated by sequential treatments of 3 days with synthetic retinoid EC23 in serum free medium, followed by a 3-day treatment with Brain-derived neurotrophic factor (BDNF) in serum free medium. Neurite length of NF200 positive cells was measured using ImageJ simple neurite tracer plugin. Laminin was used as a positive control since it has been previously described to be an optimal surface substrate for SH-SY5Y neuronal differentiation.[56] SH-SY5Y cells differentiated on laminin showed extensive and long neurite formation (**Figure 2.10**). SH-SY5Y cells differentiated on PEDOT:PSS:GOPS and PEDOT:PSS:DVS (3%) both showed formation of new neurites, showing that both are biocompatible and do not inhibit neuroregeneration. However, both laminin and PEDOT:PSS:DVS (3%) showed significantly longer neurite length when compared to GOPS. This suggests, that PEDOT:PSS cross-linked with 3% DVS increases the support for neuroregeneration and thus improves this biomaterial.

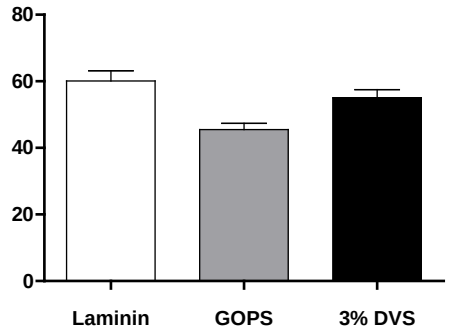

Figure 2.10. Neurite length analysis of differentiated SH-SY5Y cells cultured on PEDOT cross-linked with GOPS or 3% DVS. Statistical analysis performed with unpaired student's t-test with **&*** p<0,05.

2.3 Conclusions

In this chapter we have presented DVS as an outstanding PEDOT:PSS cross-linker. It not only provided great potential for device fabrication due to the higher conductivity and transconductance in respect to GOPS, but also a straightforward manner to create insoluble films at low temperature, making possible the incorporation of thermolabile and biological substances. The suspension has been characterized physico-chemically by UV-Vis-NIR, Raman and IR spectroscopy. Conductivity measurements conducted on the dried material confirm the high applicability, giving a result of more than the double, up to 600 S cm^{-1} (at 3% v/v) in respect to GOPS, and affirming that the addition of more cross-linker does not affect the conductivity. Biocompatibility assays were performed using L929 and SH-SY5Y cells, measuring cytotoxicity, proliferation and neurite length, showing full biocompatibility and better support for neuroregeneration when compared to GOPS cross-linked material. Furthermore, PEDOT:PSS:DVS (3%) showed a better initial cellular attachment of SH-SY5Y cells, which will be beneficial for a neural interface that has to be established. To show the applicability of PEDOT:PSS:DVS, the creation of an OECT and the measure of transconductance was tested. PEDOT:PSS:DVS channel values are high in the short and long term. This finding show its applicability in *in vivo* recording measurements. All in all in chapter 2 we demonstrated that DVS cross-linking agent provides an outstanding solution for the low temperature fabrication of cross-linked PEDOT-PSS films for bioelectronics or other organic electronic applications

2.4 Experimental Section

2.4.1 Materials and Method

PEDOT:PSS CleviosPH1000® was bought from Heraeus. Deuterated solvent and NMR tubes were bought from Deutero GmbH. 3-(Trimethoxysilyl)propyl methacrylate and soap micro-90 were supplied by Sigma Aldrich. All other chemicals were supplied from Fisher Scientific. Microscope glass slides with cut edges provided by VWR 76x26x1 mm. Round-shaped glass coverslips were supplied by OPPAC S.A. in two different sizes 1.3cm and 2.5cm of diameter. Fourier-transform Raman spectroscopy was perform on a Bruker RFS 100/S with YAG:Nd laser (1064 nm) 500 mW horizontally polarized (H) as excitation source, ROCKSOLID configuration permanently aligned as interferometer and a HeNe laser at 633 nm 1 mW as alignment excitation source. As detector Ge-diode, cooled at liquid nitrogen temperature (77 K). A 5mm mirror quartz cuvette was filled with a suspension of PEDOT:PSS:DVS diluted 1:50, running 150 scan per measure. The UV-Vis-NIR measures were obtained using a Perkin Elmer Lambda 950 between 200 nm and 1350 nm using quartz cuvette and preparing PEDOT:PSS:DVS suspension diluted 1:10. ^{1}H-NMR has been performed on a Bruker Avance 400MHz, using WATERGATE and D_2O. FT-IR spectra were recorded on a Bruker Alfa ATR.

2.4.2 PEDOT:PSS:GOPS suspension

To prepare 25 mL of aqueous dispersion: Ethylene glycol 5 mL, dodecyl benzene sulfonic acid (DBSA) 25 µL and 250 µL of (3-Glycidyloxypropyl) trimethoxysilane (GOPS) were mixed with 20 mL of PEDOT:PSS Clevios PH1000®.

2.4.3 PEDOT:PSS:DVS suspension for conductivity measurements

To prepare about 25 mL of aqueous dispersion: Ethylene glycol 1.25 mL, dodecyl benzene sulfonic acid (DBSA) 25 µL were mixed with 20 mL of PEDOT:PSS Clevios PH1000®, to this suspension different quantities of DVS were added. Once prepared, is preferable to use the dispersion right after or in the next hour.

2.4.4 PEDOT:PSS:DVS suspension for devices

The procedure is the same as PEDOT:PSS:DVS but 50 µL of (3-Glycidyloxypropyl) trimethoxysilane (GOPS) was mixed in the formulation.

2.4.5 Films preparation for biotests

Round-shaped glass coverslips in two different sizes 1.3 cm and 2.5 cm of diameter were used. Coverslips used for the measurements were previously treated for 2 h with piranha solution which was freshly prepared mixing one part of H_2O_2 and another part of H_2SO_4. Spin-coated films were made by pipetting, on a KLM SCC spin coater, in the center of the coverslip the suspension and spin coating them for 40 s at 1000 rpm (to get a film of about 100 nm). A suspension of 3% v/v of GOPS was used together with two containing 5 and 10 % v/v of DVS, prepare as described before. Once spin coated, glass slides were hard baked for 1 h at 50 °C under vacuum. To check delamination, the resulting coverslips after the drying step were put in a beaker with 20 mL of PBS 0.01 M changing this solution 3 times every 8 h.

2.4.6 Film preparation for conductivity measurements

Prior to utilization, glass slides were sonicated in a 2 %wt soap bath during 10 min, followed by sonication in an isopropanol:acetone 2:1 bath during 10 min. After sonication, the glass-slides were rinsed with isopropanol and DI water successively. Afterwards, they were activated by plasma treatment at 100 W with oxygen at 40 sccm for 30 s on a E-100 Benchtop Plasma System by PlasmaEtch, NV, USA. The solutions were spin-coated on a Laurell WS-400B-6NPP-LITE at 1000 rpm for 40 s for the ones containing DVS. For the suspension without DVS, the spin coating was 30 s at 3000 rpm. Resulting in both cases in about 100 nm thick films. Bruker Dektak profilometer was used to measure film thickness. Once spin coated, glass slides were hard baked for 40 min at 140 °C. The measurements of conductivity were performed on a 4point probe method, using a Jandel KM3-AR instrument.

2.4.7 OECT fabrication

Glass slides 76×26×1 mm were cleaned by sonication in a 2 wt% soap solution in DI water for 15 min and then in isopropanol:acetone 1:1 in volume for 15 min. Au interconnects were patterned by spin-coating S1813 (Shipley) photoresist on the glass slide, exposing it to UV light using a SUSS MJB4 contact aligner, and developed using MF-26. A 10 nm Cr adhesion layer, followed by a 100 nm Au film were deposited (Alliance Concept EVA450) and patterned using lift-off in acetone. Afterwards, an insulation layer 1.7 µm of parylene-C with 3-(Trimethoxysilyl)propyl methacrylate as adhesion promoter was deposited. A layer of soap (micro-90) and an extra sacrificial layer of parylene-C (2 µm) were deposited. The last fabrication step was the patterning of a 3.5 µm layer of photoresist, AZ9260, which was then etched using oxygen plasma using an Oxford 80 plus. In this way, channel area was defined, 100 µm width and 10 µm length. The transistor was spin coated with PEDOT:PSS containing 5% v/v ethylene glycol, 0.1% v/v dodecyl benzene sulfonic acid, 3% v/v divinyl sulfone, and 0.2% v/v of (3-glycidyloxypropyl) trimethoxysilane at 1000 rpm for 40 s, resulting in a ~100 nm thick film. After peeling off the upper layer of parylene, PEDOT:PSS:DVS channel was put in direct contact with an electrolyte solution 0.1M NaCl where the Ag/AgCl gate electrode (Warner Instruments) was submerged for measurements. Drain and Gate voltage and current were measured and applied correspondingly by a Keithley 2602A instrument.

2.4.8. Biocompatibility testing L929 and SH-SY5Y cell culture

Murine L929 cells were cultured in in high glucose Dulbecco's Modified Eagles Medium (DMEM; Sigma, Ref. D5796) supplemented with 10% Fetal Bovine Serum (FBS; Biochrom, Ref. A1020S0115) and 1% Penicillin-Streptomycin (Pen/Strep; Lonza, Ref. A3717-745E). Cells were passaged at ~80% confluence or seeded according to experimental preferences.

Human SH-SY5Y cells were cultured in Advanced D-MEM/F12 (Gibco, Ref:12634-010) supplemented with 10% FBS and 1% Pen/Strep and cells were passaged or seeded for experiments at ~80% of confluence. Both cell lines were maintained in a humidified incubator at 37 °C, 5% CO_2.

2.4.9 Cytotoxicity assay according to ISO 10993-5 guidelines

Cytotoxicity or biocompatibility of samples was assessed by MTT assay (Roche, Cell proliferation kit I) performed according to ISO 10993-5 guidelines for the extract method using the murine fibroblast cell line L929. The protocol for MTT was performed according to manufacturer instructions and all cultures and incubation steps were performed in a humidified incubator at 37 °C, 5% CO_2. Cells were seeded in a 96-well plate at a density of 10^4 cells/well. Extracts of samples or negative (high-density polyethylene, USP, Ref. 1546707) and positive controls (positive bioreaction, USP, Ref. 1071439) were generated by conditioning cell culture medium for 24h with samples of appropriate dimensions defined in ISO 10993-5. Which states that samples with a thickness below 0,5 mm should have at least a contact surface area of 6 cm^2, if thickness of samples is between 0,5 mm and 1 mm this surface area has to be at least 3 cm^2 and with a sample thickness of 1 mm and more 1,25 cm^2. 24 h after seeding, L929 cells were cultured in these medium extracts for 24h abd there after MTT was added for 4h. To dissolve purple formazan salt crystals, cell proliferation kit I solubilization solution was added for 24h and absorbance was measured at wavelength 550 nm using a Multiskan Ascent (Thermo Scientific) plater reader. Outcomes were interpreted by using unpaired Student's t-test, differences which showed $p<0.05$ were considered as significant.

2.4.10 Proliferation of SH-SY5Y cells

Proliferation of SH-SY5Y cells on the material substrates was evaluated by counting of live cells. SH-SY5Y cells were seeded in 24-well plates at a density of $4x10^4$ cells/well in Advanced D-MEM/F12 (Gibco, Ref:12634-010) supplemented with 10% FBS and 1% Pen/Strep. Cells cultured on tissue culture plastic (TCP) were used as a control condition. 24 h after seeding cell culture

medium was refreshed or live/dead assay was started in the t=0 h timepoint. Live/dead assay (Thermofisher, Ref: L3224) was performed according to manufacturer protocol. Cells were washed once with serum free culture medium where after cells were treated for 15 min with 8 µMµEthD-1 for staining of dead cells and 4 µM calcein-am for staining of live cells, provided in the kit. Imaging was done with the use of an Olympus IX51 fluorescent microscope. Proliferation of SH-SY5Y cells was evaluated by counting the amount of live cells in a minimum of 3 microscopic fields at 10x in 3 independent samples per timepoint (0, 24 and 48 h). Counting of cells was done by using the cell counter plugin of the ImageJ software.

2.4.11 Neuronal differentiation of SH-SY5Y cells and immunocytochemistry

For differentiation of SH-SY5Y cells, cells were seeded with a density of $6x10^4$ cells on laminin coated (10µg/ml) glass coverslips (control), or PEDOT:PSS:DVS films drop-casted on glass coverslips. Differentiation of SH-SY5Y cells was performed as described previously with some modifications.[57] Induction of neuronal differentiation of SH-SY5Y cells was done by sequential treatment of cells with 1µM synthetic retinoid ec23 (Amsbio, Ref. SPR002) for 3 days, followed by a 3 days treatment with human brain derived neurotrophic factor (BDNF; Sigma-Aldrich, Ref. B3795). Both steps were performed in serum free medium. For analysis of neurite formation, immunocytochemistry was performed. After rinsing with PBS 1x cells were fixed in 4% formaldehyde in PBS 1x (0.1% Triton X-100) for 12 min at 4 °C followed by rinsing twice with PBS 1x for 10min.and 1 h blocking in 1% BSA in PBS 1x at room temperature. Cells were stained with Anti-neurofilament 200 primary antibody (1:500; Sigma-Aldrich, Ref. N4142) for 1.5 h at room temperature Thereafter, cells were rinsed 2 times with PBS 1x and incubated (1:500) with Alexa 568 Goat anti-Rb IgG (H+L; Invitrogen, Ref. A11011) for 1.5h at room temperature After incubation with secondary antibody, cells were washed with PBS 1x supplemented with Hoechst (1:1000) for nuclear staining followed by normal rinsing with PBS 1x for 5 min. Coverslips were mounted onto glass slides using Permafluor (Thermo scientific, Ref. TA-006-FM)

for fluorescence imaging. Length of formed neurites was evaluated using ImageJ with the simple neurite tracer plugin and results were compared with npaired Student's t-test where $p<0.05$ was considered as significant.

2.5 References

(1) Rivnay, J.; Owens, R. M.; Malliaras, G. G. *Chem. Mater.* **2014**, *26* (1), 679.

(2) Jimison, Leslie H.Khodagholy, D.; Doublet, T.; Bernard, C.; Malliaras, G. G.; Owens, R. M. *Applications of Conducting Polymer Devices in Life Sciences*; 2013; Vol. 8.

(3) Shi, H.; Liu, C.; Jiang, Q.; Xu, J. *Adv. Electron. Mater.* **2015**, *1* (4), 1500017.

(4) Balint, R.; Cassidy, N. J.; Cartmell, S. H. *Acta Biomater.* **2014**, *10* (6), 2341.

(5) Mantione, D.; del Agua, I.; Schaafsma, W.; Diez-Garcia, J.; Castro, B.; Sardon, H.; Mecerreyes, D. *Macromol. Biosci.* **2016**, *16* (8), 1227.

(6) Isaksson, J.; Kjäll, P.; Nilsson, D.; Robinson, N. D.; Berggren, M.; Richter-Dahlfors, A. *Nat. Mater.* **2007**, *6* (9), 673.

(7) Sessolo, M.; Khodagholy, D.; Rivnay, J.; Maddalena, F.; Gleyzes, M.; Steidl, E.; Buisson, B.; Malliaras, G. G. *Adv. Mater.* **2013**, *25* (15), 2135.

(8) Mawad, D.; Artzy-Schnirman, A.; Tonkin, J.; Ramos, J.; Inal, S.; Mahat, M. M.; Darwish, N.; Zwi-Dantsis, L.; Malliaras, G. G.; Gooding, J. J.; Lauto, A.; Stevens, M. M. *Chem. Mater.* **2016**, *28* (17), 6080.

(9) Elschner, A.; Kirchmeyer, S.; Lövenich, W.; Merker, U.; Reuter, K.; Lovenich, W.; Merker, U.; Reuter, K. *PEDOT*, 1st ed.; CRC Press: Boca Raton FL USA, 2011.

(10) Zhang, S.; Hubis, E.; Girard, C.; Kumar, P.; DeFranco, J.; Cicoira, F. *J. Mater. Chem. C* **2016**, *4* (7), 1.

(11) Huang, T.-M.; Batra, S.; Hu, J.; Miyoshi, T.; Cakmak, M. *Polymer (Guildf).* **2013**, *54* (23), 6455.

(12) Xing, Y.; Qian, M.; Wang, G.; Zhang, G.; Guo, D.; Wu, J. *Sci. China Technol. Sci.* **2014**, *57* (1), 44.

(13) Ghosh, S.; Inganäs, O. *Synth. Met.* **1999**, *101* (1–3), 413.

(14) Kim, S.; Cho, A.; Kim, S.; Cho, W.; Chung, M. H.; Kim, F. S.; Kim, J. H. *RSC Adv.* **2016**, *6* (23), 19280.

(15) Cho, W.; Im, S.; Kim, S.; Kim, S.; Kim, J. *Polymers (Basel).* **2016**, *8* (5), 189.

(16) Mu Yang; Yushi Zhang; Hongze Zhang; Zhihong Li. In *10th IEEE International Conference on Nano/Micro Engineered and Molecular Systems*; IEEE, 2015; pp 149–151.

(17) Khodagholy, D.; Doublet, T.; Quilichini, P.; Gurfinkel, M.; Leleux, P.; Ghestem, A.; Ismailova, E.; Hervé, T.; Sanaur, S.; Bernard, C.; Malliaras, G. G. *Nat. Commun.* **2013**, *4*, 1575.

(18) Leleux, P.; Johnson, C.; Strakosas, X.; Rivnay, J.; Hervé, T.; Owens, R. M.; Malliaras, G. G. *Adv. Healthc. Mater.* **2014**, *3* (9), 1377.

(19) Berezhetska, O.; Liberelle, B.; De Crescenzo, G.; Cicoira, F. *J. Mater. Chem. B* **2015**, *3* (25), 5087.

(20) Williamson, A.; Rivnay, J.; Kergoat, L.; Jonsson, A.; Inal, S.; Uguz, I.; Ferro, M.; Ivanov, A.; Sjöström, T. A.; Simon, D. T.; Berggren, M.; Malliaras, G. G.; Bernard, C. *Adv. Mater.* **2015**, *27* (20), 3138.

(21) Zhang, S.; Kumar, P.; Nouas, A. S.; Fontaine, L.; Tang, H.; Cicoira, F. *APL Mater.* **2015**, *3* (1), 14911.
(22) Wang, C.; Qi, C. *Tetrahedron* **2013**, *69* (26), 5348.
(23) Lai, J.-Y. *Carbohydr. Polym.* **2014**, *101*, 203.
(24) Gkoupidenis, P.; Schaefer, N.; Garlan, B.; Malliaras, G. G. *Adv. Mater.* **2015**, *27* (44), 7176.
(25) Rivnay, J.; Leleux, P.; Ferro, M.; Sessolo, M.; Williamson, A.; Koutsouras, D. A.; Khodagholy, D.; Ramuz, M.; Strakosas, X.; Owens, R. M.; Benar, C.; Badier, J.-M.; Bernard, C.; Malliaras, G. G. *Sci. Adv.* **2015**, *1* (4).
(26) Khodagholy, D.; Rivnay, J.; Sessolo, M.; Gurfinkel, M.; Leleux, P.; Jimison, L. H.; Stavrinidou, E.; Herve, T.; Sanaur, S.; Owens, R. M.; Malliaras, G. G. *Nat. Commun.* **2013**, *4*, 3.
(27) Mantione, D.; del Agua, I.; Schaafsma, W.; ElMahmoudy, M.; Uguz, I.; Sanchez-Sanchez, A.; Sardon, H.; Castro, B.; Malliaras, G. G.; Mecerreyes, D. *ACS Appl. Mater. Interfaces* **2017**, *9* (21), 18254.
(28) Asplund, M.; Thaning, E.; Lundberg, J.; Sandberg-Nordqvist, A. C.; Kostyszyn, B.; Inganäs, O.; von Holst, H. *Biomed. Mater.* **2009**, *4* (4), 45009.
(29) Hayashi, S. *Polym. Plast. Technol. Eng.* **1988**, *27* (1), 61.
(30) Massonnet, N.; Carella, A.; Jaudouin, O.; Rannou, P.; Laval, G.; Celle, C.; Simonato, J.-P. *J. Mater. Chem. C* **2014**, *2* (7), 1278.
(31) Liu, S.; Tian, J.; Wang, L.; Luo, Y.; Sun, X. *Analyst* **2011**, *136* (23), 4898.
(32) Zhang, L.; Peng, H.; Kilmartin, P. A.; Soeller, C.; Travas-Sejdic, J. *Macromolecules* **2008**, *41* (20), 7671.
(33) Schaffer, H. E.; Heeger, A. J. *Solid State Commun.* **1986**, *59* (7), 415.
(34) Ouyang, J.; Xu, Q.; Chu, C.-W. W.; Yang, Y.; Li, G.; Shinar, J. *Polymer (Guildf).* **2004**, *45* (25), 8443.
(35) Reyes-Reyes, M.; Cruz-Cruz, I.; López-Sandoval, R. *J. Phys. Chem. C* **2010**, *114* (47), 20220.
(36) Louarn, G.; Trznadel, M.; Buisson, J. P.; Laska, J.; Pron, A.; Lapkowski, M.; Lefrant, S. *J. Phys. Chem.* **1996**, *100* (30), 12532.
(37) Cruz-Cruz, I.; Reyes-Reyes, M.; Rosales-Gallegos, I. A.; Gorbatchev, A. Y.; Flores-Camacho, J. M.; López-Sandoval, R. *J. Phys. Chem. C* **2015**, *119* (33), 19305.
(38) Kvarnström, C.; Neugebauer, H.; Ivaska, A.; Sariciftci, N. S. *J. Mol. Struct.* **2000**, *521* (1–3), 271.
(39) Nguyen, T. P.; Le Rendu, P.; Long, P. D.; De Vos, S. A. *Surf. Coatings Technol.* **2004**, *180–181*, 646.
(40) Lin, E.-W.; Boehnke, N.; Maynard, H. D. *Bioconjug. Chem.* **2014**, *25* (10), 1902.
(41) d'Arcy, R.; Siani, A.; Lallana, E.; Tirelli, N. *Macromolecules* **2015**, *48* (22), 8108.
(42) Fabretto, M.; Zuber, K.; Jariego-Moncunill, C.; Murphy, P. *Macromol. Chem. Phys.* **2011**, *212* (19), 2173.
(43) Greco, F.; Zucca, A.; Taccola, S.; Menciassi, A.; Fujie, T.; Haniuda, H.; Takeoka, S.; Dario, P.; Mattoli, V. *Soft Matter* **2011**, *7* (22), 10642.
(44) Kim, J. Y.; Jung, J. H.; Lee, D. E.; Joo, J. *Synth. Met.* **2002**, *126* (2–3),

311.
(45) Ouyang, L.; Musumeci, C.; Jafari, M. J.; Ederth, T.; Inganäs, O. *ACS Appl. Mater. Interfaces* **2015**, *7* (35), 19764.
(46) Bernards, D. A.; Malliaras, G. G. *Adv. Funct. Mater.* **2007**, *17* (17), 3538.
(47) Nikolou, M.; Malliaras, G. G. *Chem. Rec.* **2008**, *8* (1), 13.
(48) Yi, Z.; Natale, G.; Kumar, P.; Mauro, E. Di; Heuzey, M.-C.; Soavi, F.; Perepichka, I. I.; Varshney, S. K.; Santato, C.; Cicoira, F. *J. Mater. Chem. C* **2015**, *3* (25), 6549.
(49) Khodagholy, D.; Gurfinkel, M.; Stavrinidou, E.; Leleux, P.; Herve, T.; Sanaur, S.; Malliaras, G. G. *Appl. Phys. Lett.* **2011**, *99* (16), 163304.
(50) Rivnay, J.; Leleux, P.; Sessolo, M.; Khodagholy, D.; Hervé, T.; Fiocchi, M.; Malliaras, G. G. *Adv. Mater.* **2013**, *25* (48), 7010.
(51) Felix, H.; Jessica, L.; Anna, S.; Vivek, P.; Sven, I. *Front. Neurosci.* **2016**, *10*.
(52) Stavrinidou, E.; Leleux, P.; Rajaona, H.; Khodagholy, D.; Rivnay, J.; Lindau, M.; Sanaur, S.; Malliaras, G. G. *Adv. Mater.* **2013**, *25* (32), 4488.
(53) Aregueta-Robles, U. A.; Woolley, A. J.; Poole-Warren, L. A.; Lovell, N. H.; Green, R. A. *Front. Neuroeng.* **2014**, *7*, 15.
(54) Green, R. A.; Lovell, N. H.; Wallace, G. G.; Poole-Warren, L. A. *Biomaterials* **2008**, *29* (24), 3393.
(55) Thompson, B. C.; Murray, E.; Wallace, G. G. *Adv. Mater.* **2015**, *27* (46), 7563.
(56) Dwane, S.; Durack, E.; Kiely, P. A. *BMC Res. Notes* **2013**, *6*, 366.
(57) Encinas, M.; Iglesias, M.; Liu, Y.; Wang, H.; Muhaisen, A.; Cena, V.; Gallego, C.; Comella, J. X. *J. Neurochem.* **2000**, *75* (3), 991.

Chapter 3. New Carboxylic Acid Dioxythiophene (ProDOT-COOH) for Easy Functionalization of Conductive Polymers

3.1 Introduction

PEDOT, poly(3,4-ethylenedioxithiophene) is nowadays the dominant conducting polymer as transparent conducting layer, or hole injector layer for most organic electronic devices such as OLEDs, OPVs, OTFTs or electrochromic devices.[1–4] Recently, PEDOT and other polydioxythiophenes such as ProDOT are emerging also as champion materials in the field of organic bioelectronics both in the domain of biosensing and also for interaction with living cells.[5,6] Looking at the structure of EDOT or PEDOT, we can easily see that is not easy to functionalize. It is possible to substitute PSS or actuate on the anionic chain, but no directly on the EDOT scaffold.

In order to modify the monomer, only the dioxolane part is available, due that the thiophene ring is totally substituted (in the polymeric form also the position 2 and

5 are used) and breaking the conjugation will affect the conductivity. Then, act on the dioxolane ring, on the methylenes groups is the only way to introduce pendant groups and further functionalities. Looking forward on that way, in the literature is clearly notable a disequilibrium about the few works done in order to modify the proper monomer EDOT and the many works concerning the modification of all the matrix: anionic chain, solvents, dopants, crosslinkers etc. At this stage is good to have in mind that PEDOT:PSS is a commercial suspension sell by companies and the complete formulation is unknown. Then, as the suspension come already improved and stable, many research groups use it pristine, so the amount of literature behind nowadays is huge. Secondly, but not less important, is that to modify the scaffold, many synthetic chemistry steps are needed, and normally, the users of this materials are not pure chemists. As shown in **Scheme 3.1** the most used are EDOT-CH_2OH EDOT-CH_2-Cl EDOT- CH_2Br. Even if these are not synthesized directly, but derived from hydroxymethyl-EDOT or chloromethyl-EDOT, EDOT-CH_2N_3 and EDOT-CH_2-SH are used as starting materials and is worth to show them.[7–11] Noticeable, all of them present a substituent in position 2 on the dioxolane ring, normally a mono-substituted methyl group.

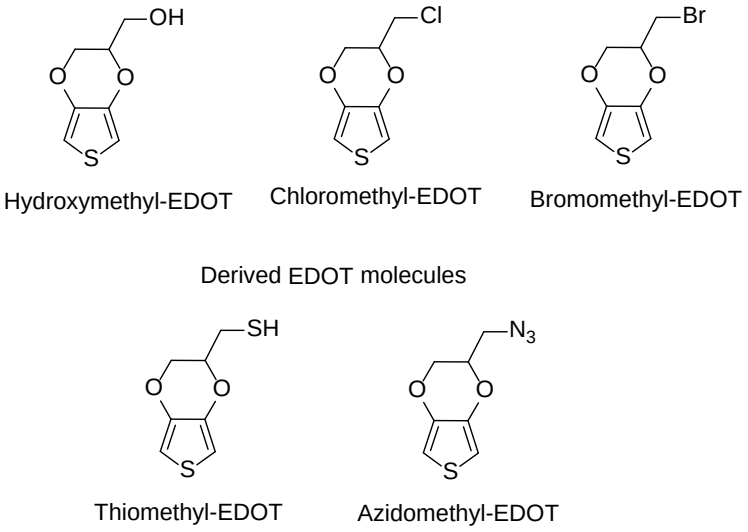

Scheme 3.1 Most used EDOT derivates.

In all these cases the synthesis of these functional EDOT monomers requires many synthetic steps.[12–15] The known routes are two: in one synthesis, there is the creation of both rings: the thiophene and the dioxolane (**Scheme 3.2** pathway #1); in the second one, the starting material is an already 3,4-substituted thiophene ring, like 3,4-dimethoxythiophene or 3,4-bromothiophene. Both ways are shown in **Scheme 3.2**.

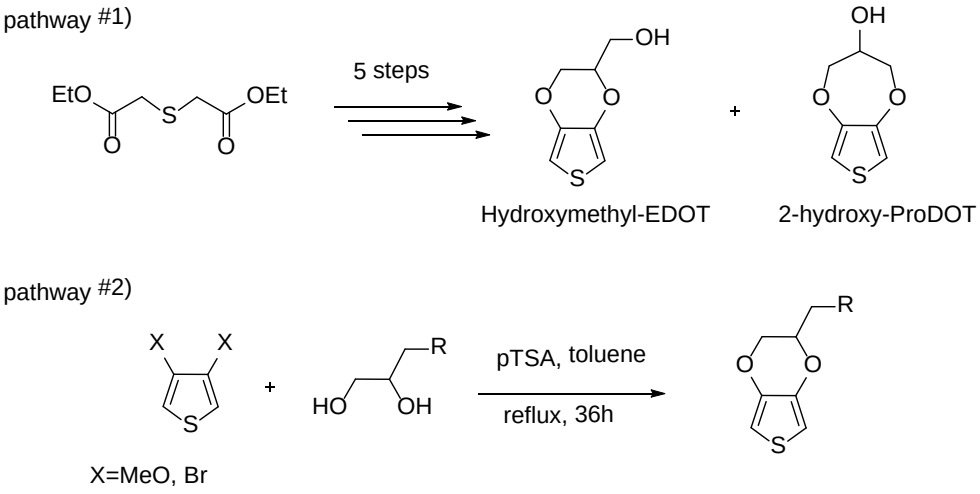

Scheme 3.2 Synthetic pathway to functionalized EDOT.

In the first pathway, even if is often present a mixture difficult to separate, the reagents are much cheaper compare to the second route, where the 3,4-disubstituted thiophene is way more expensive. The advantage of the second is the easy chemistry behind, and the high overall yield. Anyhow, for the creation of the most used derivate EDOT-CH_2OH or, if R is a better nucleophile than the hydroxyl group, the first pathway is the only approach to avoid the dioxepane derivate, as shown in **Scheme 3.3**.

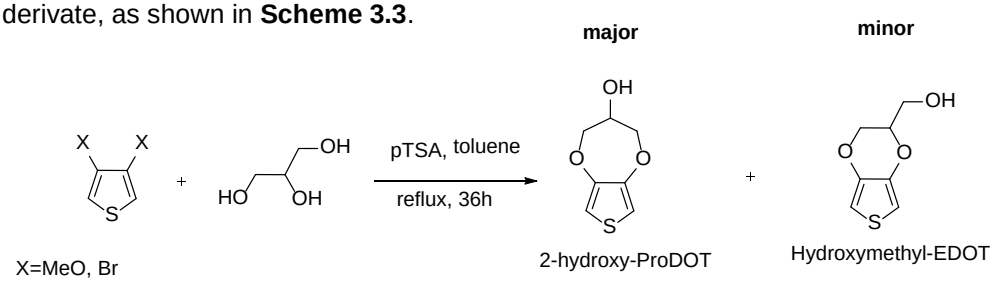

Scheme 3.3 Dioxepane side-product derivate from pathway #2.

Recently the attention is moving toward a more reactive and easy to functionalize EDOT derivative bearing a carboxylic acid. Martin et al. reported the synthesis of an EDOT functional carboxylic acid monomer in 7 steps, using pathway #1.[9] This EDOT-COOH was used to improve the adhesion of PEDOT to the electrodes. A similar PEDOT-COOH polymer was recently synthesized by Mawad et al. from EDOT-CH_2OH in 3 additional steps which formed electroconductive hydrogels to be used as scaffolds for electro-responsive cells.[16] Both examples are shown in **Scheme 3.4**.

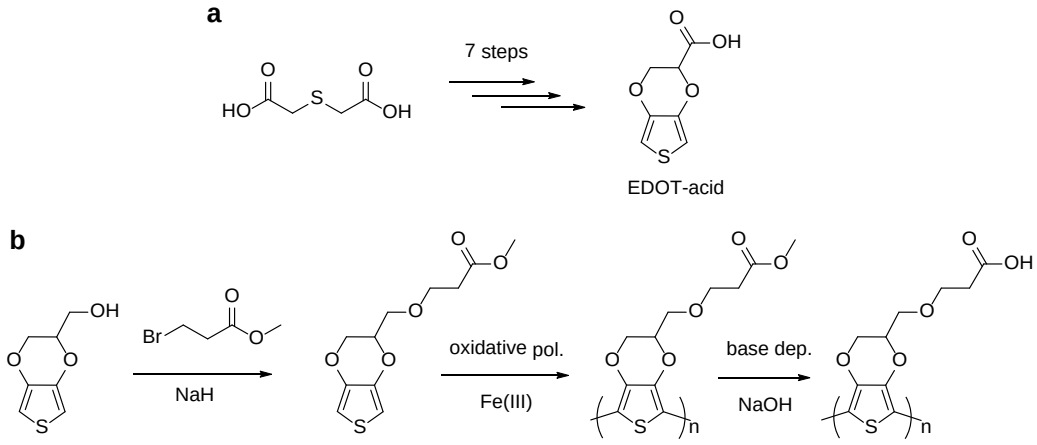

Scheme 3.4 EDOT-COOH derivate.

It is well understandable and visible from the major product in the reaction with 3,4-disubstituted thiophene and glycerol (**Scheme 3.3**), that EDOT scaffold are considered more difficult to synthesize than the ProDOT ones while the polymers present similar properties.[17–19] Following this trail, in this work, we present the synthesis of a new functional ProDOT carboxylic acid (ProDOT-COOH) molecule which can be carried out in just two steps using commercially available reagents. We also demonstrated the versatility of the monomer as precursor to synthesize a series of functional ProDOT derivatives.[20]

3.2 Results and Discussion

3.2.1 Synthesis of ProDOT-COOH

The synthesis of the ProDOT-COOH molecule is shown in **Scheme 3.5**.

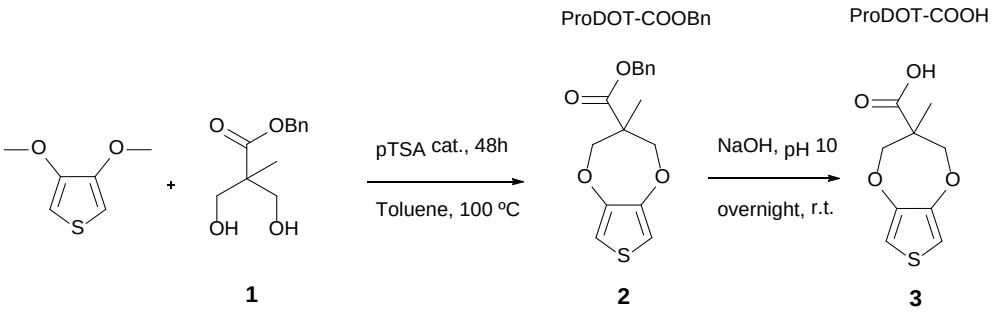

Scheme 3.5 Synthetic route to ProDOT-COOH (**3**).

We explored the use of 2,2-bis(hydroxymethyl)propanoic acid (bis-MPA) as a cheap precursor to prepare ProDOT-COOH. Our selection was based because bis-MPA is a common reagent in polyester and polycarbonate chemistry to prepare functional monomers due to simplicity of the carboxylic acid to be protected/deprotected with benzyl bromide and sodium hydroxide respectively.[21] In addition it is well-established the high reactivity of 1,3 diols towards 3,4-dimethoxythiophene in the presence of acid catalysis.[22–27] Thus, in the first step the protected bis-MPA (**1**) was reacted with 3,4-dimethoxythiophene in the presence of p-toluenesulfonic acid catalyst (PTSA) to afford ProDOT-COOBn (**2**) in high yield. Finally, a quantitative deprotection step was carried out with sodium hydroxide leading to the desired ProDOT-COOH (**3**); all the process is shown in **Scheme 3.5**. The reactions could be easily performed scaled up, because the purification process consisted only in one flash chromatography column and the starting materials are affordable in grams scale. In addition, the possibility to crystallize the product **3** (ProDOT-COOH) permitted to obtain high purity material, ready for polymerization and to be used in further reactions. In **Figure 3.1** is

displayed the ORTEP structure of ProDOT-COOH crystal and the looks like of the ProDOT-COOH powder and the ^{1}H-NMR of the pure molecule.

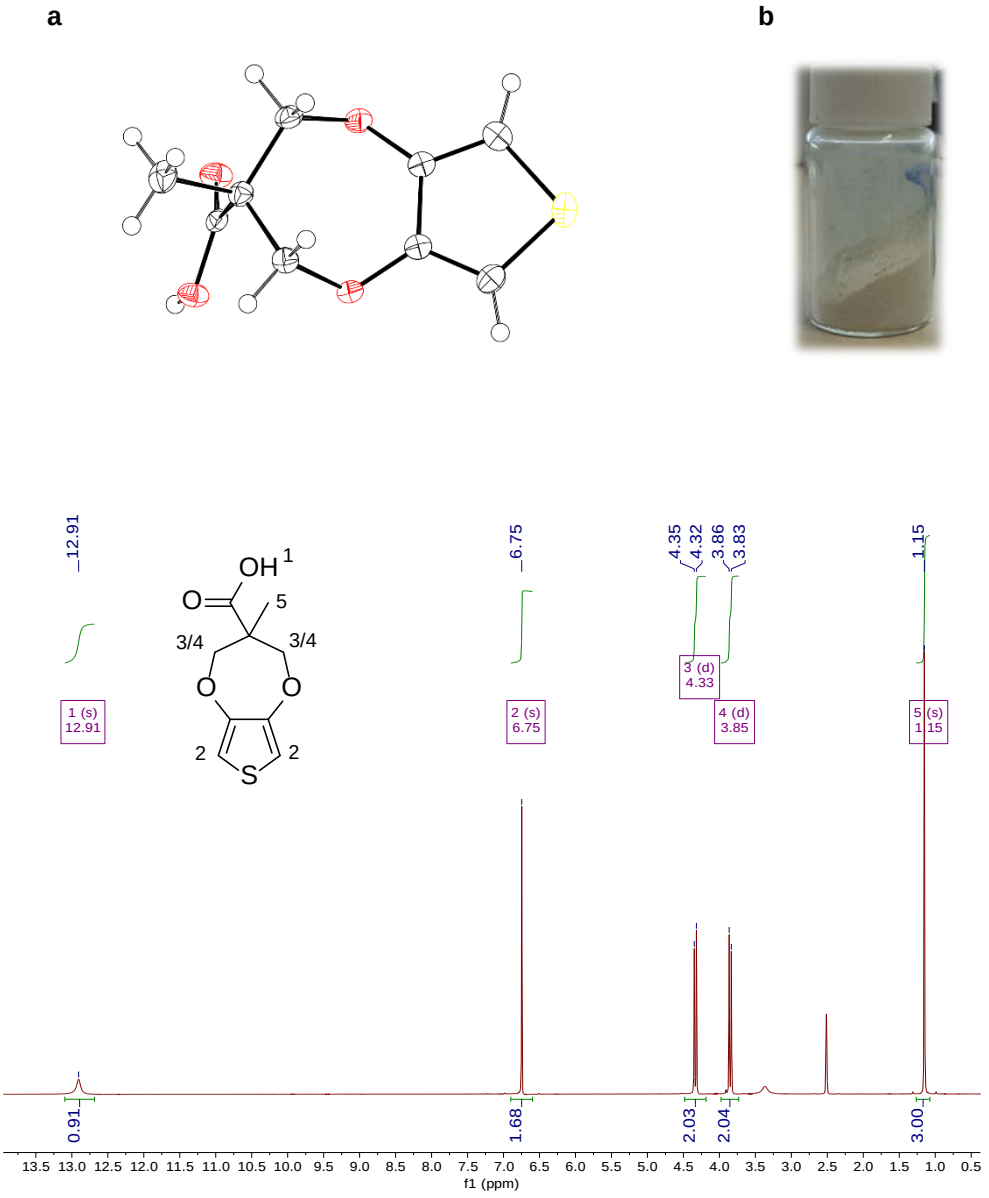

Figure 3.1 a) ORTEP structure of ProDOT-COOH at 150 K and 50 % probability, b) looks like of ProDOT-COOH powder, b) ^{1}H-NMR of ProDOT-COOH.

3.2.2 Polymerizations of ProDOT-COOH

Next, we investigated the polymerization of the functional monomer ProDOT-COOH (**Scheme 3.7**).

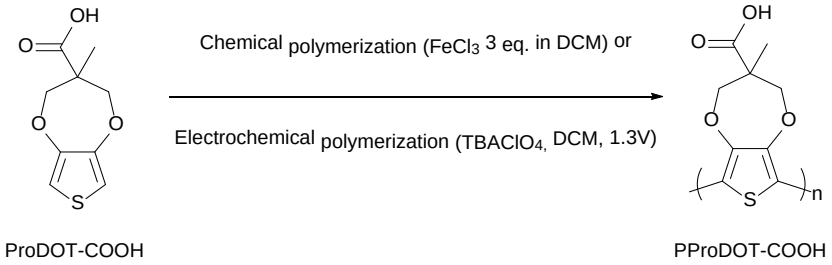

Scheme 3.7 Polymerization routes of PProDOT-COOH.

First, the electrochemical polymerization of ProDOT-COOH (**3**) was carried out by cyclic voltammetry using 0.1 M $TBAClO_4$ (tetrabutylammonium perchlorate) as electrolyte in dichloromethane (DCM) in a standard three electrode cell (**Figure 3.2**).

Similarly, to other ProDOT monomers, the irreversible oxidation of thiophene group that occurred at potentials higher than 1.3 V, formed on top of the working electrode a dark violet. The polymer simultaneously dissolved in the electrolyte leading to a

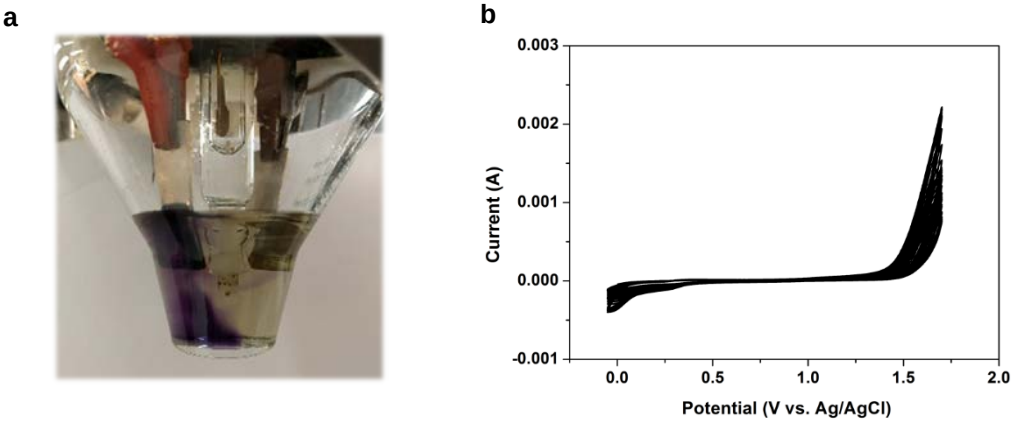

Figure 3.2 a) Electrochemical cell setup. b) Cyclic voltammograms of the electrochemical polymerization of ProDOT-COOH (10-2 M) in 0.1 M $TBAClO_4$ acetonitrile solution, using a 1 cm2 platinum working electrode, switching potential from -0.05 V to 1.7 V at a 20 mV s-1 scan rate

violet solution of the polymer. Meanwhile, the chemical polymerization was carried out by treating a solution 0.1 M of the ProDOT-COOH (**3**) in dichloromethane with 3 equivalents of Iron trichloride overnight. The chemical oxidative polymerization leaded to the quantitative formation of a dark solid precipitate. The poly(ProDOT-COOH) polymer was purified by dialysis and recovered as a solid dark blue powder.

3.2.3 Characterization of ProDOT-COOH

The ATR-FTIR (**Figure 3.3**) confirmed the chemical nature of the poly(ProDOT-COOH) showing a strong and a broad band at 3100 cm^{-1} due to the stretching of OH from the carboxylic acid, an enlarged signal at 1600cm^{-1} due to the stretching of the carbonyl of the carboxylic acid.
A strong band, attributed to the double bond of the poly(thiophenes) at 1350cm^{-1} was also observed. Interestingly, the poly(ProDOT-COOH) was soluble in slightly basic water and allowed the spin-coating of this material and the formation of thin films. The “blueish” films showed an electronic conductivity value of 0,01 S/cm as measured by 4-point probe method.

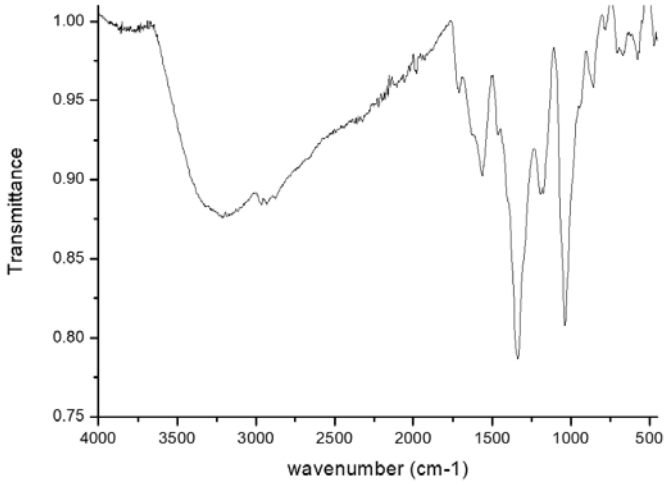

Figure 3.3 ATR FT-IR PProDOT-COOH

3.2.4 ProDOT-COOR: functionalizations and characterizations

Besides its polymerizability, ProDOT-COOH can be used as a versatile precursor for the synthesis of a variety of functional ProDOT monomers. Thus, three different functional moieties were coupled to ProDOT-COOH, i.e. Dopamine (DA), hydroxyl-TEMPO and tetraethylene glycol (TEG), as shown in **Scheme 3.8**. First, dopamine is known to be an useful molecule for its energy storage and adhesion properties.[28,29] TEMPO is a popular nitroxide stable-radical which can be applied into batteries due to its high redox potential and reversible redox processes.[30] Very recently our group has been demonstrated the synthesis of a PEDOT-TEMPO derivative, which showed unique electronic properties.[30] Replacing PEDOT with ProDOT-COOH makes the synthetic route cheaper and more efficient. Polyethyeleneglycol or TEG moieties are known functionalities which are used in bio-surfaces as well as ion conducting materials.[31]

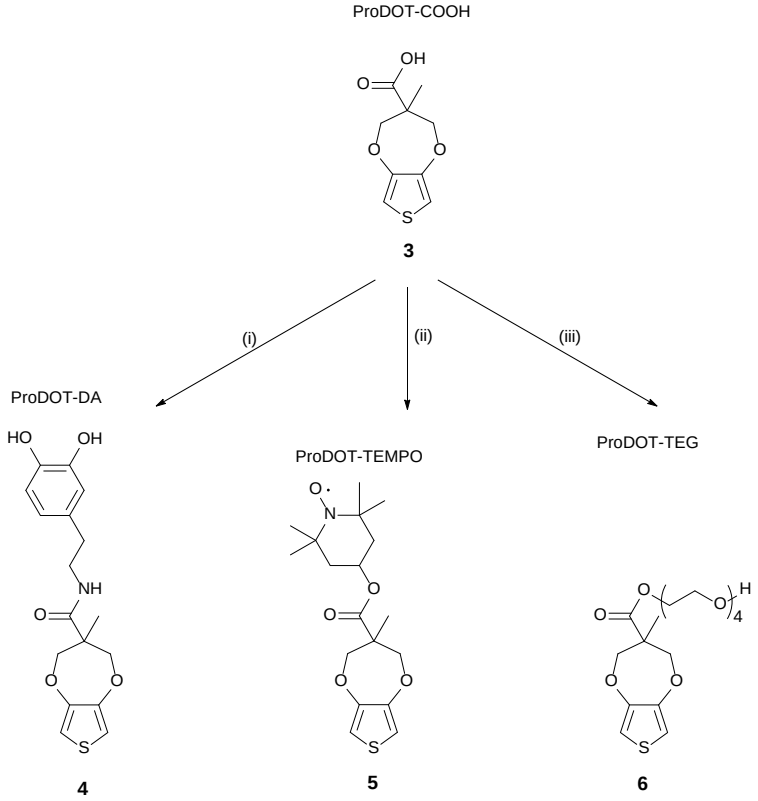

Scheme 3.8 ProDOT-COOH functionalization. (i) Dopamine Hydrochloride, HATU/DIEA. (ii) 4-hydroxy-TEMPO, DIC/DMAP cat. (iii) Tetraethylene glycol, HATU/DIEA.

Our aim, connecting the TEG group is to bring the properties of TEG to the poly(ProDOT) as well as to create a mixed ionic-electronic conductive material, due to the TEG and thiophene part. [32,33]

The synthesis of the ProDOT derivatives has been performed using common esterification coupling agents such as DCC-DMAP or HATU-DIEA.[34] Using HATU-DIEA, together with water soluble monomers such as dopamine and TEG, allowed isolation of the product simply with an extraction, without using any chromatographic technique, making this method easy to proceed and to scale-up. The full characterization of the three new monomers (**4**-**6**) is shown in section *3.4 Experimental Section.* Then the three new monomers were electropolymerized in acetonitrile or dichloromethane, with a monomer concentration of 10mM and using $TBAClO_4$ 0.1 M as electrolyte. The cyclic voltammograms of the monomers, together with their onset potential for the oxidation of thiophene ring are shown in **Figure 3.4**.

a

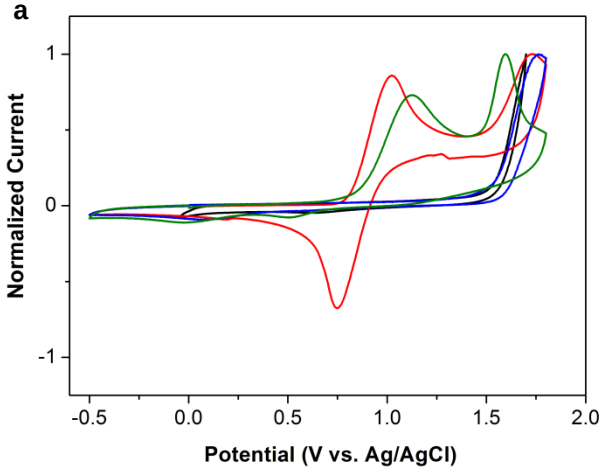

b

Monomer	E_{onset} (V)
ProDOT-COOH	1.54
ProDOT-DA	1.50
ProDOT-TEMPO	1.53
ProDOT-TEG	1.56

Figure 3.4 a) Cyclic voltammograms of ProDOT-R monomers (10-3 M) in acetronitrile or dichloromethane solution with 0.1 M $TBAClO_4$ electrolyte at 20 mVs-1 scan rate: ProDOT-COOH (black/ACN), ProDOT-DA (green/ACN), ProDOT-TEMPO (red/DCM) and ProDOT-TEG (blue/DCM). b) Table with the onset potentials of the thiophene ring in the various monomers.

By this method, the functional poly(ProDOT) polymers were obtained as violet films onto the surface of the working electrode. The electrodeposited films were later electrochemically characterized by cyclic voltammetry in monomer free solutions (**Figure 3.5**). It was noticeable that two redox processes were presented in polyProDOT-DA and polyProDOT-TEMPO polymers, due to the redox properties of their bearing groups. The catechol scaffold of dopamine was oxidized at 1.15 V (A2, Figure 1a) and reduced at 0.0 V (C2), while the nitroxide radical of TEMPO was oxidized at 0.85 V (A2, Figure 1b) and reduced at 0.78 V (C2). On the other hand, PProDOT-TEG underwent just one redox reaction (A1/C1), related to the polythiophene backbone due to the redox inactivity of its bearing group. As expected, the redox peaks of the thiophene backbone (A1/C1) were present in the three polymers with oxidation potentials (A1) between 0.2 V and 0.6 V and reduction potentials (C1) between -0.55 V and 0 V. This variation in the potentials is very likely to be caused by the different chemical nature of the pendant groups and the various solvents used for the electrochemical polymerization and characterization.

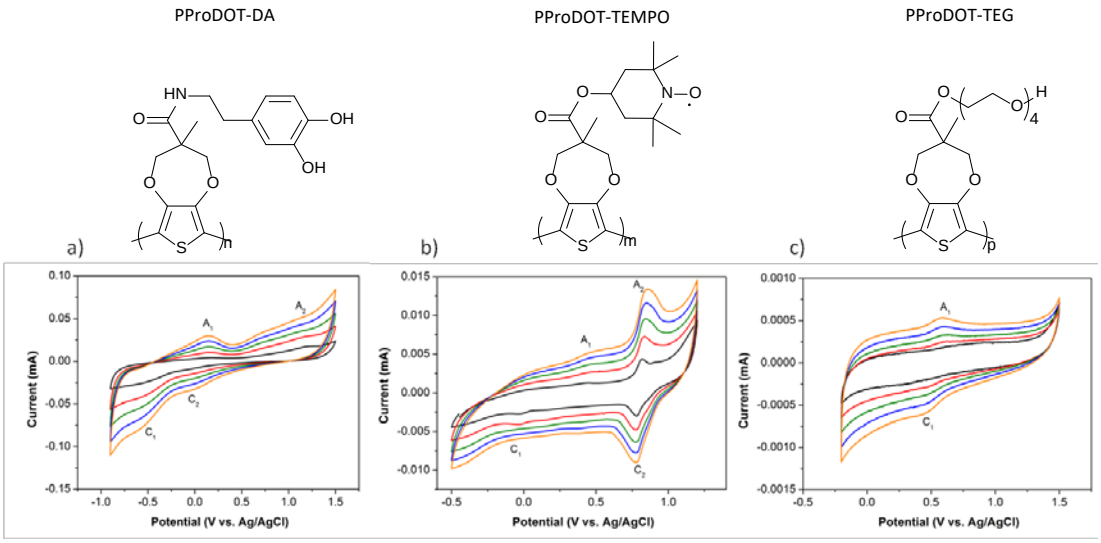

Figure 3.5 Figure 1. Cyclic voltammograms of the electro polymerized films at 5, 7.5, 10, 15 and 20 mV s-1 scan rates and their respective chemical polymer structures. a) PProDOT-DA in 0.1 M $TBAClO_4$ in ACN, b) PProDOT-TEMPO and c) PProDOT-TEG in 0.1 M $TBAClO_4$ in DCM.

3.3 Conclusions

Summarizing, in this third chapter, we present in this chapter a simple way to synthesize an easy functionalizable new ProDOT base molecule, bearing a carboxylic acid. The synthesis already present in literature consists of many steps, needing a strong organic chemistry background. In this chapter, we present a two steps synthesis, that could be performed also without a deep knowledge in organic synthesis. This molecule has been polymerized chemically and electrochemically. In the first case, the chemical polymerization is the most use in literature in order to form stable suspensions; on the other hand, the electrochemical one has been spready use to cover object, obtain a “surfactant free” polymer or to get highly pure conductive layer. In both cases the polymerization succeed, resulting in a violet-dark conductive polymer. Even in the absence of surfactant, the suspension presents a quite high conductivity, due to the absence of an insulator part. Using ProDOT-COOH as reagent, we synthetized three new functional ProDOT molecules. The new ProDOT molecules were functionalized with electroactive dopamine or TEMPO moieties, or biologically relevant tetraethylene glycol. These ProDOT monomers were electropolymerized to demonstrate the possibility to create functional conductive electroactive materials and to demonstrate the really presence of the electroactive species like dopamine and TEMPO. The easy synthesis and the facile esterification demonstrates the strong versatility of this new ProDOT-COOH that could be applied in many areas, mainly, in all that application that need a covalent linkage in between the conductive polymer and the substituent. Moreover, this molecule has the advantage of an ease co-polymerizability with EDOT, opening up to a mixed conductive copolymer.

3.4 Experimental Section

3.4.1 Materials and Method

Reactant and reagents were obtained Sigma-Aldrich, solvents were obtained from Fischer Scientific and used without further purification. 1D and 2D-NMR spectra were recorded at ambient temperature with a 400 MHz Bruker Avance III. The following abbreviations are used to describe peak patterns where appropriate: br = broad, s = singlet, d = doublet, t = triplet, q = quartet, m= multiplet, dd = doublet of doublets. Coupling constants (J) are reported in Hertz (Hz). TLC were carried out on aluminum precoated plates (silica gel 40-60Å 400mesh, F254, Aldrich) using hexane:ethyl acetate (Hex:AcOEt) (v/v) as eluent. Silica gel high-purity grade, pore size 60 Å, 230-400 mesh particle size 40-63 µm was use for flash column chromatography. Fourier Transform Infrared Spectroscopy (FTIR) measurements were performed on a Brüker Alpha-p FTIR spectrometer. Spectra were collected from 4000 to 250 cm^{-1} with the following settings: 42 scans per sample and spectral resolution: 4 cm^{-1}. High resolution mass spectrometry (HRMS) has been measured by direct injection in a Waters modelo SYNAPTTM G2 HDMSTM, using a Q-TOF detector and positive electrospray ionization ESI^+.

*3.4.2 Synthesis of MPA-OBn (**1**)*

The synthesis of 1 has been performed as previously describe in literature. Briefly: in a 500mL round bottom flask, 50g (0.373 mol, 1eq) of 2,2-Bis(hydroxymethyl) propionic acid was dissolve in 250mL of dimethylformamide (DMF) together with 24g (0.429 mol, 1.15eq) KOH and stirred for 1 hour at 100 ºC. Then, benzyl bromide 76.54g (53.23mL, 0.448 mol, 1.2eq) was added dropwise with a pressure-compensating dropping funnel and stirred at 100 ºC overnight. After, DMF was evaporated off and the residue dissolved with EtOAc (250mL) and washed with water (3x100mL). The organic phase was dried over Na_2SO_4, the solid separated by filtration and the solvent evaporated under

vacuum. The product is a viscous colorless oil that tent to crystallize. The characterization of the resulting molecule matched perfectly the literature.[35]

^{1}H NMR (400 MHz, Chloroform-d) δ 7.64 – 7.08 (m, 5H), 5.23 (s, 2H), 3.96 (d, J = 11.4 Hz, 2H), 3.76 (d, J = 11.1 Hz, 2H), 1.11 (s, 3H) ppm.

*3.4.3 Synthesis of ProDOT-OBn (**2**)*

To an argon degassed solution of 3,4-Dimethoxythiophene 5 g (34.7 mmol, 1 eq) in 200 mL of toluene, 10.1 g (45 mmol, 1.3 eq) of MPA-OBn (**1**) were dissolved. Then a catalytic amount of p-Toluenesulfonic acid monohydrate 0.66g (3.47 mmol, 0.05eq) was added and the mixture heated at 100 °C for 48 hours. The blue mixture was filtered and the toluene remove under vacuum. The blue oily residue was directly charged in a flash column chromatographic using hexane:ethyl acetate (EtOAc) 9:1 (Rf= 0.52), to afford **2** as a colorless oil (5.5g, 52%). FT-IR ν_{max}/cm^{-1} 3109 (=C-H), 2975, 2939 (C-H), 1727 (C=O) and 1480 (C=C), 1134, 1027.

^{1}H NMR (400 MHz, DMSO-d_6) δ 7.48 – 7.25 (m, 5H, Ph), 6.79 (s, 2H, (-CH)$_2$-S), 5.20 (s, 2H,-CH$_2$-Ph), 4.42 (d, *J* = 12.2 Hz, 2H, C-CH$_2$-C), 3.87 (d, *J* = 12.2 Hz, 2H, C-CH$_2$-C), 1.16 (s, 3H, -CH$_3$) ppm. ^{13}C NMR (101 MHz, DMSO-d_6) δ 172.64 , 149.21 , 135.96 , 128.45 , 127.98 , 127.49 , 106.15 , 75.02 , 66.01 , 50.09 , 18.02 ppm.

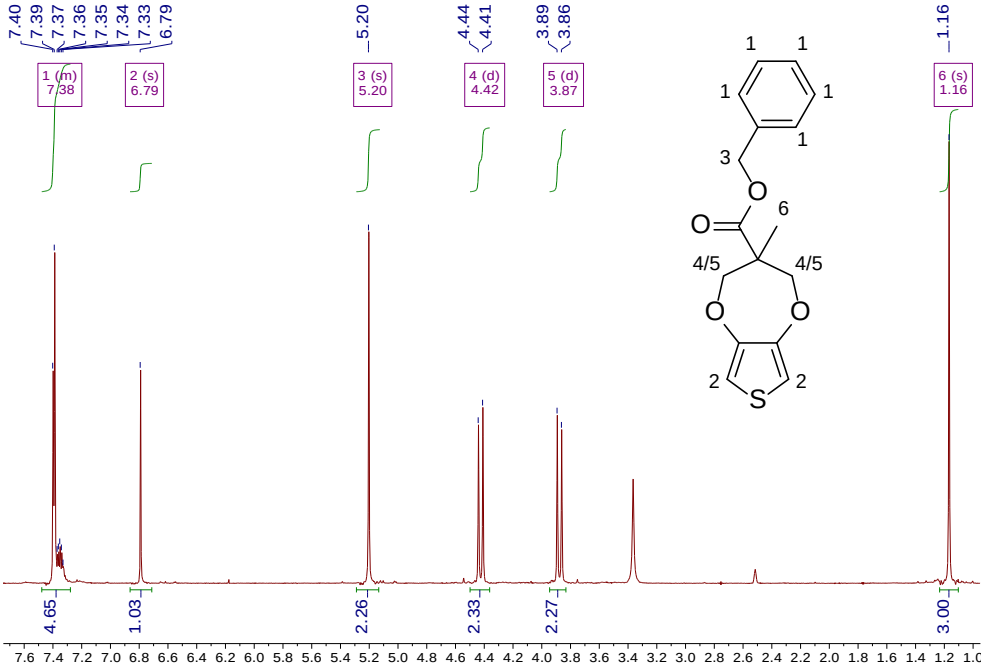

Figure 3.6 ^{1}H NMR of ProDOT-OBn (**2**)

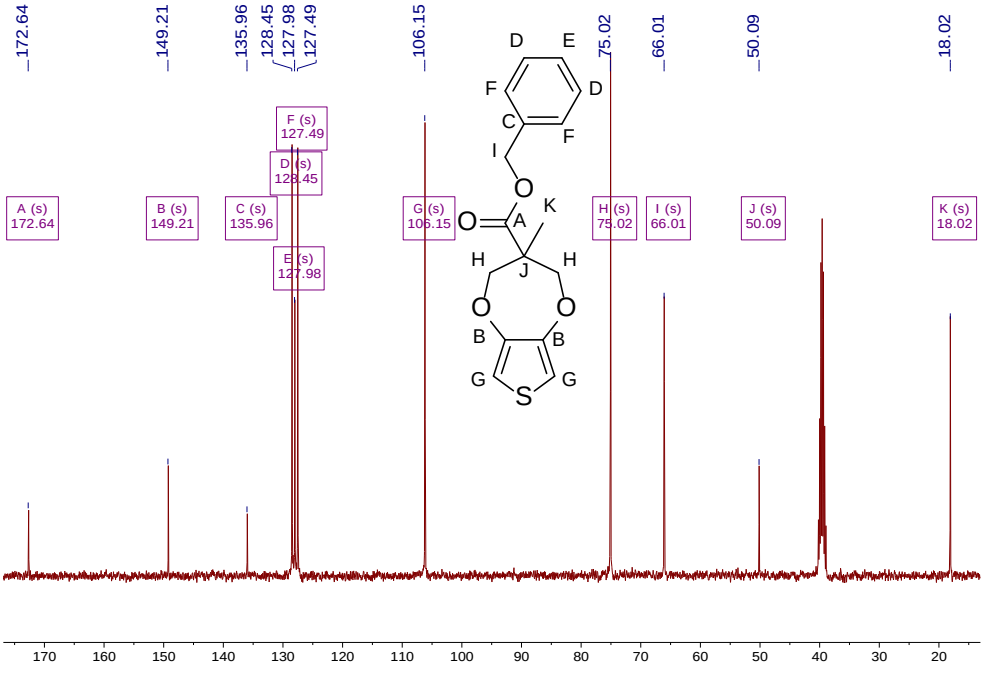

Figure 3.7 ^{13}C NMR of ProDOT-OBn (**2**)

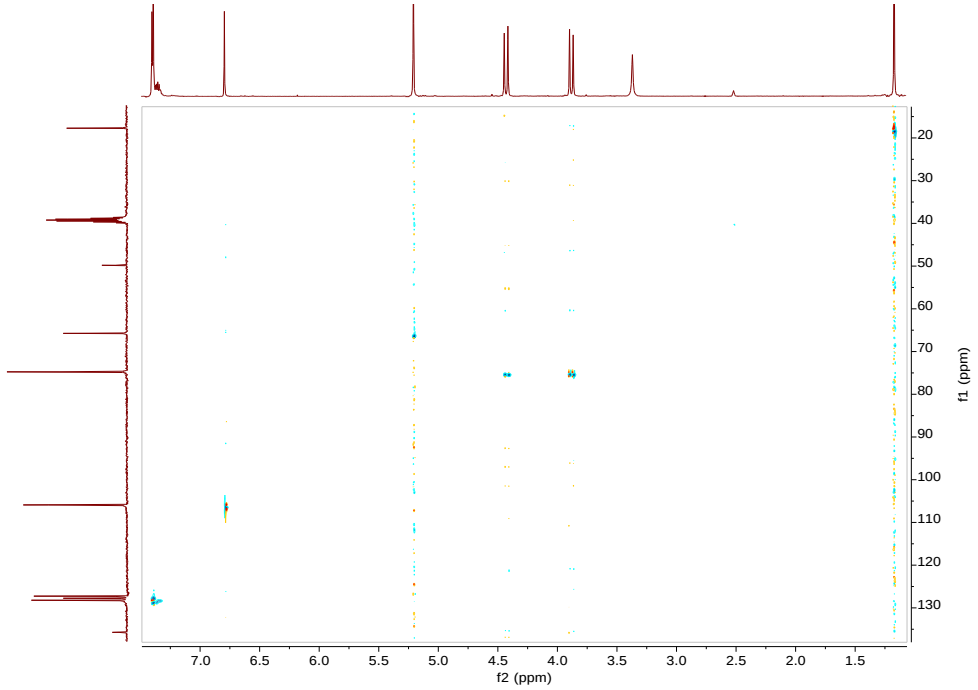

Figure 3.8 ^{1}H-^{13}C HSQC of ProDOT-OBn (**2**)

*3.4.4 Synthesis of ProDOT-COOH (**3**)*

To a solution of ProDOT-OBn (**2**) 1g (3.3 mmol) in a tetrahydrofurane (THF):water 3:2 100mL, was added NaOH 0.32 g (8 mmol) and let stirred overnight at room temperature. To the mixture was then added diethyl ether and the aqueous phase bring to pH acid with a solution of HCl 1M. The organic phase was washed with water (50mL) and brine (50mL). The organic layer was dried with Na_2SO_4, filtered and the solvent remove under vacuum, to afford 3 as an off white solid (0.70g, ≈100%). Recrystallization could be performed with Hexane/DMC, affording colorless crystals CCDC 1530638. Mp 159 °C. Ft-IR ν_{max}/cm^{-1} 3119 (COO-H), 3109 (=C-H), 2905 (C-H), 1697 (C=O) and 1485 (C=C), 796 (C=S).

^{1}H NMR (400 MHz, DMSO-d6) δ 12.91 (bs, 1H, -COOH), 6.75 (s, 2H, $(-CH)_2$-S), 4.33 (d, J = 12.1 Hz, 2H, C-CH_2-C), 3.85 (d, J = 12.2 Hz, 2H, C-CH_2-C), 1.15 (s, 3H, $-CH_3$) ppm. ^{13}C NMR (101 MHz, DMSO-d6) δ 174.59 , 149.22 , 105.76 , 75.18 , 49.46 , 18.24 ppm. HRMS *m/z* 237.0205 $[MNa]^+$.

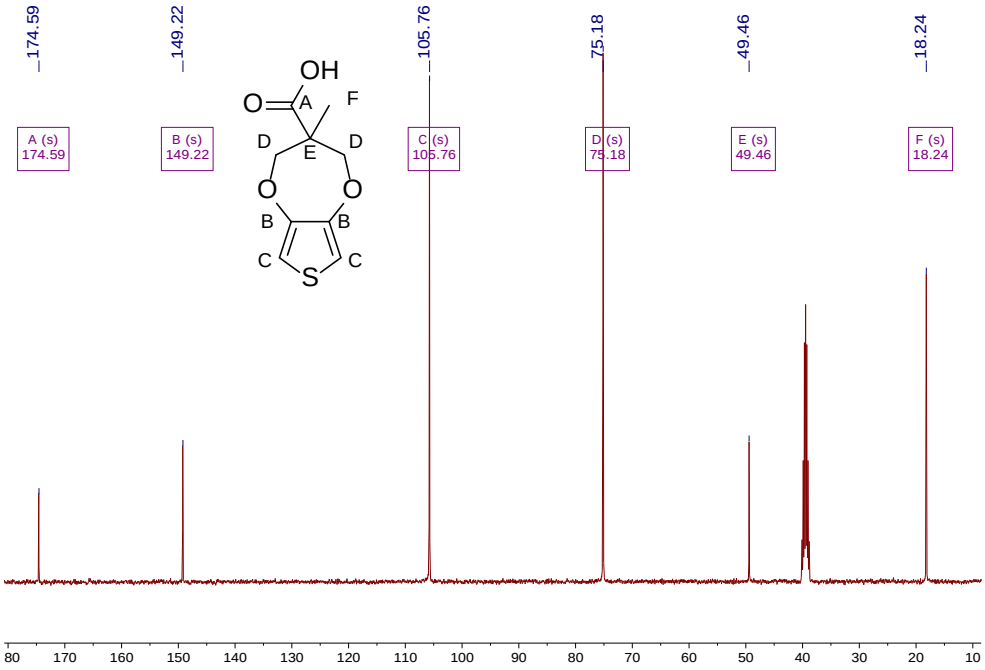

Figure 3.10 ^{13}C NMR of ProDOT-COOH (**3**)

*3.4.5 Synthesis of ProDOT-DA (**4**)*

In a round bottom flask, 0.5g (2.34 mmol, 1 eq) of ProDOT-COOH (**3**) has been dissolved in 30 mL of anhydrous DMF, together with diisopropylethylamine (DIPEA) 1.35 mL (10 mmol, 3.3 eq) and 1-[Bis(dimethylamino)methylene]-1H-1,2,3-triazolo[4,5-b]pyridinium 3-oxide hexafluorophosphate (HATU) 0.977 g (2.57 mmol, 1.1 eq). After 30 minutes 3,4-dihydroxyphenethylamine (Dopamine) 0.662 g (3.5 mmol, 1.5eq) has been added and let stirred overnight at room temperature. After, DMF was remove under vacuum and the product dissolve in 100mL of EtOAc. The organic phase was washed with water (3x50mL), dried over Na_2SO_4 and the solvent remove under vacuum, affording **4** as a yellow powder (0.69 g, 85%). Mp 126 °C. Ft-IR ν_{max}/cm^{-1} 3379 (NH), 3150 (OH, br), 3116 (=C-H), 2928 (C-H), 2702 (Ph), 1635 (C=O) and 1477 (C=C), 776 (C=S).

^{1}H NMR (400 MHz, DMSO-d6) δ 8.73 (s, 1H, HO-Ph), 8.62 (s, 1H, HO-Ph), 7.72 (t, J = 5.7 Hz, 1H, -NH-CO-), 6.75 (s, 2H, (-CH)$_2$-S), 6.69 – 6.52 (m, 2H, Ph), 6.42 (d, J = 8.1 Hz, 1H, Ph), 4.30 (d, J = 12.2 Hz, 2H, C-CH$_2$-C), 3.85 (d, J = 12.2 Hz,

2H, C-CH_2-C), 3.22 (q, J = 6.9 Hz, 2H, -NH-CH_2-CH_2-Ph), 2.62 – 2.43 (m, 2H, -NH-CH_2-CH_2-Ph), 1.10 (s, 3H, -CH_3) ppm. ^{13}C NMR (101 MHz, DMSO-d6) δ 172.01 , 149.35 , 145.06 , 143.52 , 130.19 , 119.38 , 116.05 , 115.46 , 105.81 , 75.66 , 49.54 , 40.94 , 34.54 , 18.26 ppm. HRMS *m/z* 372.0865 $[MNa]^+$.

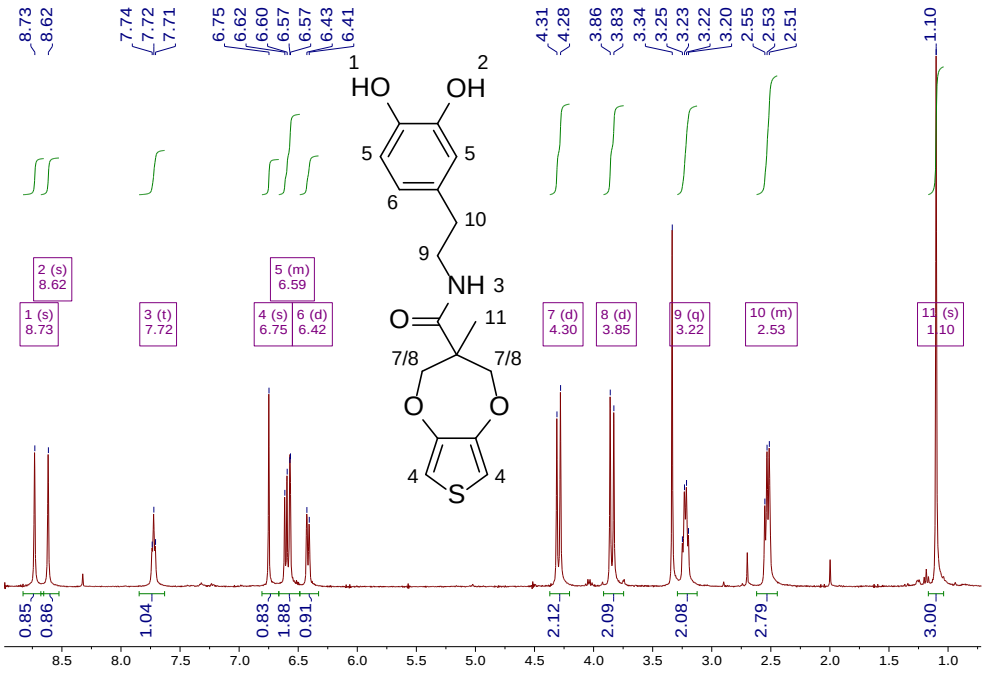

Figure 3.11 ^{1}H NMR of ProDOT-DA (**4**)

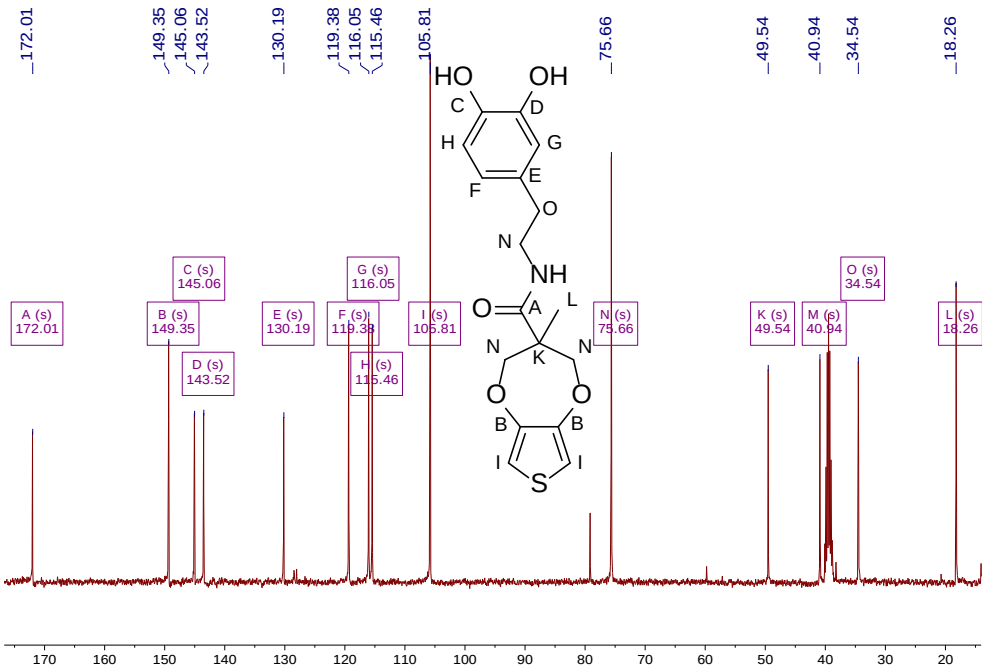

Figure 3.12 ^{13}C NMR of ProDOT-DA (**4**)

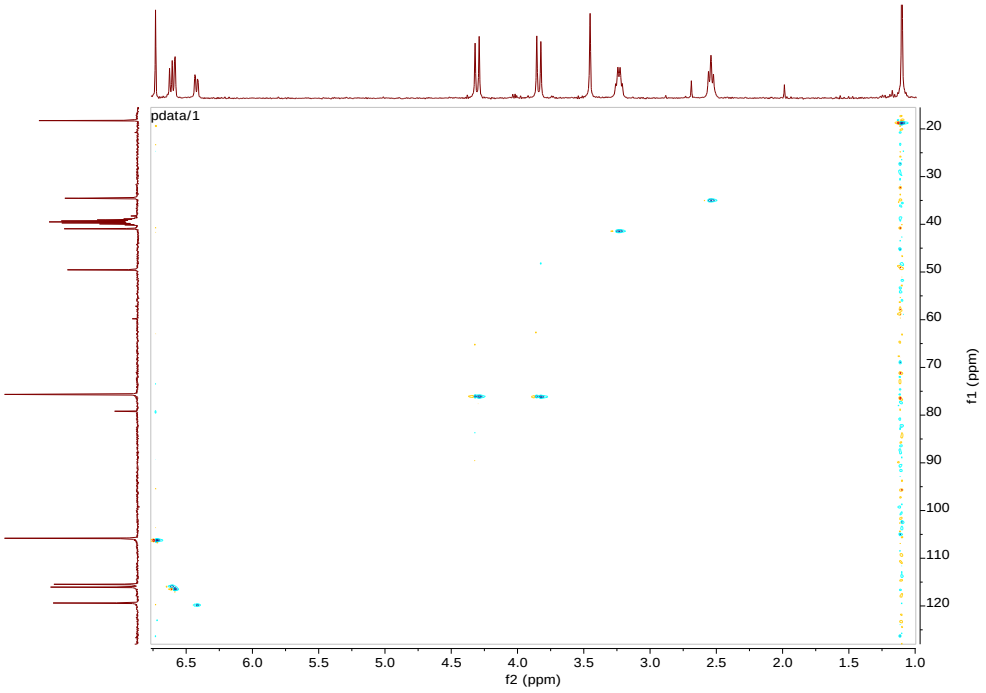

Figure 3.14 ^{1}H-^{13}C HSQC of ProDOT-DA (**4**)

*3.4.6 Synthesis of ProDOT-TEMPO (**5**)*

To a solution of ProDOT-COOH (**3**) 0.5g (2.34 mmol, 1 eq) in 75 mL of dry DCM, DCC 5.5 g (2.57 mmol, 1.1 eq) was added and let stirring for 30 minutes. Afterwards, 4-Hydroxy-TEMPO 0.489 g (2.80 mmol, 1.2 eq) and DMAP 0.029 g (0.23 mmol, 0.1 eq) were added and the reaction mixture was kept 24 h at room temperature. After the reaction completion, monitored by TLC, the reaction mixture was filtered, to eliminate the urea salts precipitated during the reaction. The product containing filtrate was diluted with extra 250 mL of DCM and rinsed 3 times with 100 mL of water. The organic phase was dried over Na_2SO_4, and concentrated. The concentrated product was loaded onto a silica gel column and purified by flash column chromatography using a mixture of hexane:EtOAc 8:2 (Rf=0.46) to give **5** as an orange powder (0.72 g, 84 %). Mp 104 °C. Recrystallization could be performed using Hexane/DCM, affording deep reddish crystals CDCC 1530781. Ft-IR ν_{max}/cm^{-1} 3108 (=C-H), 2973, 2936 (C-H), 1716 (C=O) and 1474 (C=C), 1129, 1025, (N-O·). ^{1}H NMR (400 MHz, Ph-NHNH2, DMSO-d6) δ ≈6.75 (Ph-$NHNH_2$ overlapped), 5.03 (t, J = 11.5 Hz, 1H, -O-C*H*-$(CH_2)_2$), 4.37 (d, J = 12.2 Hz, 2H, C-CH_2-C), 3.84 (d, J = 12.2 Hz, 2H, C-CH_2-C), 1.87 (dd, J = 12.2, 4.0 Hz, 2H, -O-CH-(C*H*$_2)_2$), 1.50 (t, J = 11.8 Hz, 2H, -O-CH-(C*H*$_2)_2$), 1.15 – 1.08 (m, 12H, $(CH_3)_4$) ppm. ^{13}C NMR (101 MHz, Ph-$NHNH_2$, DMSO-d6) δ 172.30 , 149.23 , 106.04 , 74.97 , 67.21 , 57.92 , 49.89 , 43.33 , 31.97 , 20.54 , 18.02 ppm. HRMS *m/z* 391.1424 $[MNa]^+$.

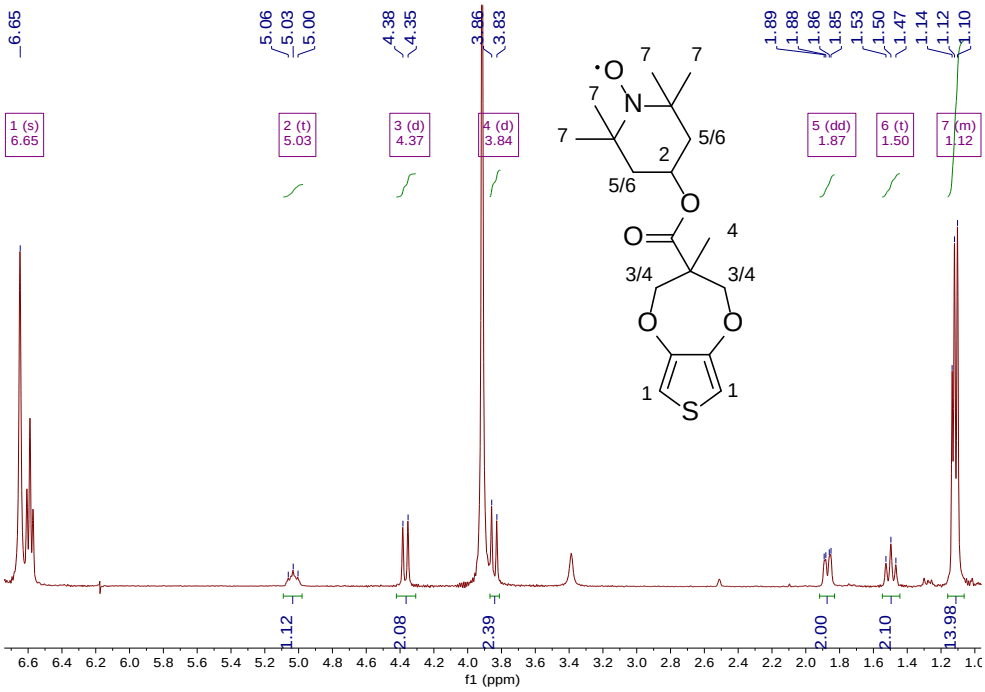

Figure 3.15 ^{1}H NMR of ProDOT-TEMPO (**5**)

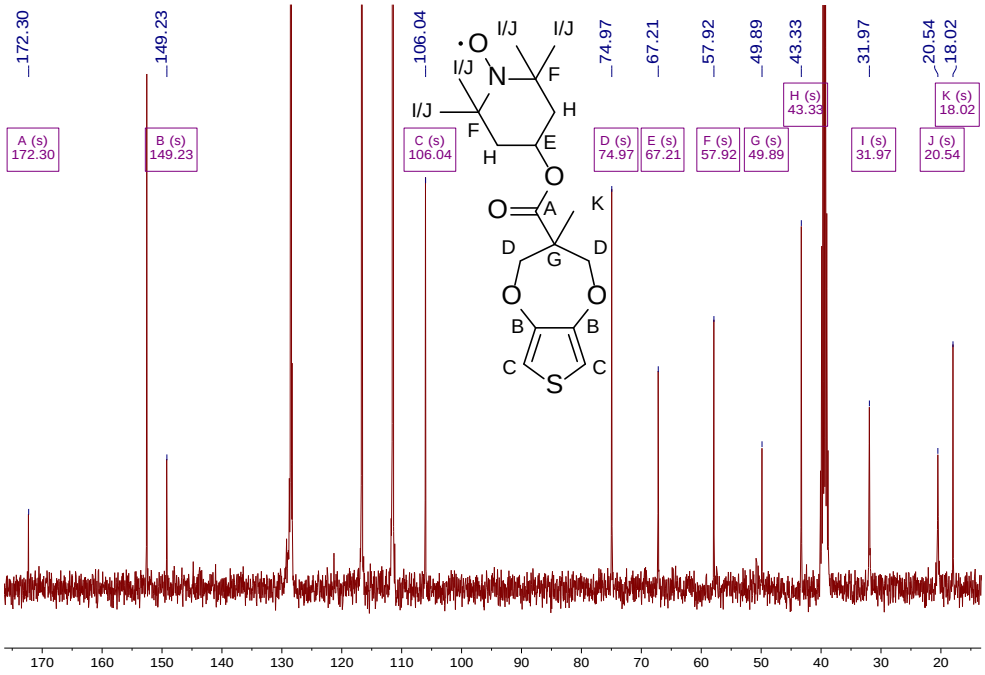

Figure 3.16 ^{13}C NMR of ProDOT-TEMPO (**5**)

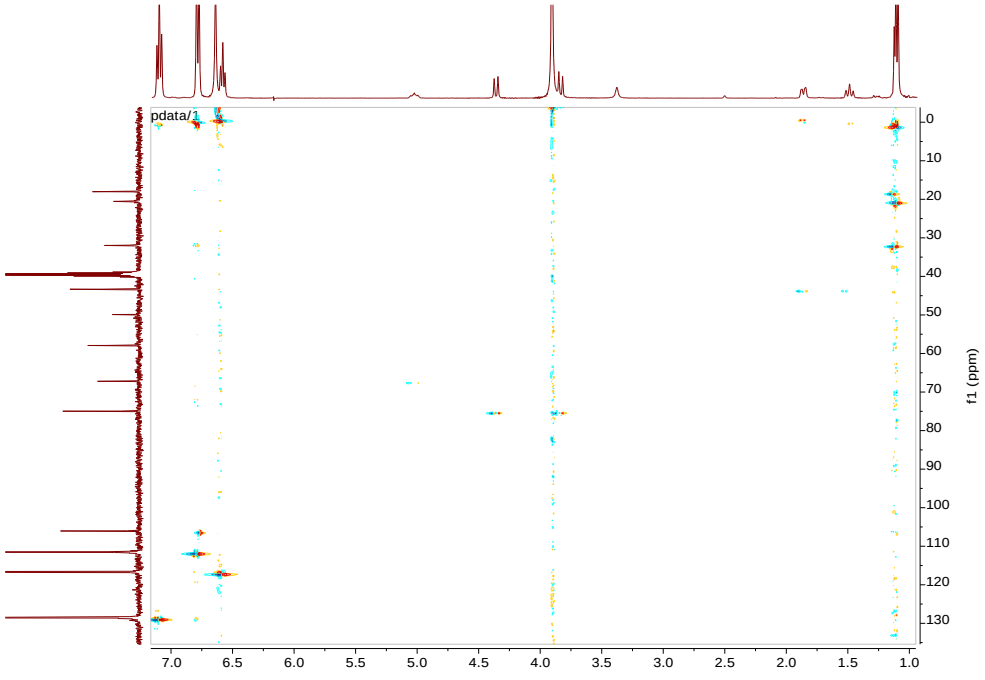

Figure 3.17 ^{1}H-^{13}C HSQC of ProDOT-TEMPO (**5**)

*3.4.7 Synthesis of ProDOT-TEG (**6**)*

In a round bottom flask, 0.5g (2.34 mmol, 1 eq) of ProDOT-COOH (**3**) has been dissolved in 30 mL of anhydrous DMF, together with diisopropylethylamine (DIPEA) 0.829 mL (10 mmol, 2.04 eq) and 1-[Bis(dimethylamino)methylene]-1H-1,2,3-triazolo[4,5-b]pyridinium 3-oxide hexafluorophosphate (HATU) 0.906 g (2.38 mmol, 1.02 eq). After 30 minutes Tetraethylene glycol (TEG) 12.43 mL (3.5 mmol ,10 eq) has been added and let stirred overnight at room temperature. After, DMF was remove under vacuum and the product dissolve in 100mL of EtOAc. The organic phase was washed with water (3x50mL), dried over Na_2SO_4 and the solvent remove under vacuum, affording **6** as a light brown viscous oil (0.67 g, 74%). Ft-IR v_{max}/cm-1 3448 (-OH), 3111 (=C-H), 2859 (C-H), 1726 (C=O) and 1472 (C=C), 1028, (-C-O-).

^{1}H NMR (400 MHz, DMSO-d_6) δ 6.76 (s, 2H, (-CH)$_2$-S), 4.57 (t, *J* = 5.5 Hz, 1H, -OH), 4.35 (d, *J* = 12.2 Hz, 2H, C-C*H*$_2$-C), 4.22 (t, *J* = 4.8 Hz, 2H, CO-O-CH$_2$), 3.85 (d, *J* = 12.2 Hz, 2H, C-C*H*$_2$-C), 3.62 (t, *J* = 4.8 Hz, 2H, -C*H*$_2$-OH), 3.56 – 3.44 (m, 10H, -O-C*H*2-C*H*2-O), 3.40 (t, *J* = 5.2 Hz, 2H, -O-C*H*2-C*H*2-O), 1.15 (s, 3H, -CH$_3$) ppm. ^{13}C NMR (101 MHz, DMSO-d_6) δ 172.76 , 149.17 , 106.02 , 74.94 , 72.33 , 69.81 , 69.75 , 68.11 , 63.90 , 60.20 , 49.99 , 18.07 ppm. HRMS *m/z* 413.1257 [MNa]$^+$.

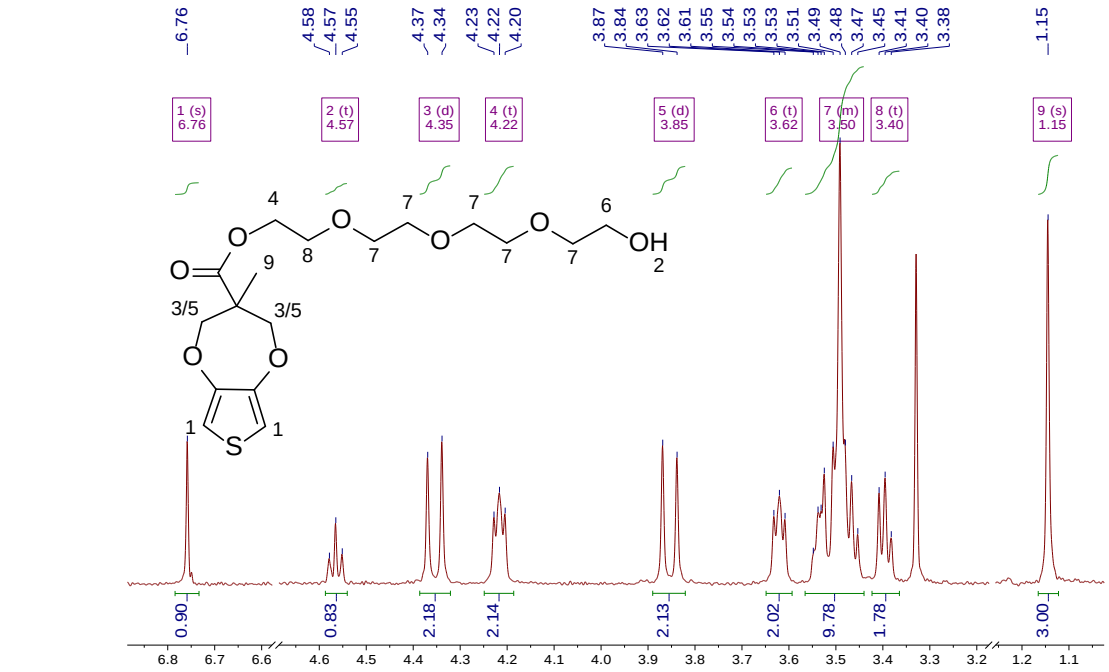

Figure 3.18 ^{1}H NMR of ProDOT-TEG (**6**)

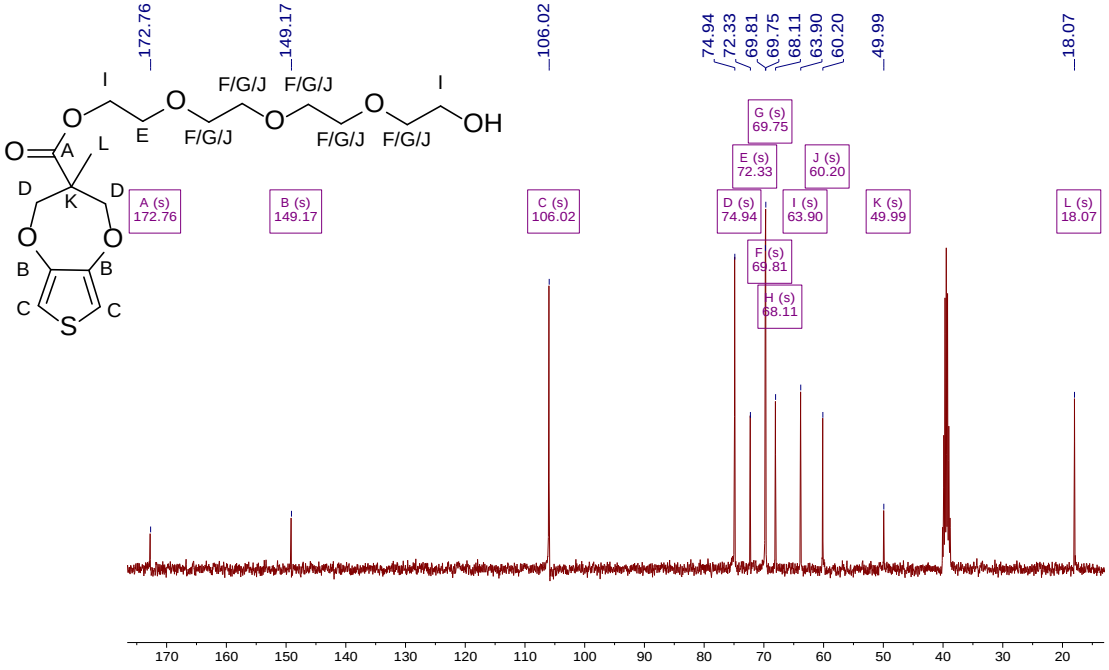

Figure 3.19 ^{13}C NMR of ProDOT-TEG (**6**)

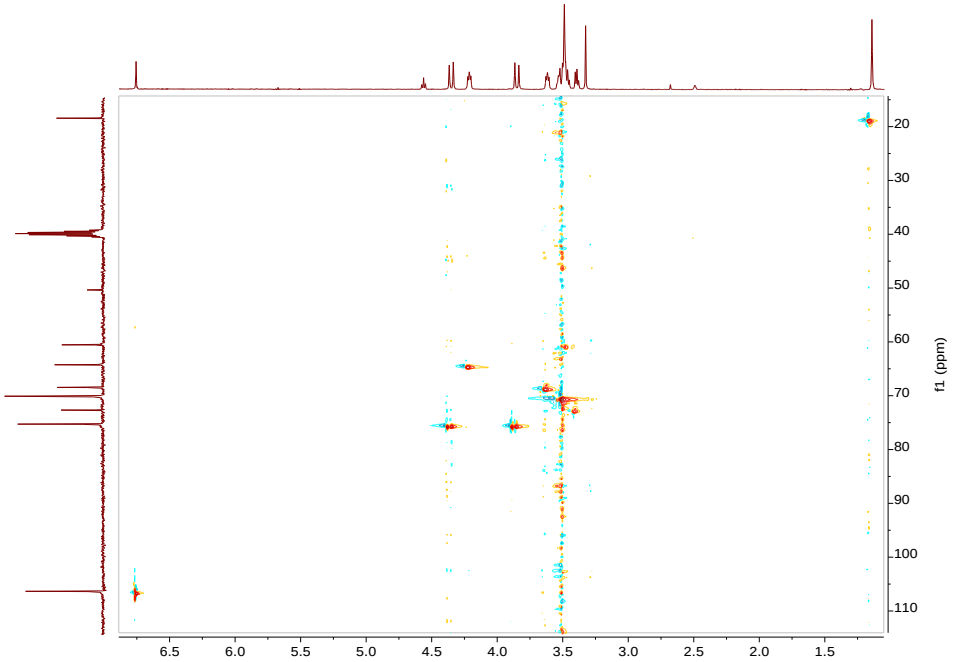

Figure 3.20 ^{1}H-^{13}C HSQC of ProDOT-TEG (**6**)

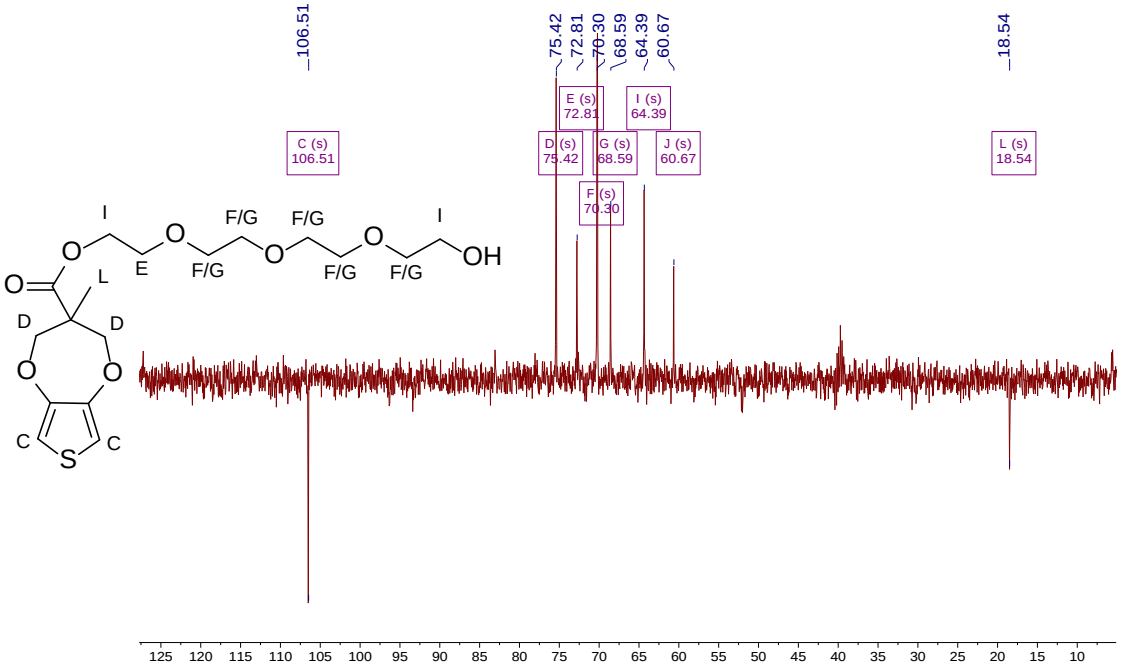

Figure 3.21 ^{13}C DEPT-135 of ProDOT-TEG (**6**)

3.4.8 Crystallography information

Intensity data were collected on an Agilent Technologies Super-Nova diffractometer, which was equipped with monochromated Cu ka radiation (l= 1.54184 Å) and Atlas CCD detector. Measurement was carried out at 150.00(10) K with the help of an Oxford Cryostream 700 PLUS temperature device. Data frames were processed (united cell determination, analytical absorption correction with face indexing, intensity data integration and correction for Lorentz and polarization effects) using the Crysalis software package.[36] The structure was solved using Olex2[37] and refined by full-matrix least-squares with SHELXL-97.[38] Final geometrical calculations were carried out with Mercury[39] and PLATON[40] as integrated in WinGX.[41] For the ProDOT-TEMPO crystal there is a disorder in two positions of part of the one of the molecules (75/25) of the asymmetric unit. The measured crystal is a no merohedral twin. The structure has been refined as a 2-component twin (85/15 %) used hklf5 file of the majority component.

*ProDOT-COOH (**3**) CCDC 1530638*

Crystal Data		*Collection and Refinement*	
Formula	C9 H10 O4S1	Difractomet.	Agilent SuperNovaCu
Formula Weight	214.23	Detector	CCD (Atlas)
Crystal System	monoclinic	Temperature (K)	149.99(10)
Space group	P 2_1/n (No.14)	λ(CuKα) (Å)	1.54184
a (Å)	10.2478(2)	Monochromator	Multilayer optic
b (Å)	8.15230(10)	Collimator (mm)	0.2
c (Å)	12.1782(3)	Scan mode	ω rotation
α(°)	90	Scan width (°)	1.0
β(°)	112.322(2)	Time per frame(s)	(Total, h) 2;8 (14)
γ(°)	90	Interval of θ (°)	4.66, 69.95
V (Å^3)	941.16(3)	(hkl) minimum	(-12 -9 -15)
Z	4	(hkl) maximum	(12 9 15)
Dx (g·cm^{-3})	1.512	Reflections measures	7253
μ (CuKα) (mm^{-1})	2.98	Reflections ind.($R_{int.}$)	1762(0.026)
F (000)	448	Reflections observ. [I>2σ (I)]	1706
Morphology	prism	Absorption correction	Analytical
Colour	colourless	Solution	OLEX2
Size (mm)	0.31 x 0.41 x 0.49	Refinement	SHELXL97(14/7)
		Number of parameters	129
		Number of restrictions	0
		Δ/σmaximum	0.000
		Δ/σmedium	0.000
		Δρmaximum (eÅ^{-3})	0.184
		Δρminimum (eÅ^{-3})	-0.226
		S (GOF)	1.054
		Secondary extinction coeff.[b]	0
		R(F) (I>2σ_I, all)	0.0310, 0.0320
		Rw(F2)[a] (I>2σ_I ,all)	0.0801, 0.0802

[a] Refine weighting: $1/[\sigma 2(Fo^2)+(0.0435P)^2+ 0.4880P]$ where $P = [Max(F_o^2,0)+2F_c^2]/3$.
[b] Secondary extinction type SHELXL: $F_c^* = kF_c[1+0.001F_c^2\lambda^3/sen(2\theta)]^{-1/4}$

*ProDOT-TEMPO (**5**) CCDC 1530781*

Crystal Data		*Collection and Refinement*	
Formula	C18 H26 N1 O5 S1	Difractomet.	Agilent SuperNova Cu
Formula Weight	368.46	Detector	CCD (Atlas)
Crystal System	monoclinic	Temperature (K)	150.01(4)
Space group	P 2_1/n (No.14)	λ(CuKα) (Å)	1.54184
a (Å)	6.1625(2)	Monochromator	Multilayer optic
b (Å)	61.602(2)	Collimator (mm)	0.2
c (Å)	9.9660(3)	Scan mode	ω rotation
α(°)	90	Scan width (°)	1.0
β(°)	94.243(3)	Time per frame(s)	(Total, h) 2;8 (14)
γ(°)	90	Interval of θ(°)	2.89, 69.00
V (Å^3)	3773.0(2)	(hkl) minimum	(-6 -74 -11)
Z(Z')	8(2)	(hkl) maximum	(2 69 12)
Dx (g·cm^{-3})	1.297	Reflections measures	32949
μ (CuKα) (mm^{-1})	1.754	Reflections ind. ($R_{int.}$)	7293(0.082)
F (000)	1576	Reflections observ. [I>2σ (I)]	6164
Morphology	prism	Absorption correction	Analytical
Colour	orange	Solution	OLEX2
Size (mm)	0.29 x 0.26 x 0.15	Refinement	SHELXL97(14/7)
		Number of parameters	480
		Number of restrictions	30
		Δ/σmaximum	0.001
		Δ/σmedium	0.000
		Δρmaximum (eÅ^{-3})	0.561
		Δρminimum (eÅ^{-3})	-0.594
		S (GOF)	1.174
		Secondary extinction coeff.[b]	0
		R(F) (I>2σ$_I$, all)	0.0917, 0.1008
		Rw(F2)[a] (I>2σ$_I$,all)	0.2507, 0.2548

[a] Refine weighting: $1/[\sigma 2(Fo^2)+(0.0435P)^2+ 0.4880P]$ where $P = [Max(F_o^2,0)+2F_c^2]/3$.
[b] Secondary extinction type SHELXL: $F_c^* = kF_c[1+0.001F_c^2\lambda^3/sen(2\theta)]^{-1/4}$

3.4.9 Electrochemical measurements

The electrochemical polymerization and characterization were performed on an Autolab PGSTAT302N by using the standard three-electrode configuration with platinum sheets (with an area of 1 cm^2) as working and counter electrodes and an Ag/AgCl (3 M KCl) as reference electrode.

The electrochemical polymerizations of ProDOT-COOH and ProDOT-TEG monomers were investigated by cyclic voltammetry in 0.1 M $TBAClO_4$ acetonitrile and 0.1 M $TBAClO_4$ DCM solution, respectively. On the other hand, the electrochemical polymerizations of ProDOT-TEMPO and ProDOT-DA were studied by chronoamperometry, applying 1.7 V for 30 minutes in 0.1 M $TBAClO_4$ DCM and 0.1 M $TBAClO_4$ acetonitrile solution, respectively. The monomer concentration used was 10^{-2} M for all the cases.

3.5 References

(1) Rivnay, J.; Owens, R. M.; Malliaras, G. G. *Chem. Mater.* **2014**, *26* (1), 679.
(2) Berggren, M.; Richter-Dahlfors, A. *Adv. Mater.* **2007**, *19* (20), 3201.
(3) Martin, D. C.; Malliaras, G. G. *ChemElectroChem* **2016**, *3* (5), 686.
(4) Asplund, M.; Nyberg, T.; Inganäs, O. *Polym. Chem.* **2010**, *1* (9), 1374.
(5) Feldman, K. E.; Martin, D. C. *Biosensors* **2012**, *2* (4), 305.
(6) Martin, D. C.; Povlich, L. K.; Feldman, K. E. *Mater. Matters* **2010**, *5.3*, 68.
(7) NG, S. C.; CHAN, H. S. O.; YU, W.-L. *J. Mater. Sci. Lett.* **1997**, *16* (10), 809.
(8) Caras-Quintero, D.; Bäuerle, P. *Chem. Commun.* **2002**, No. 22, 2690.
(9) Povlich, L. K.; Cho, J. C.; Leach, M. K.; Corey, J. M.; Kim, J.; Martin, D. C. *Biochim. Biophys. Acta - Gen. Subj.* **2013**, *1830* (9), 4288.
(10) Bu, H.-B.; Götz, G.; Reinold, E.; Vogt, A.; Schmid, S.; Blanco, R.; Segura, J. L.; Bäuerle, P. *Chem. Commun.* **2008**, No. 11, 1320.
(11) Stéphan, O.; Schottland, P.; Le Gall, P.-Y.; Chevrot, C.; Mariet, C.; Carrier, M. *J. Electroanal. Chem.* **1998**, *443* (2), 217.
(12) Kumar, A.; Welsh, D. M.; Morvant, M. C.; Piroux, F.; Abboud, K. A.; Reynolds, J. R. *Chem. Mater.* **1998**, *10* (13), 896.
(13) Damaceanu, M.-D.; Gilsing, H.-D.; Schulz, B.; Arvinte, A.; Bruma, M. *RSC Adv.* **2014**, *4* (94), 52467.
(14) Godeau, G.; Ben Taher, Y.; Pujol, M.; Guittard, F.; Darmanin, T. *J. Fluor. Chem.* **2016**, *191*, 90.
(15) Mishra, S. P.; Sahoo, R.; Ambade, A. V.; Contractor, A. Q.; Kumar, A. *J. Mater. Chem.* **2004**, *14* (12), 1896.
(16) Mawad, D.; Artzy-Schnirman, A.; Tonkin, J.; Ramos, J.; Inal, S.; Mahat, M. M.; Darwish, N.; Zwi-Dantsis, L.; Malliaras, G. G.; Gooding, J. J.; Lauto, A.; Stevens, M. M. *Chem. Mater.* **2016**, *28* (17), 6080.
(17) Wolfs, M.; Darmanin, T.; Guittard, F. *Eur. Polym. J.* **2013**, *49* (8), 2267.
(18) Rodríguez-Calero, G. G.; Conte, S.; Lowe, M. A.; Gao, J.; Kiya, Y.; Henderson, J. C.; Abruña, H. D. *Electrochim. Acta* **2015**, *167*, 55.
(19) Sahoo, R.; Mishra, S. P.; Kumar, A.; Sindhu, S.; Narasimha Rao, K.; Gopal, E. S. R. *Opt. Mater. (Amst).* **2007**, *30* (1), 143.
(20) Mantione, D.; Casado, N.; Sanchez-Sanchez, A.; Sardon, H.; Mecerreyes, D. *J. Polym. Sci. Part A Polym. Chem.* **2017**, *55* (17), 2721.
(21) Appel, R.; Fuchs, J.; Tyrrell, S. M.; Korevaar, P. A.; Stuart, M. C. A.; Voets, I. K.; Schönhoff, M.; Besenius, P. *Chem. - A Eur. J.* **2015**, *21* (52), 19257.
(22) Kim, J.; Kim, B.; Anand, C.; Mano, A.; Zaidi, J. S. M.; Ariga, K.; You, J.; Vinu, A.; Kim, E. *Angew. Chemie Int. Ed.* **2015**, *54* (29), 8407.
(23) Diouf, A.; Darmanin, T.; Dieng, S. Y.; Guittard, F. *J. Colloid Interface Sci.* **2015**, *453*, 42.
(24) Godeau, G.; Amigoni, S.; Darmanin, T.; Guittard, F. *Appl. Surf. Sci.* **2016**, *387*, 28.
(25) Darmanin, T.; Guittard, F. *Mater. Chem. Phys.* **2014**, *146* (1), 6.

(26) Otley, M. T.; Alamer, F. A.; Zhu, Y.; Singhaviranon, A.; Zhang, X.; Li, M.; Kumar, A.; Sotzing, G. A. *ACS Appl. Mater. Interfaces* **2014**, *6* (3), 1734.
(27) Welsh, D. M.; Kloeppner, L. J.; Madrigal, L.; Pinto, M. R.; Thompson, B. C.; Schanze, K. S.; Abboud, K. A.; Powell, D.; Reynolds, J. R. *Macromolecules* **2002**, *35* (17), 6517.
(28) Patil, N.; Falentin-Daudré, C.; Jérôme, C.; Detrembleur, C. *Polym. Chem.* **2015**, *6* (15), 2919.
(29) Milroy, C. A.; Manthiram, A. *ACS Energy Lett.* **2016**, *1* (4), 672.
(30) Casado, N.; Hernández, G.; Veloso, A.; Devaraj, S.; Mecerreyes, D.; Armand, M. *ACS Macro Lett.* **2016**, *5* (1), 59.
(31) Hou, S.; Burton, E. A.; Simon, K. A.; Blodgett, D.; Luk, Y.-Y.; Ren, D. *Appl. Environ. Microbiol.* **2007**, *73* (13), 4300.
(32) Abraham, K. M.; Jiang, Z.; Carroll, B. *Chem. Mater.* **1997**, *9* (9), 1978.
(33) Jung, H.-G.; Hassoun, J.; Park, J.-B.; Sun, Y.-K.; Scrosati, B. *Nat. Chem.* **2012**, *4* (7), 579.
(34) *N,N'-dicyclohexylcarbodiimide - 4-dimethylaminopyridine; HATU - N,N-diisopropylethylamine*.
(35) Ihre, H.; Hult, A.; Fréchet, J. M. J.; Gitsov, I. *Macromolecules* **1998**, *31* (13), 4061.
(36) CrysAlisPro, Agilent Technologies, Version 1.171.37.31 (release 14-01-2014 CrysAlis171 .NET)(compiled Jan 14 2014, 18:38:05). .
(37) Dolomanov, O. V.; Bourhis, L. J.; Gildea, R. J.; Howard, J. A. K.; Puschmann, H. *J. Appl. Crystallogr.* **2009**, *42* (2), 339.
(38) Sheldrick, G. M. *Acta Crystallogr. Sect. A Found. Crystallogr.* **2008**, *64* (1), 112.
(39) Macrae, C. F.; Bruno, I. J.; Chisholm, J. A.; Edgington, P. R.; McCabe, P.; Pidcock, E.; Rodriguez-Monge, L.; Taylor, R.; van de Streek, J.; Wood, P. A. *J. Appl. Crystallogr.* **2008**, *41* (2), 466.
(40) Spek, A. L. *J. Appl. Crystallogr.* **2003**, *36* (1), 7.
(41) Farrugia, L. J. *J. Appl. Crystallogr.* **1999**, *32* (4), 837.

Conclusions

During this Ph.D. thesis, I put my efforts into developing new materials/routes which overcome some of the actual limitations of the successful PEDOT:PSS dispersion. As we have seen in literature, this conductive polymer has been used and is still in use in many fields: from bioelectronic to chemistry, from electronical engineering to the modern medicine. The scientific community is searching new strategies to improve and enhance different properties of this young material in order to create day by day better devices and innovative tools.

Bioelectronic, nowadays an emerging field, is demanding innovative materials to create futuristic devices like brain implants or smart tissues. PEDOT:PSS is today the best candidate. Due to its conductivity, mechanical properties, transparency and ease of handling, PEDOT:PSS has become the gold standard. In this work we have develop new PEDOT:PSS-base and -like materials, for bioelectronic applications. New materials or synthetic routes in order to overcome some of the limitations of PEDOT:PSS such as low biocompatibility, cross-linking strategies or new (bio)functional polymers have been investigated. Following this, the thesis was divided in three chapters, each one concerning one modification as discussed bellow.

In the first chapter, we have presented a simple synthetic strategy to create PEDOT dispersion doped with glycosaminoglycans biopolymers. The resulting multi-purpose conductive suspensions were broadly characterized by following the kinetics of the reaction, DLS and UV-Vis-NIR. PEDOT/GAGS materials assessed not only biocompatibility in terms of cell viability, but also do not interfere with physiological functions using cell line CCF-STTG1 and SH-SY5Y. A remarkable observation was that the novel PEDOT:GAGs were shown to be more supportive for neuroregenerative processes, compared to commercial PEDOT:PPS, as shown by longer neurite length of differentiated SH-SY5Y cells. In addition, was shown where SH-SY5Y cells were partially protected from H_2O_2 induced cell death.

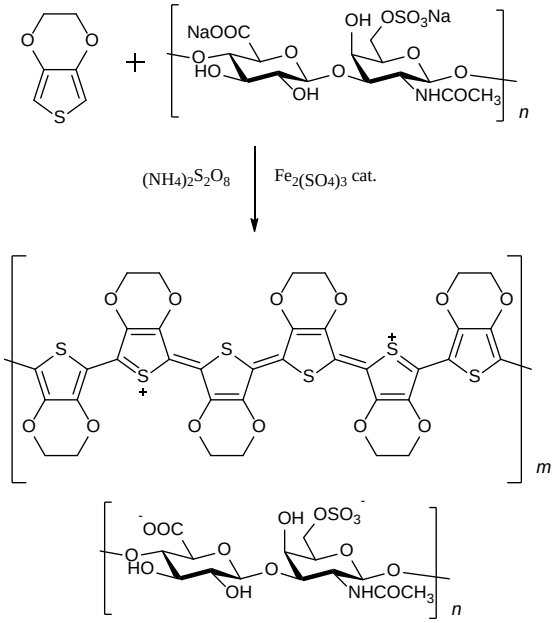

Figure C.1 Schematic representation of cross-linking reaction of PEDOT:PSS film by DVS. a) Oxidative chemical polymerization of EDOT with GAG (e.g. CS).

In the second chapter, we have presented DVS as an outstanding PEDOT:PSS cross-linker, providing better properties than the currently employed silane derivate GOPS. The PEDOT:PSS:DVS has been characterized physical-chemically by UV-Vis-NIR, Raman and IR spectroscopy. Conductivity measurements conducted on the dried material confirm the high applicability, giving a result of more than the double, up to 600 S cm^{-1} (at 3% v/v) in respect to GOPS, and confirming that the addition of more cross-linker does not affect the conductivity. Biocompatibility assays were performed using L929 and SH-SY5Y cell lines, measuring cytotoxicity, proliferation and neurite length, showing full biocompatibility and better support for neuroregeneration when compared to GOPS cross-linked material. To show the applicability of PEDOT:PSS:DVS, the creation of an OECT and the measure of transconductance was tested. PEDOT:PSS:DVS channel values are high in the short and long term. This finding shows its applicability in *in vivo* recording measurements.

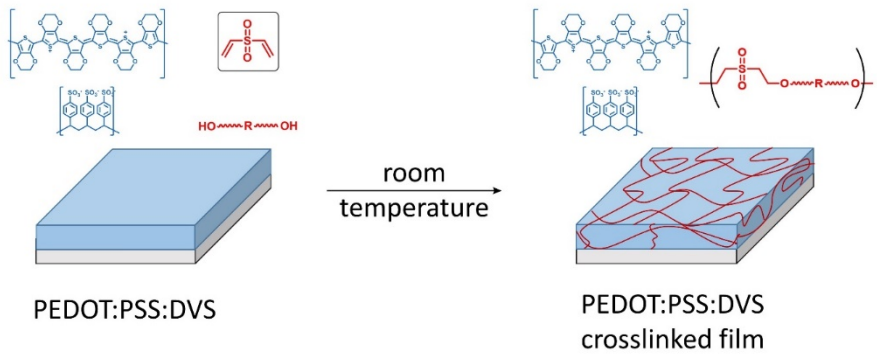

Figure C.2 Schematic representation of cross-linking reaction of PEDOT:PSS film by DVS.

In the third chapter, we presented a simple way to synthesize an easy functionalizable new ProDOT base molecule, bearing a carboxylic acid. The synthesis already present in literature consists of many steps, needing a strong

organic chemistry background. In this chapter, we present a two steps synthesis, that could be performed also without a deep knowledge in organic synthesis. This molecule has been polymerized chemically and electrochemically. Even in the absence of surfactant, the chemically polymerized suspension presents a quite high conductivity, due to the absence of an insulator part. Using ProDOT-COOH as reagent, we synthetized three new functional ProDOT molecules. The new ProDOT molecules were functionalized with electroactive dopamine or TEMPO moieties, or biologically relevant tetraethylene glycol. These ProDOT monomers were electropolymerized to demonstrate the possibility to create functional conductive electroactive materials and to demonstrate the really presence of the electroactive species like dopamine and TEMPO.

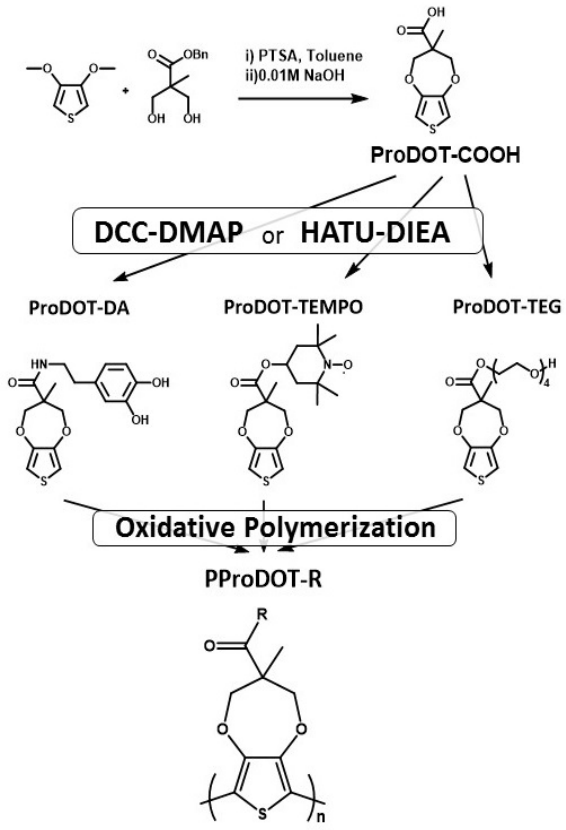

Figure C.3 ProDOT-COOH synthesis and functionalization using, Dopamine Hydrochloride, 4-hydroxy-TEMPO and Tetraethylene glycol.

Resumen

Cuando hablamos de materiales poliméricos o plásticos es de sentido común asociarlos con aislantes térmicos y eléctricos. De hecho, desde pequeños, en la escuela, nos enseñan como los hilos de cobre y, en general, los aparatos electrónicos, están cubiertos de plástico para poderlos manejar. Pero eso es sólo parcialmente correcto. Si hablamos cronológicamente, el primer material polimérico era capaz de conducir la electricidad. ¿Raro? Empecemos a explorar ese mundo desde el principio.

El primer plástico ampliamente conocido es la Bakelita, un buen aislante, que fue desarrollada por Leo Bakeland en Yonkers, cerca de Nueva York en 1907 (**Esquema R.1a**).[1] Sin embargo, hay que resaltar que el primer material polimérico fue sintetizado por H. Letheby en el Hospital de Londres casi cincuenta años antes. Sin darse cuenta este profesor sintetizó un material oscuro, aparentemente no muy útil, utilizando una solución de anilina y poniendo electricidad entre dos electrodos de platino (**Esquema R.1b**).[2] Ese fue el primer gran descubrimiento en la historia de los polímeros y de los polímeros conductores.

Hoy en día, el descubrimiento más reseñable de los polímeros conductores se debe a tres investigadores, que ganaron el premio nobel en química en el año 2000: Alan J. Heeger, Alan MacDiarmid and Hideki Shirakawa.[3] En 1977 los

tres completaron lo que se entiende como el primer artículo científico completo sobre los polímeros conductores. En el artículo hablan de un derivado de poliacetileno, que oxidándose, genera un polímero con una excelente conductividad eléctrica.

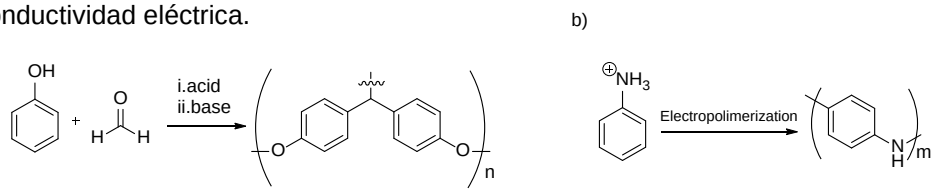

Esquema R.1 a) reacción y estructura de la Bakelite, b) reacción de polimerización electroquímica de la anilina.

Numerosas publicaciones científicas han seguido en la literatura de las últimas décadas este trabajo, intentando mejorar dos factores: la conductividad y la estabilidad. El desafío más grande fue la lucha contra la estabilidad de los polímeros conductores en medio acuoso. Muchos de esos polímeros, o no eran estables, o no podían ni tan siquiera ser expuestos a la humedad. La solución llego cuando los investigadores de Bayer Jonas Heywang y Werner Schmidtberg patentaron en 1988 el poli-3,4-etilenedioxotiofeno (PEDOT) el protagonista principal de esta historia.[4] Una semana después publicaron otra patente donde lo sintetizaban directamente en agua, utilizando como estabilizante y/o dopante otro polímero el poliestireno sulfonado (PSS).[5] En el **Esquema R.2** podemos ver como la cadena de polímero conductor, cargada positivamente, es estabilizada por el poliestireno cargado negativamente. Actualmente este material es vendido por diferentes empresas, las cuales han optimizado la formulación para crear un material estable, con una alta conductividad y que se puede utilizar en diferentes campos. Podemos dividir las áreas de aplicación del PEDOT:PSS en diferentes sectores como por ejemplo la electrónica y energía, optoelectrónica y salud. En electrónica se utiliza como agente antiestático o como recubrimiento transparente y conductor en diferentes dispositivos electrónicos como móviles o tabletas. En el campo de la optoelectrónica las aplicaciones son muy diversas desde células solares, transistores, a ventanas inteligentes de tipo electrocrómico a dispositivos

emisores de luz (OLEDs). En el campo de la salud las aplicaciones son muy variadas como sensores de H_2O_2 and O_2,[6] NO_2,[7] and O_3[8], humedad,[9] acidez,[10] concentraciones de iones,[11] y una larga variedad de moléculas biológicas como encimas,[12] anticuerpos[13] y ácido desoxirribonucleico (DNA).[14]

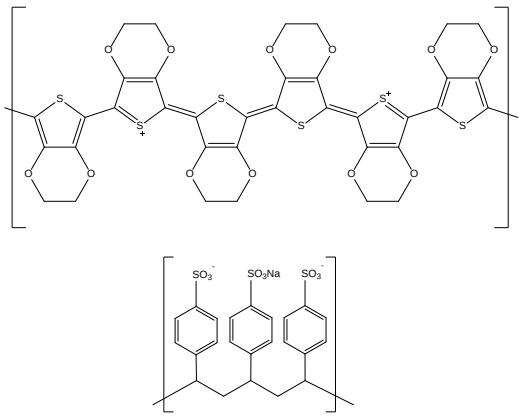

Esquema R.2 PEDOT:PSS.

La bioelectrónica, disciplina donde la biología y la electrónica se unen, ofrece un gran número de oportunidades de aplicación de nuevos materiales que combinan biocompatibilidad, biofuncionalidad, naturaleza “soft”, conductividad eléctrica o iónica. A día de hoy el PEDOT:PSS es el material más utilizado en diferentes dispositivos bioelectrónicos como biosensores, OTFTs (transitores orgánicos), sensores cutáneos y sondas cerebrales.[15] Sin embargo, el PEDOT:PSS tiene una serie de limitaciones como su falta de biocompatibilidad, la necesidad de un proceso de reticulación para estabilizarlo en medio acuoso o la escasa biofuncionalidad. Por esta razón, el objetivo principal de esta tesis ha sido modificar la formulación y la estructura de PEDOT:PSS hacia un material con mejores prestaciones en bioelectrónica. Como sugiere la **Figura R.1**, hemos dividido el trabajo en tres partes.

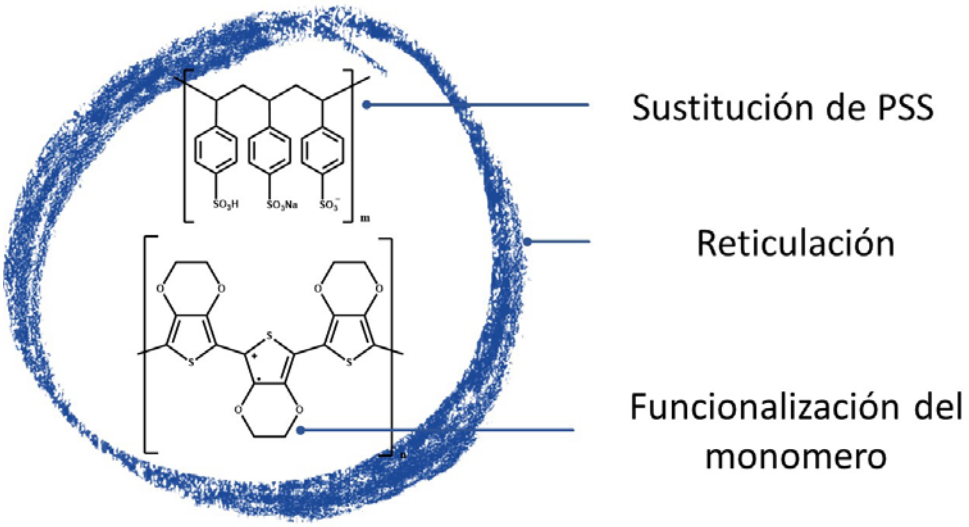

Figura R.1 Esquema de los capítulos.

En el primer capítulo hemos sustituido el polímero aniónico PSS con otros más bio-tolerante. El PSS presenta, en disolución con PEDOT, protones residuales junto a los grupos sulfonados que dañan las células y reducen la compatibilidad del material final. Buscando en la literatura una clase de polímeros naturalmente biocompatibles y cargados negativamente, nos hemos encontrado con los Glicosaminoglicanos (GAGs). Estos polímeros están presentes en nuestro cuerpo y llevan grupos sulfonatos y carboxilatos, los cuales pueden interaccionar con la cadena de PEDOT y estabilizar la carga positiva como se observa en el **Esquema R.3**. Durante la tesis hemos sintetizado una serie de dispersiones de PEDOT:GAGS con ácido hialurónico, sulftato de condroitina y Heparina. Sustituyendo el PSS con los GAGs, obtuvimos materiales que presentaron conductividad ligeramente más baja, pero con mejor bio-compatibilidad. En el caso de los materiales de PEDOT:sulfato de condroitina, es posible añadir al material un efecto antiinflamatorio muy útil en vista de un implante corporal, para contrastar la inflamación resultante.

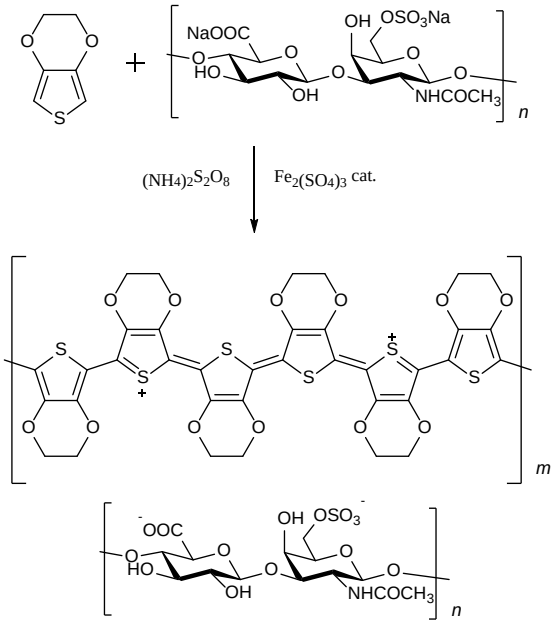

Esquema R.3 Esquema de polimerización oxidativa de EDOT con sulfato de condroitina.

En el segundo capítulo nos hemos enfocado en introducir en la formulación de PEDOT:PSS un nuevo agente reticulante. El PEDOT:PSS es una dispersión acuosa, una vez secado el material, si lo introducimos de nuevo en un ambiente acuoso se re-disolverá. Para solucionar este problema necesitamos de un agente reticulante. El reactivo más utilizado es un derivado del silicio, el glicidoxipropiltrimetóxi silane (GOPS). Las desventajas de este silano, es que es muy difícil de quitar el exceso y que la reticulación reduce la conductividad final del material. En nuestro caso utilizamos otro tipo de molécula orgánica con base divinilica. El divinilsulfona (DVS), es un reticulante muy conocido en bioquímica, que se utiliza para reticular, biomoléculas. Sustituyendo GOPS por DVS, se puede llegar a una conductividad tres veces mayor, sin perder propiedades mecánicas. El exceso es fácil de quitar, porque el punto de ebullición del compuesto divinilico es 25ºC á 2mmHg contra los 120ºC á 2mmHg del GOPS (**Figura R.2**). Se investigó el uso de PEDOT:PSS reticulado

con DVS en transistores orgánicos, los cuales demostraron ser muy estables a lo largo de los días en contacto con una solución acuosa de tampón fosfato. Estas condiciones abren las puertas para poder utilizar estos materiales directamente en contacto con células. Para comprobar eso, se ha medido la biocompatibilidad utilizando L929 fibroblastos, unas células comunes en nuestro tejido conectivo y en los músculos y utilizando SH-SY5Y. Estas últimas son células que simulan células cerebrales. Los resultados de biocompatibilidad han sido buenos para la primera categoría de células y excelente para la segunda. El DVS, no crea una red extraña como el GOPS y deja que esta categoría de células crezca más.

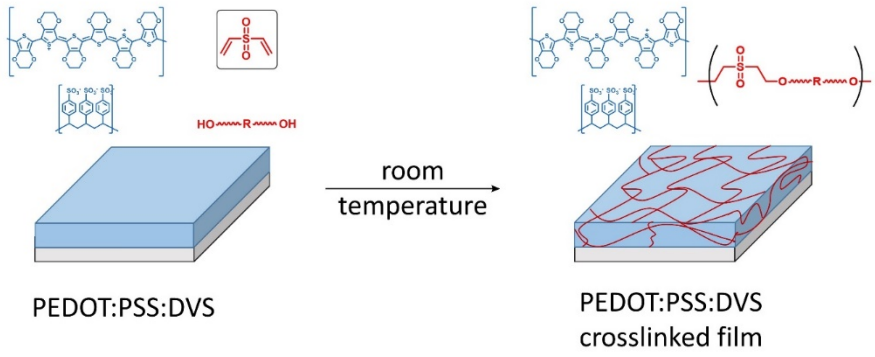

Figura R.2 Schematic representation of cross-linking reaction of PEDOT:PSS film by DVS.

En el último capítulo, hemos hablado de como intervenir directamente en la estructura molecular de la parte conductora. Para pode llevarlo a cabo hemos elegido cambiar el enfoque del EDOT. Hemos visto como el principal producto secundario en la reacción para la síntesis del EDOT-CH_2OH es un derivado con un anillo dioxepanico. En literatura, todavía, están presentes polímeros conductores que se basan en esa molécula llamada ProDOT. Mucho más fácil de sintetizar y mucho más barata, el ProDOT presenta el diseño perfecto para llevar un grupo funcional en el metileno del medio. Protegiendo el ácido 2,2-

Bis(hydroxymethyl)propiónico (bisMPA), un ácido comercial muy barato, con un grupo bencílico, podemos condensarlo con el 3,4-dimetoxytiofeno. Desprotegiendo ese último, obtenemos un ProDOT-COOH en dos simples pasos (**Esquema R.4**).

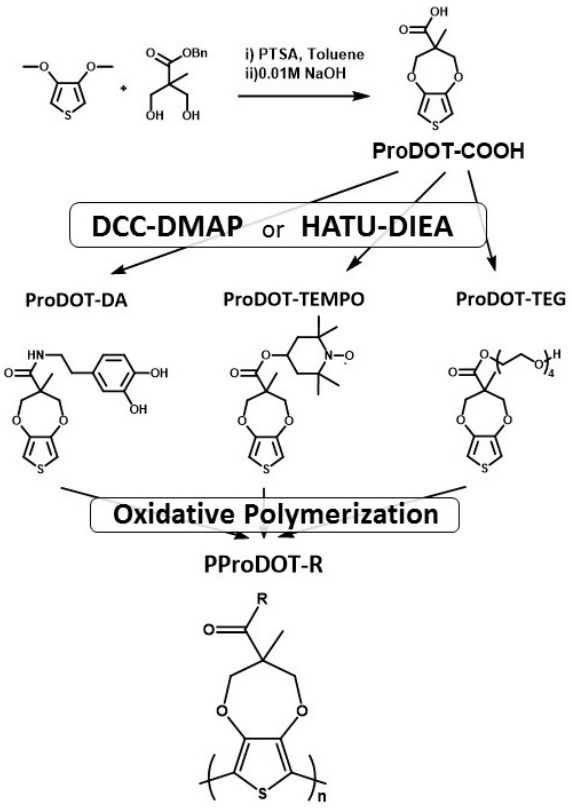

Esquema R.4 Reacciones de síntesis de ProDOT-COOH y siguientes condensaciones.

Ese derivado ha sido polimerizado químicamente y electroquímicamente, obteniendo en los dos casos un polímero conductor morado. Para demonstrar la facilidad de funcionalización de la parte carboxílica, hemos condensado tres diferentes moléculas orgánicas, cada una con una peculiar característica electroquímica. Hemos utilizado: Dopamina, dada su capacidad redox en la

parte aromática; el TEMPO ((2,2,6,6-Tetrametilpiperidin-1-yl)oxíl, dada su capacidad redox siendo un radical libre y tetraetileneglicol, dada su capacidad a quelar cationes como litio. Hemos utilizados dos diferentes protocolos de condensación, para demonstrar la viabilidad y la solidez de la molécula: DCC (N,N'-diciclohexílcarbodiimida)/DMAP (4-dimetilaminopiridina) y HATU/DIPA (N,N'-diisopropiletilamina) (**Esquema R.4**).

En conclusión, durante esta tesis doctoral se han desarrollado nuevos polímeros orgánicos conductores para su aplicación en bioelectrónica. Partiendo del material más famoso y utilizado hoy en día el PEDOT:PSS, se han podido mejorar propiedades como la biocompatibilidad, estabilidad y funcionabilidad. Todo ello, nos ha llevado a nuevos materiales que pueden servir para mejorar diferentes aplicaciones como sensores, electrodos cutáneos o scaffolds para ingeniería tisular.

Bibliografía

(1) https://www.acs.org/content/acs/en/education/whatischemistry/landmarks/bakelite.html (accessed March 2, 2017). .

(2) Letheby, H. *J. Chem. Soc.* **1862**, *15* (0), 161.

(3) Shirakawa, H.; Louis, E. J.; MacDiarmid, A. G.; Chiang, C. K.; Heeger, A. J. *J. Chem. Soc. Chem. Commun.* **1977**, No. 16, 578.

(4) Jonas, F.; Heywang, G.; Schmidtberg, W. Neue polythiophene, verfahren zu ihrer herstellung und ihre verwendung. DE3813589, 1988.

(5) Jonas, F.; Heywang, G.; Schmidtberg, W. Feststoff-elektrolyte und diese enthaltende elektrolyt-kondensatoren. DE3814730, 1988.

(6) Torsi, L.; Dodabalapur, A.; Sabbatini, L.; Zambonin, P. . *Sensors Actuators B Chem.* **2000**, *67* (3), 312.

(7) Hu, W.; Liu, Y.; Xu, Y.; Liu, S.; Zhou, S.; Zhu, D.; Xu, B.; Bai, C.; Wang, C. *Thin Solid Films* **2000**, *360* (1–2), 256.

(8) Bouvet, M.; Leroy, A.; Simon, J.; Tournilhac, F.; Guillaud, G.; Lessnick, P.; Maillard, A.; Spirkovitch, S.; Debliquy, M.; de Haan, A.; Decroly, A. *Sensors Actuators B Chem.* **2001**, *72* (1), 86.

(9) Nilsson, D. *Sensors Actuators B Chem.* **2002**, *86* (2–3), 193.

(10) Bartic, C.; Palan, B.; Campitelli, A.; Borghs, G. *Sensors Actuators B Chem.* **2002**, *83* (1–3), 115.

(11) Dabke, R. B.; Singh, G. D.; Dhanabalan, A.; Lal, R.; Contractor, A. Q. *Anal. Chem.* **1997**, *69* (4), 724.

(12) Bartlett, P. N.; Wang, J. H.; Wallace, E. N. K. *Chem. Commun.* **1996**, No. 3, 359.

(13) Kanungo, M.; Srivastava, D. N.; Kumar, A.; Contractor, A. Q. *Chem. Commun.* **2002**, No. 7, 680.

(14) Krishnamoorthy, K.; Gokhale, R. S.; Contractor, A. Q.; Kumar, A. *Chem. Commun.* **2004**, No. 7, 820.

(15) Nikolou, M.; Malliaras, G. G. *Chem. Rec.* **2008**, *8* (1), 13.

List of acronyms

ACN	Acetonitrile
ATR-FTIR	Attenuated total reflection – Fourier transformed infrared spectroscopy
BDNF	Brain-derived neurotrophic factor
CCDC	The Cambridge crystallographic data centre
CNS	Central nervous system
CS	Chondroitin sulfate
CV	Cyclic voltammetry
DBSA	4-DodecylBenzeneSulfonic Acid
DCC	N,N'-Dicyclohexylcarbodiimide
DCM	Dichloromethane
DEPT	Distortionless Enhancement by Polarization Transfer
DIEA	N,N-DiIsopropylEthylAmine
DMAP	4-DiMethylAminoPyridine
DMF	Dimethylformamide
DMSO-d6	Dimethylsulfoxide hexadeuterated
DVS	Divinylsulfon**e**
EDOT	3,4-ethylenedioxythiophene

ESI	Electrospray ionization
EtOAc	Ethyl acetate
FT-IR	Fourier transformed infrared spectroscopy
GAG	Glycosaminoglycan
GOPS	(3-Glycidyloxypropyl)trimethoxysilane
HA	Hyaluronic acid
HATU	1-[Bis(dimethylamino)methylene]-1H-1,2,3-triazolo[4,5-b]pyridinium3-oxidhexafluorophosphate
HBGF	Heparin-Binding Growth Factors
HEP	Heparin
HPLC	High pressure liquid chromatography
HRMS	High Resolution Mass Spectroscopy
HSQC	Heteronuclear Single Quantum Coherence Spectroscopy
ISO	International Standardization Organization
MDOT	3,4-MethyleneDiOxyThiophene
MTT	3-(4,5-dimethylthiazol-2-yl)-2,5-diphenyltetrazolium bromide
NaPSS	Sodium PolyStyreneSulfonate
NIR	Near Infra-Red
NGF	Neuronal Growing Factor
NMR	Nuclear Magnetic Resonance
OECT	Organic Electrochemical Transistor
OLED	Organic Light-Emitting Diode
OPV	Organic Photo Voltaic
ORTEP	Oak Ridge Thermal-Ellipsoid Plot Program
OTFT	Organic thin film transistor
PBS	Phosphate Buffer Saline
PEDOT	3,4-EthyleneDiOxoThiophene
ProDOT	3,4-PROpileneDiOxoThiophene

PSS	PolyStyreneSulfonate
pTSA	ParaToluneneSulfonic Acid
Q-TOF	Quadrupole Time-Of-Flight mass spectrometer
ROS	Reactive Oxygen Species
$TBAClO_4$	TetraButhylAmmonium Perchlorate
TEG	TetraEthylene Glycol
TEM	Transmission electron microscopy
TEMPO	(2,2,6,6-TEtraMethylPiperidin-1-yl)Oxyl
Tos	Tosyl
UV	Ultra-Violet
Vis	Visible
YAG	Yttrium Aluminium Garnet

Curriculum Vitæ

Daniele Mantione

daniele.mantione@ehu.es **,** mantione89@gmail.com

Education:

PhD student in Applied chemistry and polymeric materials, University of the Basque Country, San Sebastian, Spain, 2013-2017.

M.S. in Chemistry, University of study of Pavia, Pavia, Italy, 2013.

B.S. in Chemical sciences, University of study of Pavia, Pavia, Italy, 2011.

Professional Experience:

2013–2017 Innovative Polymers Group**,** POLYMAT-UPV/EHU, supervisors: Prof. David Mecerreyes and Dr. Haritz Sardon, Av. Tolosa 72 Ed. Korta, 20018 San Sebastian, Spain.

01/2017-07/2017 IBM Almaden Reseach Center, supervisor: Dr. James Hedrick, 650 Harry Rd. 95120 San Jose, CA, USA.

06/2015 BEL, Ecole National Superieure des Mines de Saint-Etienne, Prof. George Malliaras, Campus Georges Charpak, 880 Route de Mimet, 13120 Gardanne, France.

Languages:

Italian (C2), English (C1), Spanish (C1), French(A1)

Awarded Grants and Honors:

2017 Global Training Fellowship from the Council of San Sebastian-Spain.

2013 Doctoral grant from the European Union (Marie Curie Fellow, OLIMPIA Project, ITN, FP7).

2013 EDISU-University of Pavia Thesis Prize

Publications:

1. Iñaki Gomez, **Daniele Mantione**, Olatz Leonet, Alberto J. Blazquez, David Mecerreyes* *Hybrid Sulfur-Selenium Copolymers as Cathodic Materials for Lithium Batteries* (submitted)

2. Isabel del Agua, **Daniele Mantione**, Sara Marina, C. Pitsalidis, M. Ferro, Ana Sanchez-Sanchez, R.M. Owens, George Malliaras, David Mecerreyes *Conducting Polymer Scaffolds based on PEDOT and Xanthan Gum for live-cell Monitoring* (In preparation)

3. **Daniele Mantione**,[1] Isabel del Agua,[1] Ana Sanchez-Sanchez,* David Mecerreyes* *Conductive polydioxythiophene (PEDOT) type materials for bioelectronics* Polymers **2017**, 9, 354.

4. Ludmila Irene Ronco, Andere Basterretxea, **Daniele Mantione**, Robert H. Aguirresarobe, Roque Javier Minari, Luis Marcelino Gugliotta, David Mecerreyes, Haritz Sardon* *Temperature responsive PEG-based polyurethanes "à la carte"* Polymer **2017**, 122, 117.

5. **Daniele Mantione**, Nerea Casado, Ana Sanchez-Sanchez, Haritz Sardon, David Mecerreyes* *Easy-to-Make Carboxylic Acid Dioxythiophene Monomer (ProDOT-COOH) and Functional Conductive Polymers* Journal of Polymer Chemistry Part A **2017**, 55, 2721.

6. Isabel del Agua, **Daniele Mantione**, Nerea Casado, Ana Sanchez-Sanchez, George Malliaras, David Mecerreyes* *Conducting Polymer Iongels Based on PEDOT and Guar Gum* ACS Marco Letter **2017**, 6, 473.

7. Sofiem Garmendia,[1] **Daniele Mantione**,[1] Silvia Alonso de Castro, Coralie Jehanno, Lezama Luis, James L. Hedrick, David Mecerreyes, Luca Salassa, Haritz Sardon* *Polyurethane based organic macromolecular contrast agent (PU-ORCA) for magnetic resonance imaging* Polym. Chem. **2017**, 8, 2693.

8. **Daniele Mantione**, Isabel del Agua, Wandert Schaafsma, Ilke Uguz, Mohammed ElMahmoudy, Ana Sanchez-Sanchez, Haritz Sardon, Begoña Castro, George Malliaras * David Mecerreyes* *Low-Temperature Cross-Linking of PEDOT:PSS Films Using Divinylsulfone* ACS Appl. Mater. Interfaces **2017**, 9, 18254.

9. Guiomar Hernandez, Mehmet Isik, **Daniele Mantione**, Afshin Pendashteh, Paula Navalpotro, Devaraj Shanmukaraj, Rebeca Marcilla, David Mecerreyes* *Redox-active poly(ionic liquid)s as active materials in energy storage applications*. J. Mater. Chem. A, **2017**.[10.1039/C6TA10056B]

10. Marta Ribeiro, Maria P. Ferraz, Fernando J. Monteiro, Maria H. Fernandes, Marisa M. Beppu, **Daniele Mantione** and Haritz Sardon* *Antibacterial silk fibroin/nanohydroxyapatite hydrogels with silver and gold nanoparticles for bone regeneration* Nanomedicine: Nanotechnology, Biology and Medicine **2017**, 13, 231.

11. Jessica S. Desport,[1] **Daniele Mantione**,*[1] Mónica Moreno, Haritz Sardon, María J. Barandiaran, David Mecerreyes* *Synthesis of three different galactose-based methacrylate monomers for the production of sugar-based polymers* Carbohydrate research **2016**, 232, 50.

12. **Daniele Mantione**, Isabel del Agua, Wandert Schaafsma,* Javier Diez, Begona Castro, Haritz Sardon, David Mecerreyes* *Poly(3,4-ethylenedioxythiophene):GlycosAminGlycan (PEDOT:GAG) aqueous*

Dispersions: Towards Electrically Conductive Bioactive Materials for Neural Interfaces Macro. Biosci **2016**, 16, 1227.

13. Ana Sanchez-Sanchez,* Andere Basterrechea, **Daniele Mantione**, Agustin Etxeberria, Cristina Elizetxea, Haritz Sardon, David Mecerreyes* *Organo-mediated bulk polymerization of ε-Caprolactam and its Copolymerization with ε-Caprolactone using sulfonic acids* J. Polym. Sci., Part A **2016**, 54, 2394.

14. **Daniele Mantione**, Olatz Olaizola Aizpuru, Misal Giuseppe Memeo, Bruna Bovio, and Paolo Quadrelli* *4-Heterosubstituted Cyclopentenone Antiviral Compounds: Synthesis, Mechanism, and Antiviral Evaluation*. European J. Org. Chem. **2016**, 983.

15. Sonia Zulfiqar,* **Daniele Mantione**, Omar El Tall, Muhammad Ilyas Sarwar, Fernando Ruipérez, Alexander Rothenberger, David Mecerreyes. *Nanoporous amide networks based on tetraphenyladamantane for selective CO2 capture*. J. Mater. Chem. A **2016**, 8190.

16. Haritz Sardon,* Jeremy P. K. Tan, **Daniele Mantione**, Julian M. W. Chan, David Mecerreyes, James L. Hedrick, and Yi Yan Yang *Thermoresponsive Random Poly(ether urethane) based Nanoparticles with Tailorable LCSTs for Anticancer Drug Delivery*. Macromol. Rapid Comm. **2015,** 1761.

17. Ana M. Fernandes, **Daniele Mantione**, Raquel Gracia, Jose R. Leiza, Maria Paulis, and David Mecerreyes* *From Polymer Latexes to Multifunctional Liquid Marbles* ACS Appl. Mater. Interfaces **2015**, 7, 4433.

18. Misal Giuseppe Memeo, **Daniele Mantione**, Bruna Bovio, Paolo Quadrelli* *RuO4-Catalyzed Oxidation Reactions of N-Alkylisoxazolino-2-azanorbornane Derivatives: An Expeditious Route to Tricyclic g-Lactams* Synthesis **2011**, 13, 2165.

[1] These authors contribute equally.

Communications:

1. ACS 253rd National Meeting 2-6/0/2017 Moscone Center, San Francisco California, USA. **Daniele Mantione**, Ana Sanchez-Sanchez, Haritz

Sardon, David Mecerreyes *Innovative carboxylic acid functional Propylene dioxythiophene (ProDOT-COOH) monomer for Bioelectronics.*

2. 1st International Conference on Indigenous Resource 14-15/04/2016 Kotli, AJ&K, Pakistan. **Daniele Mantione**, Isabel del Agua, Haritz Sardon, David Mecerreyes *Innovative PEDOT/Biopolymer Aqueous Dispersions for Bioelectronic*
3. IEEE Roma 27-30/07/2015 Largo Angelicum 1 - 00184 Roma Italy, **Daniele Mantione**, Isabel del Agua, Haritz Sardon, David Mecerreyes *Innovative EDOT/Biopolymer Aqueous Dispersions for Bioelectronic.*
4. Joint Summer School of the European Projects CONTEST–OLIMPIA–EAGER 26-28/05/2014 Fraunhofer EMFT- Hansastrasse 27d - 80686 Munich, Germany. 5. **Daniele Mantione**, Isabel del Agua, Wandert Schaafsma, Javier Diez, Begona Castro, Haritz Sardon, David Mecerreyes *Poly(3,4–ethylenedioxythiophene):GlycosAminGlycan (PEDOT:GAG) aqueous Dispersions: Towards Electrically Conductive Bioactive Materials for Neural Interfaces.*

Posters:

1. POLYMAT Spotlight 21-24/06/2016 Palacio Miramar, 20018 Donostia-San Sebastian, Spain. Sonia Zulfiqar, **Daniele Mantione**, Omar El Tall, Muhammad Ilyas Sarwar, Fernando Ruipérez, Alexander Rothenberger and David Mecerreyes *Nanoporous Amide Networks Based on Tetraphenyladamantane for Selective CO_2 Capture.*
2. 1st BIOMAPP 19-20/10/2015 BiomaGune Miramon Pasealekua, 182, 20009 Donostia-San Sebastian, Spain. Sofiem Garmendia, **Daniele Mantione**, Haritz Sardon, Silvia Alonso-de Castro, Luca Salassa, David

Mecerreyes *Polyurethane based Organic Radical Contrast Agent for Magnetic Resonance Imaging*.

3. European polymers federation EPF 2015 meeting 21-26/06/2015 Kerstin Wustrack -Institut für Polymer Dresden e.V. (IPF) Hohe Str. 6-01069 Dresden Germany, Sonia Zulfiqar, Muhammad Ilyas Sarwar **Daniele Mantione**, Haritz Sardon David Mecerreyes *Amide based polymeric ionic liquids for CO2 capture.*
4. 4th Brazil-Spain Organic chemistry workshop 2-4/07/2014 Conference Room – Ed. Korta – Av. Tolosa 72 – 20018 Donostia-San Sebastian Spain, **Daniele Mantione**, Dimitrios Tsangournos, Nerea Casado, Haritz Sardon, David Mecerreyes *Synthesis of functionalized EDOT monomers for Bioelectronics.*

Work Experience:

1. Summer vacancies 2008-2009-2010 Laboratory Technician, samples collection and production control *La Versa* s.p.a.(Winery), via Francesco Crispi 15, 27047 Santa Maria Della Versa, Pavia, Italy.
2. Summer vacancies 2007 (40 days) and Easter vacancies (10 days) 2008 Laboratory technician Analysis of solid, liquid and gas intermediate of oil refining *E.N.I.* spa, Piazzale Enrico Mattei 46, 27039 Sannazzaro de' Burgondi, Pavia, Italy.